
[All ETDs from UAB](#)

[UAB Theses & Dissertations](#)

2016

Behavioral and developmental abnormalities in SULT4A1 deficient zebrafish

Francis Crittenden
University of Alabama at Birmingham

Follow this and additional works at: <https://digitalcommons.library.uab.edu/etd-collection>



Part of the [Medical Sciences Commons](#)

Recommended Citation

Crittenden, Francis, "Behavioral and developmental abnormalities in SULT4A1 deficient zebrafish" (2016).
All ETDs from UAB. 1438.
<https://digitalcommons.library.uab.edu/etd-collection/1438>

This content has been accepted for inclusion by an authorized administrator of the UAB Digital Commons, and is provided as a free open access item. All inquiries regarding this item or the UAB Digital Commons should be directed to the [UAB Libraries Office of Scholarly Communication](#).

BEHAVIORAL AND DEVELOPMENTAL ABNORMALITIES IN
SULT4A1 DEFICIENT ZEBRAFISH

by

FRANCIS CRITTENDEN

JOHN M. PARANT, COMMITTEE CHAIR
STEPHEN BARNES
CHARLES N. FALANY
TIMOTHY W. KRAFT
LORI McMAHON
ROSALINDA ROBERTS

A DISSERTATION

Submitted to the graduate faculty of The University of Alabama at Birmingham,
In partial fulfillment of the requirements for the degree of
Doctor of Philosophy

BIRMINGHAM, ALABAMA

2015

Copyright by
Francis Crittenden
2015

BEHAVIORAL AND DEVELOPMENTAL ABNORMALITIES IN
SULT4A1 DEFICIENT ZEBRAFISH

FRANCIS CRITTENDEN

PHARMACOLOGY AND TOXICOLOGY

ABSTRACT

Since its identification in 2000, sulfotransferase (SULT) 4A1 has presented an enigma to the field of cytosolic SULT biology. SULT4A1 is exclusively expressed in neural tissue, is highly conserved, and has been identified in every vertebrate studied to date. Despite this singular level of conservation, no substrate or function for SULT4A1 has been identified. Previous studies demonstrated that SULT4A1 does not bind the obligate sulfate donor, 3'-phosphoadenosine-5'-phosphosulfate (PAPS), yet SULT4A1 is classified as a SULT superfamily member based on sequence and structural similarities to the other SULTs. In this study, RNA-seq was used to search for alterations in gene expression in 72 hours post fertilization zebrafish larvae following transient SULT4A1 knockdown (KD) utilizing splice blocking morpholino oligonucleotides (MOs). This study demonstrates that transient inhibition of SULT4A1 expression in developing zebrafish larvae results in the up-regulation of several genes involved in phototransduction. SULT4A1 KD was verified by immunoblot analysis and quantitative real-time PCR (qPCR). Gene regulation changes identified by deep RNA sequencing were validated by qPCR. Transcription activator-like effector nucleases (TALENs) were also used to generate heritable mutations in the SULT4A1 gene of zebrafish. The mutation consists of an 8 nucleotide deletion within the second exon of the gene, resulting in a frameshift mutation and premature stop codon after 132 AA. During early adulthood, casual observations were made that mutant zebrafish were exhibiting excessively sedentary behavior during

the day. These observations were inconsistent with published reports on activity in zebrafish which are largely diurnal organisms and are highly active during the day. Thus, a decrease in activity during the day represents an abnormal behavior and warranted further systematic analysis. EthoVision video tracking software was used to monitor activity levels in wild type and mutant fish over 48 hours of a normal light/dark cycle. *SULT4A1* mutant fish were shown to exhibit increased inactivity bout length and frequency as well as a general decrease in daytime activity levels when compared to their WT counterparts.

Keywords: Sulfotransferase, zebrafish, transcription activator-like effector nuclease, morpholino, phototransduction, activity levels

DEDICATION

To Dr. Richard Cunningham Crittenden and Josie Lynn Falany

ACKNOWLEDGEMENTS

I would like to thank my mentor, Dr. Charles N. Falany for his support and guidance which began long before I joined his lab. I would like to thank my committee members, Dr. John M. Parant, Dr. Timothy R. Kraft, Dr. Rosalinda Roberts, Dr. Stephen Barnes, and Dr. Lori McMahon for their genuine interest in and support of my work. I also thank all of the staff at the UAB Zebrafish Research Facility as well as the faculty and collaborators who volunteered their time, expertise, and support including Dr. Alan Kaleuff, Dr. Thomas Van Groen, Dr. Karen Gamble, and Dr. Dongquan Chen. A very special thanks goes to Becky Warnix for her relentless positivity in helping me navigate the bureaucracy of UAB.

TABLE OF CONTENTS

ABSTRACT.....	<i>iii</i>
DEDICATION.....	<i>v</i>
ACKNOWLEDGEMENTS.....	<i>vi</i>
LIST OF TABLES.....	<i>x</i>
LIST OF FIGURES.....	<i>xi</i>
LIST OF ABBREVIATIONS.....	<i>xiv</i>
CHAPTER	
1 INTRODUCTION.....	1
Drug Metabolism and Pharmacokinetics.....	1
Sites of Xenobiotic Metabolism.....	2
Phase I Drug Metabolism.....	3
Phase II Drug Metabolism.....	4
Sulfotransferases.....	6
Mechanism.....	9
Structure/function Relationship.....	11
Heterogeneity.....	12
The Orphan Enzyme SULT4A1.....	15
Tissue Distribution and Expression Regulation.....	17
Biochemical Properties of SULT4A1.....	18
Psychopathology.....	22
Specific Aims.....	25
Zebrafish as a Model Organism for the Study of SULT4A1.....	25
Aim 1.....	29
Aim 2.....	30
Aim 3.....	30
2 METHODS.....	32
Zebrafish Lines and Maintenance.....	32
Lysate Collection.....	32

Bradford Analysis of Protein Concentrations	33
SULT4A1 Protein Expression Knockdown by Morpholino Injection	34
Immunoblot Analysis	34
RNA Isolation and Quantification	36
Reverse Transcription of RNA	37
Quantitative Real-Time PCR	37
RNA-Seq.....	38
Co-Immunoprecipitation of 6H-Flag-zfSULT4A1	39
Adding the Flag Tag	39
Preparing the Flag-zfSULT4A1 Construct for Cloning into pPROEX	40
Ligation of Flag-zfSULT4A1 Construct into pPROEX Plasmid and	
Expression in BL21 E. coli	41
Purifying 6His-Flag-zfSULT4A1	41
Pulldown Phase 1	42
Pulldown Phase 2.....	43
SDS Gel Separation and MS/MS Analysis	43
DNA Gel Electrophoresis	46
Immunohistochemistry of SULT4A1 in Rat Retinas.....	46
Preparing Eye Sections	46
Staining Eye Sections	46
Production of pAb to zfSULT4A1.....	47
Gel Filtration Chromatography of zfSULT4A1	49
Generation of SULT4A1 Mutant Zebrafish Using TALENs	50
TALEN Target Site Selection and Assembly	50
Microinjection of Zebrafish Embryos.....	52
Extraction of Genomic DNA from Embryos and Adult Zebrafish.....	52
Identification and Verification of SULT4A1 Mutant Zebrafish Line	53
High Resolution Melting Analysis.....	53
Dynamic Modeling of SULT4A1 ^{Δ15} Mutant Protein.....	58
Behavioral Analysis in Zebrafish.....	59
Larval Visual-Motor Response.....	59
Novel Tank Test.....	62
Social Preference Test.....	63
Activity Analysis of SULT4A1 Mutant Zebrafish	64
 3 RESULTS	 66
 Aim 1	 66
SULT4A1 Expression in Brain and Eye of Adult Zebrafish	66
Localization of SULT4A1 Within the Retina.....	68
SULT4A1 MO Effectiveness and Lack of Toxicity.....	72
SULT4A1 KD Induces Up-Regulation of Phototransduction Genes in	
72 hpf Larvae	75
Aim 2	79
Visual Motor Response (VMR) Assessment in SULT4A1 KD Larvae	79
Anxiety in the Novel Tank Test.....	81

Social Preference	84
Activity Analysis	91
Dynamic Modeling of SULT4A1 ^{Δ15} Mutant Protein.....	98
Aim 3	104
Co-Immunoprecipitation of zfSULT4A1 with YLPM1	104
In-Vitro Dimerization of SULT4A1	109
4 DISCUSSION	114
Effects of SULT4A1 Expression Deficiency on Development and Gene	
Expression in Larval and Adult Zebrafish	114
Behavioral Abnormalities in SULT4A1 KD and Mutant Zebrafish.....	121
Biochemical Analysis of SULT4A1	126
Future Directions	133
REFERENCES	142
APPENDIX	
A INSTITUTIONAL ANIMAL CARE AND USE COMMITTEE	
APPROVAL	156

LIST OF TABLES

<i>Table</i>	<i>Page</i>
1 The preferred substrates and tissue localizations of the human cytosolic SULTs.....	13
2 Sequence homology of SULT4A1 across different vertebrate species	27
3 Summary of affected genes involved in phototransduction.....	77
4 Gene ontology of transcripts affected by SULT4A1 knockdown	78
5 Activity analysis in WT and SULT4A1 ^{Δ8/Δ8} fish.....	95

LIST OF FIGURES

<i>Figure</i>	<i>Page</i>
1 Metabolic elimination pathways	7
2 The cytosolic SULT cofactor.....	8
3 Reaction mechanism of sulfonate transfer with key residues	10
4 Amino acid sequence homology between human and zebrafish SULT4A1	16
5 Stereoscopic view of SULT1B1 and SULT4A1	19
6 Stereoscopic view of PAPS binding site in SULT1B1 and SULT4A1	21
7 Stereoscopic view of a surface model of SULT4A1	23
8 MO targeting of zSULT4A1 gene	35
9 Schematic of the zebrafish SULT4A1 gene.....	51
10 SULT4A1 ^{Δ15/Δ15} and SULT4A1 ^{Δ8/Δ8} screening by HRMA analysis	54
11 SULT4A1 ^{Δ15} mutation	55
12 SULT4A1 ^{Δ8} mutation.....	56
13 Immunoblot analysis of brain lysate from WT, SULT4A1 ^{Δ15/Δ15} , and SULT4A1 ^{Δ8/Δ8} fish.....	57
14 Zebrafish Larvae Light Startle Assay Contraption (ZELLSAC).....	61
15 SULT4A1 expression in adult zebrafish tissues	67
16 Immunoblot of zebrafish brain and eye lysate using anti-human	

SULT4A1 polyclonal antibody	69
17 Relative expression level of SULT4A1 in central and peripheral retina of adult AB strain zebrafish	70
18 Immunohistochemical staining of adult rat retina for SULT4A1	71
19 SULT4A1 MO effectiveness	74
20 Normal development of SCM and 4A1 MO zebrafish larvae	76
21 qPCR verification of differentially expressed phototransduction genes observed in RNA-seq data at 72 hpf	80
22 VMR assay light stimulus intensity optimization	82
23 VMR development in 76-84 hpf SCM and SULT4A1 MO - injected larvae.....	83
24 Standard 6 minute novel tank test in WT and SULT4A1 ^{Δ8/Δ8} fish	86
25 Standard 6 minute novel tank test in WT and SULT4A1 ^{Δ15/Δ15} fish	88
26 SULT4A1 ^{Δ8/Δ8} fish behavior in a social preference test	89
27 Suppressed activity in SULT4A1 ^{Δ8/Δ8} zebrafish.....	92
28 Frequency of different inactivity bout lengths	96
29 Arrhythmic Mutant Activity	99
30 Unchanged activity in SULT4A1 ^{Δ15/Δ15} zebrafish	101
31 Stereoscopic view of the position of SULT4A1 ^{Δ15} deleted residues within the putative substrate binding pocket of SULT4A1	103
32 Stereoscopic view of the involution of His111 in SULT4A1 ^{Δ15} mutant protein	105
33 Expression and purification of 6His-Flag-zSULT4A1	106
34 Activity of purified 6His-TEV Protease	108
35 The MS/MS spectrum for the two unique peptides identified in the pulldown sample	110

36 AA sequence of YPLM1.....	112
37 Dimerization of zSULT4A1	113
38 SULT4A1 species alignments.....	130

LIST OF ABBREVIATIONS

6His	6-histidine
AA	amino acid
Acetyl CoA	acetyl coenzyme A
ADH	alcohol dehydrogenase
Arr3	arrestin 3a
ASD	autism spectrum disorder
ATF-2	activating transcription factor-2
bp	base pair
Br-STL	brain Sulfotransferase-like
CNS	central nervous system
CREB	cAMP-responsive element binding protein
CRISPR	clustered, regularly interspaced, short palindromic repeats
CYP	cytochrome P450 monooxygenase
DAPI	4',6-diamidino-2-phenylindole
egf17	EGF-like-domain, multiple 7
ELB	embryo lysis buffer
ERG	electroretinogram

ERK1	extracellular signal-regulated kinase1
FDR	false discovery rate
FMO	flavin-containing monoamine oxidase
GI	gastrointestinal
grk1b	G protein-coupled receptor kinase 1 b
GST	glutathione S-transferase
guca1e	guanylate cyclase activator 1e
Hpf	hours post fertilization
HRMA	high resolution melting analysis
IHC	immunohistochemistry
IPTG	isopropyl β -D-thiogalactoside
KD	knockdown
LB	Luria-Bertani
Mbp	megabase pairs
MBP	maltose-binding protein
MO	morpholino oligonucleotide
MS	mass spectrometry
MW	molecular weight
NBP	3-n-butylphthalide
nrc	no optokinetic response c
OKR	optokinetic response
OMR	optomotor response
OPN1LW2	opsin 1 long-wave-sensitive 2

OPN1MW1	opsin 1 medium-wave-sensitive 1
OPN1SW1	opsin 1 short-wave-sensitive 1
OPN1SW2	opsin 1 short-wave-sensitive 2
PAP	3', 5'-phosphoadenosine
PAPS	3'-phosphoadenosine, 5'-phosphosulfate
PBS	phosphate-buffered saline
Pin1	peptidyl-prolyl cis/trans isomerase
PhIP	2-amino-1-methyl-6-phenylimidazo[4,5-f]pyridine
PMSF	phenylmethanesulfonylfluoride
PP2A	protein phosphatase 2A
RPC	retinal progenitor cell
SCN	suprachiasmatic nucleus
SAM	S-adenosyl methionine
SHANK3	SH3 and multiple ankyrin repeat domains 3
SULT	cytosolic sulfotransferase
TALE	transcription activator-like effector
TALLEN	transcription activator-like effector nuclease
TBS	tris-buffered saline
TEV	tobacco etch virus
T-TBS	tris-buffered saline with TWEEN20
UGT	UDP-glucuronosyltransferase
UTR	untranslated region
VMR	visual-motor response

YLPM1	YLP motif containing protein 1
ZELLSAC	zebrafish light startle assay contraption
ZT	zeitgeber time

CHAPTER 1

INTRODUCTION

Drug Metabolism and Pharmacokinetics

During the process of drug development, many prospective therapeutic agents fail to make it to market not for a lack of target site reactivity, but for a simple lack of bioavailability. For non-intravenously administered drugs, the path a compound must take to its target site can take it through many different biological tissue types, any of which may have the ability to enzymatically modify the compound. For this reason, significant effort and resources are expended to identify and characterize the enzymes responsible for these modifications.

Drug metabolizing enzymes serve several important purposes. One is to facilitate elimination from the body. Most drugs must pass through multiple lipid membranes and aqueous compartments to reach their site of action. For this reason, most drugs must be lipid soluble in their active form and are therefore difficult for the body to eliminate unless they are first modified by a phase I and/or phase II drug metabolizing enzyme. Naloxone, as one of many examples, is a highly lipophilic compound that undergoes extensive sulfonation and glucuronidation in the liver. These conjugative metabolites are more water-soluble than the parent compound and can thus be more easily eliminated in the urine (Mistry and Houston, 1987; King et al., 1996; Kurogi et al., 2012).

Another important function of metabolic enzymes is the detoxification of harmful compounds and inhibition of their biological activity. One common dietary carcinogen found in cooked meats, 2-amino-1-methyl-6-phenylimidazo[4,5-b]pyridine (PhIP), and its carcinogenic metabolite, N-hydroxy-PhIP, undergo extensive conjugation by UDP-glucuronosyltransferases (UGTs) to form non-toxic conjugates (Langouet et al., 2002). In many cases, drug metabolizing enzymes can also cause drugs to lose their biological activity. Warfarin, for example, is an anticoagulant drug which is metabolized by CYP2C9 to form biologically inactive metabolites (Gulseth et al., 2009). However, while metabolic enzymes can detoxify harmful chemicals, they also have the potential for bioactivation of otherwise harmless compounds. Such is the case with 3-n-butylphthalide (NBP), a drug used to treat cerebral ischemia (Liu and Feng, 1995). NBP is oxidized in the liver to form 3-OH-NBP, then sulfonated by cytosolic sulfotransferase (SULT) 1A1. Spontaneous cleavage of the sulfate generates a highly reactive electrophilic cation that can then bind to hepatocellular proteins and cause hepatotoxicity (Diao et al., 2014).

Sites of Xenobiotic Metabolism

In the human body, the liver is usually the principal site of drug metabolism due to its very high concentrations of metabolic enzymes and access to intestinal absorption via the hepatic portal system. Another major site of drug metabolism is the small intestine, where the vast majority of orally administered drugs are absorbed into the blood. For orally administered drugs, the gut wall and liver together are where most of the metabolism takes place. Blood leaving the gastrointestinal (GI) tract from the small intestine, via the superior mesenteric vein, and the large intestine, via the superior and inferior mesen-

teric veins, converges in the hepatic portal vein. Because all blood leaving the GI tract must pass through the hepatic portal vein and then the liver, orally administered drugs must also first travel through the GI tract and liver before reaching the general circulation. Many drugs undergo extensive metabolism during this first pass through the GI tract and liver. This is known as the first-pass effect, and every drug absorbed in the GI tract is subject to it. For example, an orally administered dose of hydromorphone will have 62% of the dose metabolized during its first pass through the gut wall and liver (Vallner et al., 1981). While the liver and small intestine account for the bulk of the metabolic activity in the body, there are many other sites of drug metabolism. In fact, nearly every tissue type is capable of drug metabolism to a certain degree, especially those which interface with the environment.

Phase I Drug Metabolism

Metabolic enzymes can be categorized into two classes: phase I enzymes, which catalyze non-conjugative reactions, and phase II enzymes which catalyze conjugative reactions. The phase I metabolic enzymes, otherwise known as the “non-synthetic” enzymes, are responsible for reactions that catalyze the reduction, oxidation, cyclization, and de-cyclization of many compounds in the body (Parkinson, 1996). By far the most prevalent family of metabolic enzymes, the cytochrome P450 monooxygenase (CYP) family, accounts for roughly 75% of all drug metabolism in humans (Danielson, 2002). The CYPs are comprised of a superfamily of membrane-bound heme proteins that localize mostly to the endoplasmic reticulum and mitochondria of the cell. In humans, there are 57 CYP isoforms in 18 distinct gene families (Nelson, 2003). The CYPs catalyze the oxi-

ductive metabolism of a wide range of compounds. The mechanism of CYP-mediated metabolism varies depending on the substrate and CYP isoform but always begins with the transfer of an electron from a donor molecule (usually NADPH) to the heme group of the CYP, thus activating it (Meunier et al., 2004). ER CYPs are typically coupled with NADPH cytochrome P450 oxidoreductase to provide a source of reduced NADPH (Meunier et al., 2004), while mitochondrial CYPs typically receive their NADPH from adrenodoxin reductase (Lambeth et al., 1976). Other examples of Phase I metabolic enzymes are the alcohol dehydrogenases (ADH), which catalyze the oxidation of alcohols to form aldehydes (Theorell and McKee, 1961), aldehyde dehydrogenases, which catalyze the oxidation of aldehydes to generate carboxyl groups (Marchitti et al., 2008), the monooxygenases, a class of enzymes which catalyze the reductive addition of a hydroxyl group to a variety of different substrates (Harayama et al., 1992), and the flavin-containing monoamine oxidases (FMO), a family of enzymes which catalyze the oxidation of monoamines (Edmondson et al., 2004).

Phase II Drug Metabolism

Phase II drug metabolizing enzymes catalyze a different sort of reaction than their phase I counterparts. While phase I enzymes primarily catalyze the oxidative or reductive modification of drugs and may not significantly alter the chemistry of a compound, phase II enzymes specialize in the conjugation of drugs to different moieties. This results in the addition of a bulky, usually charged group which can substantially alter the chemistry of a compound.

The most common phase II reaction and one which accounts for roughly 40% of phase II metabolism is glucuronic acid conjugation, or glucuronidation (Evans and Relling, 1999). These reactions are carried out by a family of enzymes known as UDP-glucuronosyltransferases (UGTs). In the glucuronidation reaction, the glucuronyl group of UDP-glucuronide is conjugated onto the drug at a nucleophilic functional group of oxygen, nitrogen, sulfur, or carbon (King et al., 2000). The resulting glucuronosyl-drug conjugates are known as glucuronides. The ability of the UGTs' to conjugate to such a wide variety of functional groups allows them to play an important role in the detoxification of a wide range of substrates. Another notable phase II drug metabolizing enzyme superfamily is the SULTs. Discussed in detail below, the SULTs catalyze the transfer of a sulfonate group from 3'-phosphoadenosine, 5'-phosphosulfate (PAPS) onto a hydroxyl or amine group of the substrate (Tibbs et al., 2014). Glutathione S-transferases (GSTs) are an extremely diverse group of enzymes that catalyze the transfer of the reduced form of glutathione (γ -glutamyl-cysteinyl-glycine) onto drug molecules (Armstrong, 1991). Another diverse group of phase II enzymes, the acetyltransferases, catalyze the acetylation of a wide variety of compounds, such as hydralazine, using acetyl coenzyme A (Acetyl CoA) as the acetyl donor molecule (Timbrell et al., 1980). The methyltransferases catalyze the methylation of substrate compounds using S-adenosyl methionine (SAM) as a methyl group donor molecule (Weinshilboum, 1988). Lastly, amino acid acyl transferases are a class of enzymes that catalyze the conjugation of amino acid residues to carboxylic acid residues on their substrates (Knights et al., 2007). Typically, the amino acids conjugated in these types of reactions are Gly, Glu, Arg, and Lys (Gregus et al., 1993). The amino acid acyl transferases utilize a mechanism whereby ATP is converted to AMP and

conjugated to the substrate to form an acyl adenylate. Substituting the AMP with CoA yields a high-energy intermediate which is then conjugated to the amino group of the acceptor amino acid (Knights et al., 2007).

Typically, drugs will undergo phase I metabolism first. The addition or modification of a functional group, usually via the generation of a hydroxyl moiety, in phase I will “prime” them for their phase II conjugation and subsequent elimination from the body. However, this progression from phase I to phase II to elimination is not always the case. Some drugs are simply eliminated after phase I metabolism. Alternatively, some drugs forego phase I and are primarily metabolized by phase II enzymes. Aspirin is a drug that is conjugated with glycine and eliminated with minimal phase I metabolism (Levy and Tsuchiya, 1972). These and other possible metabolic pathways to elimination are represented in Figure 1.

Sulfotransferases

The second most common phase II drug metabolizing system is the cytosolic SULT superfamily (Evans and Relling, 1999). The SULTs comprise a superfamily of enzymes that catalyze a metabolic reaction wherein a sulfonate moiety is transferred from the obligate donor, PAPS (Figure 2), onto the substrate in conjugation to a hydroxyl group or primary amine group. The substrate is generally rendered biologically inactive and more water soluble, facilitating its elimination from the body (Tibbs et al., 2014).

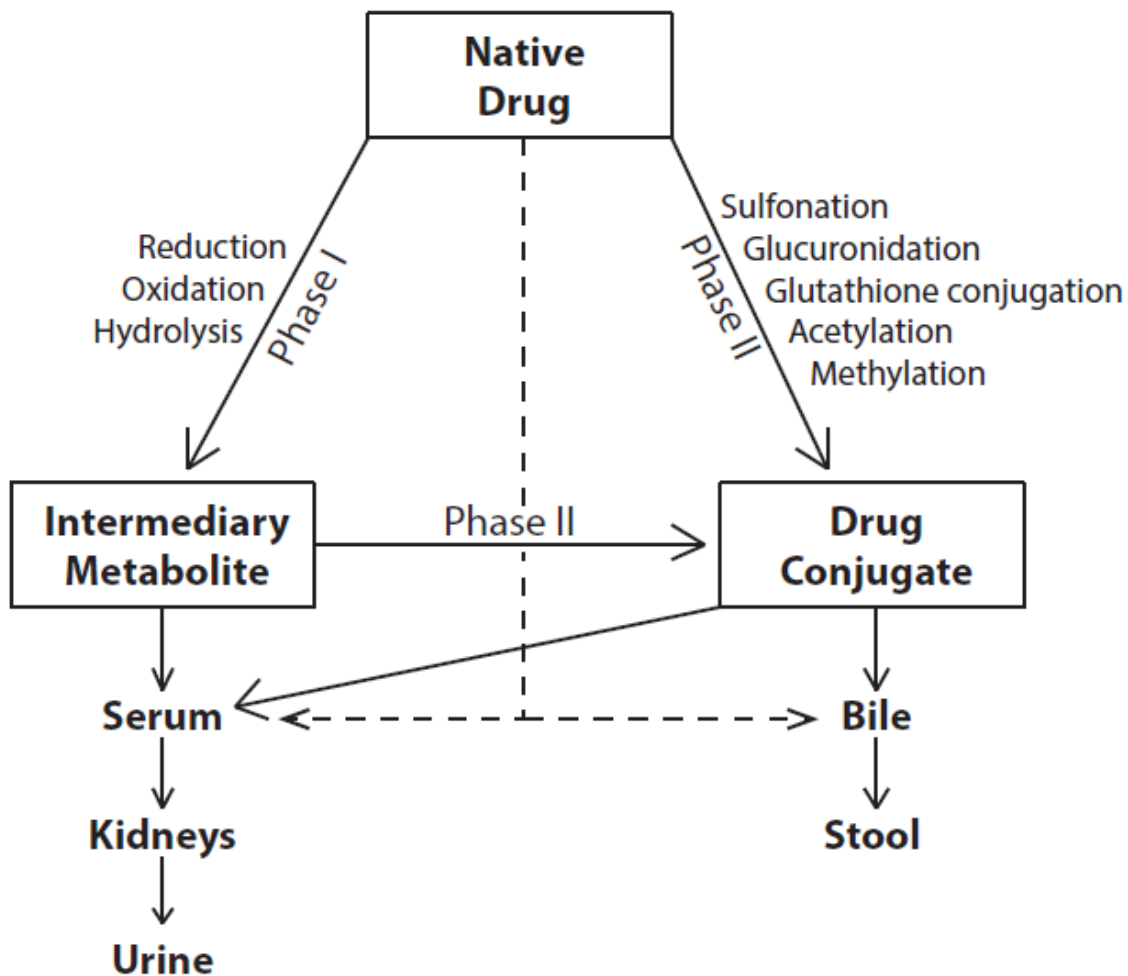


Figure 1. Metabolic elimination pathways. Shown is a schematic representation of the possible pathways for a drug to be rendered water-soluble and eliminated from the body. Often times, a native drug will first undergo a phase I metabolic modification before being conjugated to glucuronic acid or another moiety in a phase II reaction and then being eliminated in either the urine or stool. Less commonly, drugs can undergo phase II conjugation and elimination without any phase I modification.

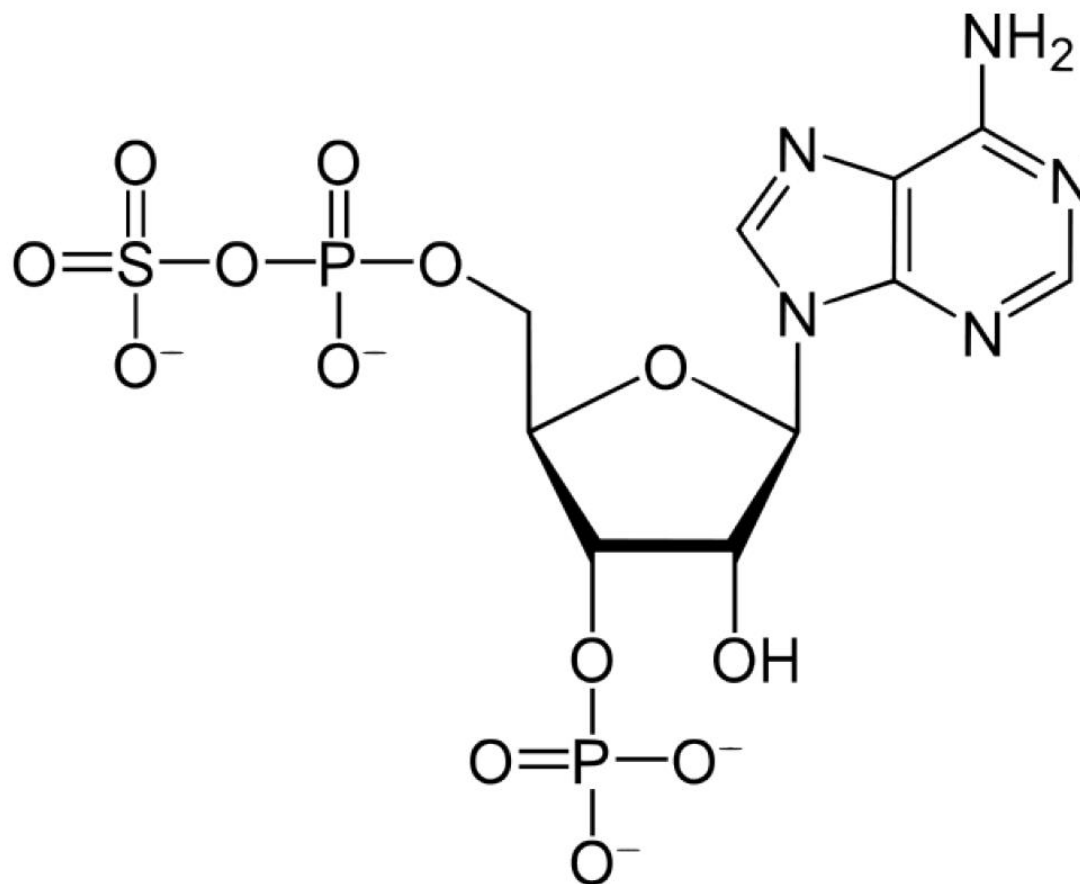


Figure 2. The cytosolic SULT cofactor. Shown here is the cytosolic SULT cofactor, 3'-phosphoadenosine, 5'-phosphosulfate (PAPS). PAPS is the obligate donor of the sulfonate group in sulfation reactions catalyzed by the SULTs.

Mechanism

The mechanism by which the SULTs catalyze the sulfonation of substrates is mediated by the key amino acid residues His 109, Lys 48, Lys 107, and Ser 135. These residues, numbered according to their position on human SULT1B1, are mostly conserved across the catalytically active SULTs (Kakuta et al., 1998; Ong et al., 1999). The sulfonate transfer proceeds via an in-line attack by the substrate's nucleophilic acceptor group on the exposed sulfate of PAPS. This attack is facilitated in large part by the amino acid (AA) residue His 109, which deprotonates the substrate's acceptor hydroxyl group, allowing the exposed oxygen to make its nucleophilic attack. The importance of this residue is reinforced by the observation that mutation of His 109 renders the SULTs catalytically inactive (Kakuta et al., 1998). Lys 107 is only conserved across the SULT1 family and is thought to play a role in the reaction mechanism by acting in concert with His 109 to position the substrate nucleophile and stabilize the transition state of the sulfonate group being transferred (Teramoto et al., 2009). Lys 48 is also thought to facilitate the hydrolysis of the PAP-sulfonate bond by interacting with the nucleophilic oxygen on the phosphate of PAPS and stabilizing the transition state, while Ser 135 assists the hydrolysis of PAPS by modulating the position of Lys 48 (Pedersen et al., 2002; Teramoto et al., 2009). These residue interactions as well as the reaction transition state are represented in Figure 3.

The process of substrate and PAPS binding can occur one of two ways: either the substrate binds first, or PAPS binds first. In most cases, whether the substrate or PAPS binds first has little to no effect on the reaction kinetics. In some cases, however, kinetic studies have shown that the substrate will have a higher affinity for the PAPS-bound

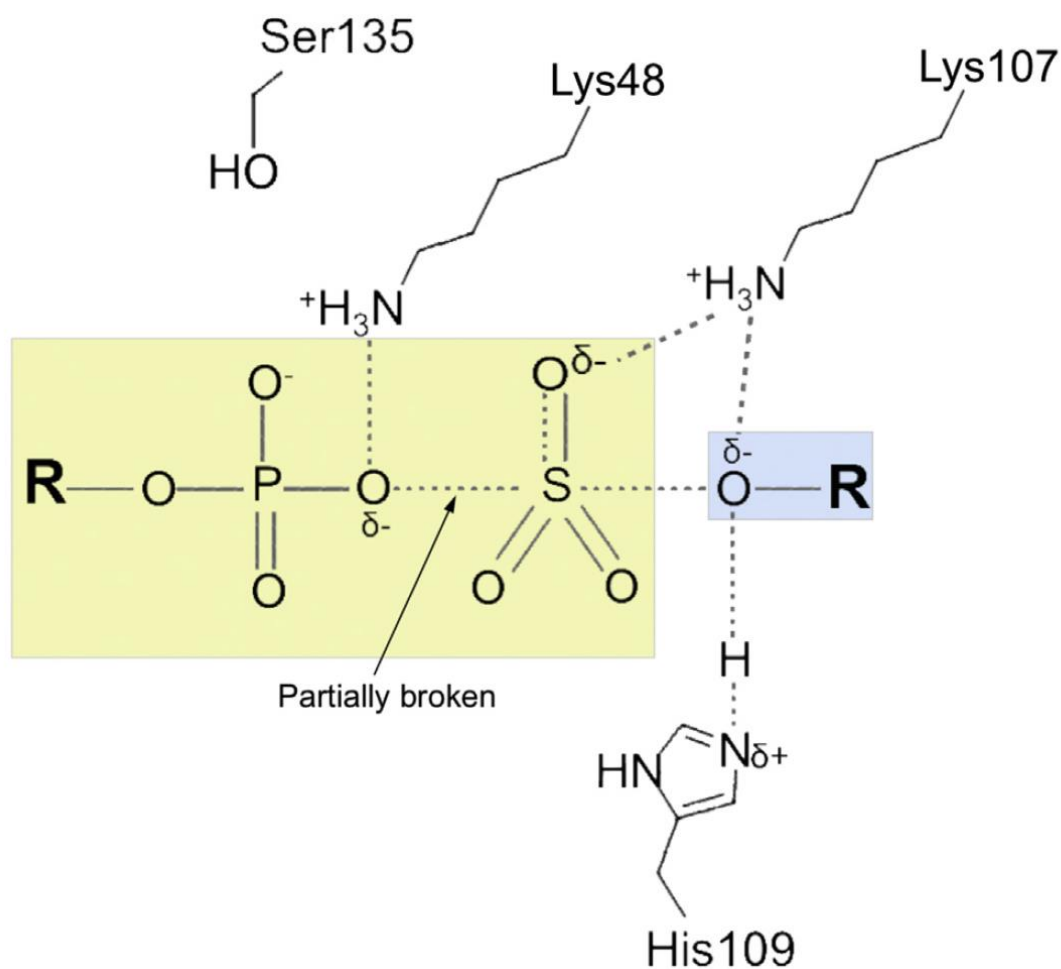


Figure 3. Reaction mechanism of sulfonate transfer with key residues. The blue highlight denotes the substrate; yellow represents the cofactor, PAPS. Residues are numbered according to their position on SULT1B1. The reaction proceeds via an attack from the nucleophilic O of the substrate on the S of PAPS. His 109 facilitates this by acting as a nucleophile and deprotonating the substrate hydroxyl group. Lys 107 assists in positioning the nucleophile and stabilizing the transition state. Lys 48 also assists in stabilizing the transition state, and its position is modulated by Ser 135.

enzyme. SULT1B1 has been shown to bind α -naphthol with higher affinity when PAP is already bound (Allali-Hassani et al., 2007). This can be explained by the observation that PAP/PAPS binding induces the constriction of the substrate binding pocket, giving the enzyme a higher affinity for small molecule substrates (Cook et al., 2013b; Cook et al., 2013c).

Structure/function Relationship

Several key structural features are conserved across all of the catalytically active SULTs. The core tertiary structure of the enzymes consists of a series of β -pleated sheets that make up the backbone of the proteins (Allali-Hassani et al., 2007). This rigid structure provides a foundation which confers stability to the protein. The surface of each protein has two openings: one that allows the substrate to enter and another that allows PAPS to enter. The PAPS binding pocket is highly conserved among the SULTs in its size, charge distribution, and positioning (Kakuta et al., 1998; Ong et al., 1999). Trp 53 and Arg 131, two conserved residues, facilitate the tight binding of PAPS while other residues such as Lys 48 facilitate the sulfonate transfer (Dong et al., 2012). The substrate binding pocket is less conserved than the PAPS binding pocket, which allows a wider variety of compounds to bind and be sulfonated. The substrate binding pocket is defined by three flexible loop regions in the SULT1 isoforms and two in the SULT2 isoforms (Tibbs et al., 2014). The loop known as loop 3 is comprised of residues Pro 238 through Thr 262 (in SULT1B1) and is especially important in regulating the substrate specificity of the SULTs (Cook et al., 2013a). This loop sits on the surface of the proteins and effectively forms a lid over the substrate binding pocket. Dynamic modeling has shown this

loop to be very flexible in the unbound protein. However, the lid stabilizes when the protein is bound to PAPS (Tibbs et al., 2014). This is why almost all of the more complete SULT crystal structures are co-crystallized with either PAPS or PAP. The only near-complete SULT crystal structure without either PAPS or PAP is SULT2A1 (Rehse et al., 2002). The stabilization of loop 3 induced by PAPS binding also has the effect of constricting the size of the substrate binding pocket by as much as 257 \AA^3 (Tibbs et al., 2014). Our lab has shown that this structural rearrangement can have significant effects on substrate specificity and reaction kinetics (Cook et al., 2010).

The SULTs exist *in vivo* as homodimers. This property of SULTs is imparted by the highly conserved dimerization domain with the sequence KxxxTVxxxE (Petrotchenko et al., 2001). The importance of this dimerization domain remains poorly understood, although its high level of conservation suggests an important purpose. Although many SULTs possess identical dimerization domains, no heterodimers have yet been reported.

Heterogeneity

Just as individual SULT isoforms share sequence homology with the other isoforms within their respective families, they also share a similar substrate affinity. Members of the SULT1 family typically have a higher affinity for phenolic compounds than do members of the SULT2 family, which typically have a higher affinity for 3β -hydroxysteroids (Glatt et al., 2001; Coughtrie, 2002). The catalytically active SULT isoforms can sulfonate a variety of different endogenous and exogenous compounds, summarized in Table 1. This table demonstrates the heterogeneity of the SULTs'

Table 1: The preferred substrates and tissue localizations of the human cytosolic SULTs

Isoform	Reactive Compounds	Endogenous	Exogenous	Tissue Localization
1A1	phenols, polyphenols	4-Methylphenol	oxymorphone	brain, GI, liver
1A2	phenols	-	naloxone	GI, liver
1A3	catecholamines	6-hydroxydopamine	hydromorphone	GI
1B1	phenols	3, 3',5-triiodothyronine	3-hydroxybenzo pyrene	GI, liver
1C2	phenols	-	p-nitrophenol	kidney, thyroid, GI
1C3	-	-	-	-
1C4	phenols, estrogens	2-hydroxy-E2	naloxone	kidney, ovary, spinal cord
1E1	estrogens	estrone	ethinyl estradiol	GI, liver
2A1	hydroxysteroids	dehydroepiandrosterone	butorphanol	GI, liver
2B1	3-beta-hydroxysteroids	dehydroepiandrosterone	-	prostate, placenta, skin
4A1	-	-	-	Brain, retina

substrate specificity, even among members of the same family or subfamily. For example, SULT1E1 is recognized as being a highly active estrogen SULT despite its classification in the SULT1 family. Similarly, SULT1A3 is classified in the SULT1A family based on global amino acid sequence similarity. However, SULT1A3 displays a higher affinity towards the monoamine neurotransmitters than the small phenolic compounds sulfated by SULT1A1 and SULT1A2. In studies considering only the small-molecule binding profiles of the human SULTs, SULT1A3 tends to cluster more with members of the SULT1C subfamily (Allali-Hassani et al., 2007).

The SULTs are expressed in a wide variety of tissue and cell types throughout the body, most notably in the GI tract and liver (Table 1). All three members of the SULT1A subfamily are expressed at various points in the GI tract while SULT1A1 and 1A3 also are expressed in the brain (Salman et al., 2009; Kurogi et al., 2013). SULT4A1, the subject of this dissertation, is also expressed in the brain, but as of yet no substrate or function has been identified for this orphan enzyme (Falany et al., 2000). Of the SULT1 family, the SULT1C subfamily has the most heterogeneous distribution with SULT1C2 expression in the adult kidney, thyroid, and GI tract (Her et al., 1997) and SULT1C4 expression in the adult kidney, ovary, and spinal cord (Sakakibara et al., 1998). Recent evidence suggests that the SULT1C subfamily also displays heterogeneity of expression over the course of human development. SULT1C2 expression has been observed in the fetal kidney and liver, but not in the adult liver (Stanley et al., 2005). Similarly, SULT1C4 is expressed widely throughout the fetus, particularly in the lung, kidney, and heart. By adulthood, however, the protein can no longer be detected in the lung or heart (Sakakibara et al., 1998). Most SULTs localize exclusively to the cytosol with one nota-

ble exception being SULT2B1b. This isoform, which is expressed in the skin, prostate, brain, and placenta (He et al., 2004; Higashi et al., 2004; Salman et al., 2011), has been shown to localize in the nucleus in the placenta in a manner that appears related to serine phosphorylation of the carboxy-terminal peptide (He et al., 2004; He and Falany, 2006).

The Orphan Enzyme SULT4A1

In 2000, our lab identified and cloned a novel SULT-like protein in cDNA libraries of the human and rat brain. It shared many sequence and structural homologies to the known SULTs, but researchers were unable to demonstrate any catalytic activity, earning it the name, “Brain Sulfotransferase-like” (Br-STL) (Falany et al., 2000). Br-STL was later renamed to SULT4A1 in accordance with the current standardized SULT nomenclature (Blanchard et al., 2004). This classification as a SULT was based upon sequence as well as structural similarities to the other SULTs, despite its apparent lack of catalytic activity. One characteristic that sets SULT4A1 apart from the other SULTs is its singular level of sequence conservation when compared to the other SULTs. It is the only member of the SULT gene family in humans which has not been reported to contain at least one exonic polymorphism (Hildebrandt et al., 2007). Furthermore, SULT4A1 has been identified in every vertebrate species investigated to date with exceptional AA sequence conservation. For example, zebrafish and humans, two species which share no other homologous SULTs, have SULT4A1 genes which are 87% identical and 92% similar in sequence (Figure 4) (Crittenden et al., 2014). Such a high level of conservation suggests an important conserved function, but as of yet a function that has not been identified.

```

hSULT4A1 MAESEAE TPSTPGEFESKYFEFHGVRLPPFCRGKMEEIANFPVRPSDVWI 50
zSULT4A1 MAESEVDTPSTPIEYESKYFEHHGVRLPPFCRGKMDEIANFSLRSSDIWI 50
***** . ***** * . ***** ***** . ***** . * ** . **

hSULT4A1 VTYPKSGT SLLQEVVYLV SQGADPDEIGLMNIDEQLPVLEYPQPGLDI IK 100
zSULT4A1 VTYPKSGT SLLQEVVYLV SQGADPDEIGLMNIDEQLPVLEYPQPGLLEII Q 100
***** . *****

hSULT4A1 ELTSPRLIKSH LPYRFLPSDLHNGDSKVIYMARNPKDLVVSYYQFHRSLR 150
zSULT4A1 ELTSPRLIKSH LPYRFLPSAMHNGEGKVIYMARNPKDLVVSYYQFHRSLR 150
***** . *****

hSULT4A1 TMSYRGTFQEFCCR FMNDKLG YGSWF EHVQEFWEHRMDSNVFLFLKYEDMH 200
zSULT4A1 TMSYRGTFQEFCCR FMNDKLG YGSWF EHVQEFWEHRMDSNVFLFLKYEDMY 200
*****

hSULT4A1 RDLVTMVEQLARFLGVSCDKAQLEALTEHCHQLVDQCCNAEALPVGRGRV 250
zSULT4A1 KDLGTLVEQLARFLGVSCDKAQLES LVESSNQLIEQCCNSEALSICRGRV 250
. ** . * . ***** . * * ** . ***** . *** . ****

hSULT4A1 GLWKDIFTVSMNEKFDLVYKQKMGKCDLTFDFYL 284
zSULT4A1 GLWKDVFTVSMNEKFDVIYRQKMAKSDLTFDFIL 284
***** . ***** . * . ***** *

```

Figure 4. Amino acid sequence homology between human and zebrafish SULT4A1. Sequences are 86.9% identical and 91.9% similar. Asterisks indicate conserved amino acids. Periods indicate a changed residue that maintains the same electrochemical properties. Key conserved features are highlighted in black and include the active site His (residue 111), the KXXFTVXXXE dimerization domain (residues 254-263), and the TYPKSGT PAPS binding domain (residues 52-58).

Note: From “Inhibition of SULT4A1 expression induces up-regulation of phototransduction gene expression in 72-hour postfertilization zebrafish larvae” by F. Crittenden, H. Thomas, C. M. Ethen, Z. L. Wu, D. Chen, T. M. Kraft, J. M. Parant, and C. N. Falany, 2014, *Drug Metabolism and Disposition*, 42, p. 947. Copyright 2014 by The American Society for Pharmacology and Experimental Therapeutics. Reprinted with permission.

Tissue Distribution and Expression Regulation

SULT4A1 is expressed extensively throughout the central nervous system (CNS) (Falany et al., 2000; Liyou et al., 2003). In humans and rats, immunohistochemical studies have shown it to have especially strong immunoreactivity in the neurons of the choroid plexus, cerebral cortex, cerebellum, thalamus, pituitary, medial temporal lobe, and lentiform nucleus (Liyou et al., 2003). SULT4A1 appears to have different levels of expression and subcellular localizations depending on where it is expressed within the CNS. In the cerebral cortex, especially strong expression was observed in the lamina 5 pyramidal neurons of the motor cortex. Throughout most of the brain, SULT4A1 was shown to localize mostly to the soma and dendrites of neurons. In the thalamus, punctate granular staining suggests a synaptic localization as well (Liyou et al., 2003). The reliability of these immunohistochemical studies, however, is suspect. Given the highly conserved nature of SULT4A1 among vertebrates, the protein is not highly immunogenic. As a result, most antibodies to SULT4A1 are not reliable. SULT4A1 is expressed in a number of glioblastoma cell lines as well including LN229 and U251, although it does not appear to be oncogenic (Sun et al., 2012). Its expression in these lines can be slightly induced by treatment with resveratrol. Translation of SULT4A1 appears to be driven by the transcription factors cAMP-responsive element binding protein (CREB) and activating transcription factor-2 (ATF-2) and can be induced by μ -opioid stimulation (Butcher et al., 2010).

In mice, there appears to be disequilibrium of expression of SULT4A1 between adult males and females. In male mice, brain levels of SULT4A1 mRNA remained similar to female brain levels until the animals reached the age of 30 days. At this point,

mRNA levels in the female brain increased while those in the male brain remained relatively constant. As adults, female mice displayed 4-fold higher levels of SULT4A1 mRNA than their male counterparts (Alnouti and Klaassen, 2006).

There is conflicting evidence for expression of SULT4A1 outside the central nervous system. Although no SULT4A1 has been detected outside the CNS by northern or western blot analysis, partial transcripts have been detected throughout the body (Falany et al., 2000; Alnouti and Klaassen, 2006; Crittenden et al., 2014; Sidharthan et al., 2014). In humans, much of this is due to a splice variant which results in an additional exon between the sixth and seventh exons and a premature stop codon (Falany et al., 2000; Sidharthan et al., 2014). This splice variant has been detected by PCR in the human thymus, spleen, testis, prostate, placenta, ovaries, kidney, colon, and small intestine (Sidharthan et al., 2014).

Biochemical Properties of SULT4A1

Structurally, SULT4A1 shares many common features with the other SULTs. Comparison of the crystal structure to that of the other SULTs reveals a remarkable conservation of structures such as the β -sheet backbone, catalytic His, dimerization domain, and key amino acid residues necessary for the binding of PAPS (Figure 5). In fact, most of the resolved crystal structure of hSULT4A1 (1ZD1) (Allali-Hassani et al., 2007) lines up very well with that of the catalytically active SULTs. Because of the conserved dimerization domain, SULT4A1 has been shown to exist as a homodimer *in vitro* (Sidharthan et al., 2014).

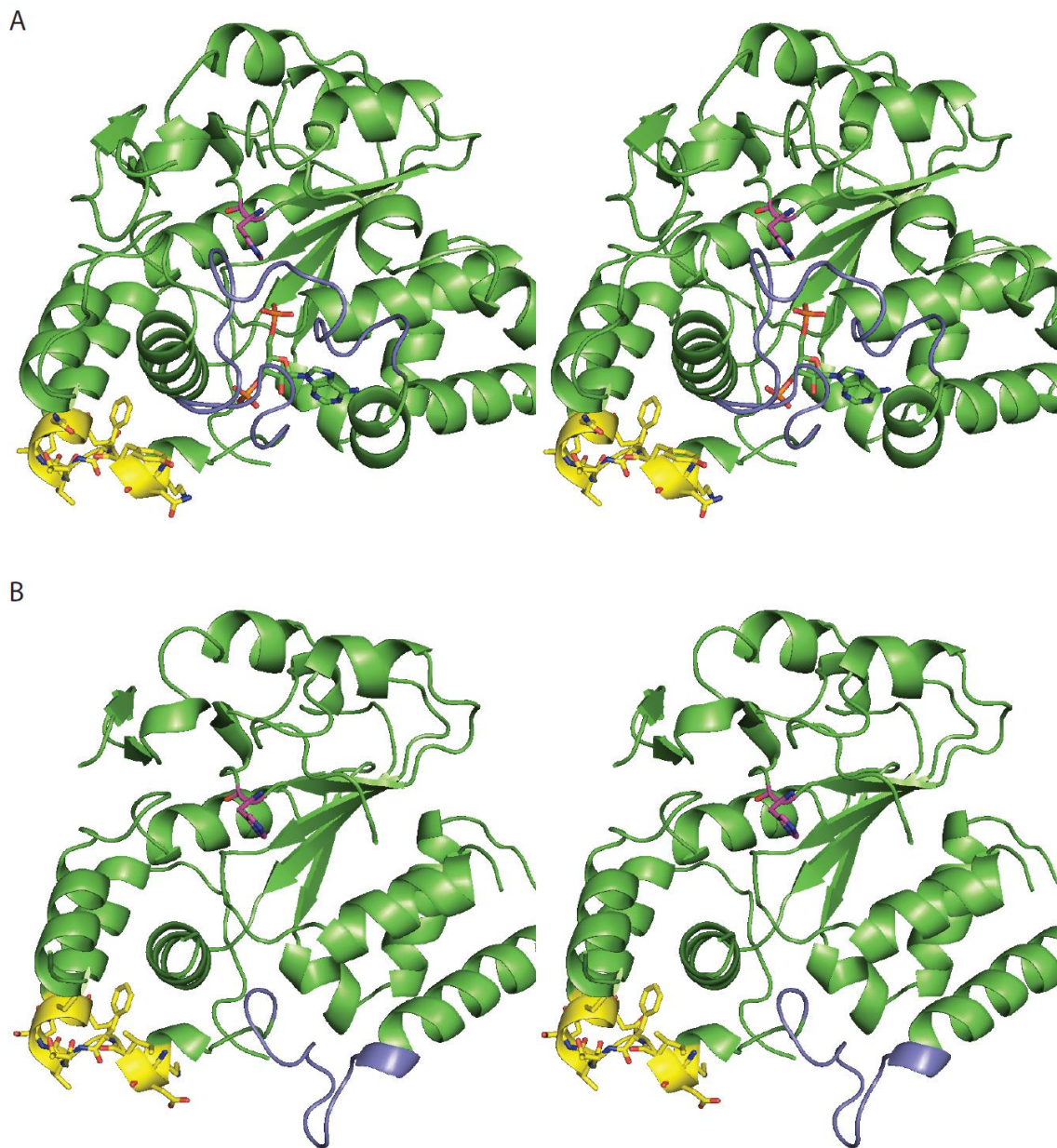


Figure 5. Stereoscopic view of SULT1B1 and SULT4A1. (A) SULT1B1 (2Z5F) and (B) SULT4A1 (1ZD1). Important conserved domains are colored as follows: dimerization domain (yellow), loop 3 (blue), and active site histidine (magenta). SULT1B1 is pictured here with PAP (green, blue, and orange) bound.

Unlike the other SULTs, SULT4A1 has a demonstrated inability to bind the co-factor, PAPS (Allali-Hassani et al., 2007). This inability is likely due to one of the few prominent structural differences between SULT4A1 and the other SULTs. The sequence spanning from Gln 236 to Gly 248, known as “loop 3” in the SULTs, is substantially shorter in SULT4A1 than in the other SULTs (Figure 5). In the catalytically active SULTs, this loop is 24 residues long and effectively forms a lid over the substrate binding pocket. Variations in the sequence of this loop are responsible for much of the variation in substrate specificity seen in the SULTs (Cook et al., 2013a). Loop 3 is very flexible, and has only been fully resolved in the crystal structure of the active SULTs when bound to either PAP or PAPS (Tibbs et al., 2014). In SULT4A1, however, loop 3 is much shorter (only 13 amino acids) and relatively more rigid. The only available crystal structure for SULT4A1 has many unresolved sequences, but loop 3 did fully resolve despite the fact that the protein was not co-crystallized with PAP or PAPS. The positioning of loop 3 in the crystal structure may help explain why SULT4A1 has no demonstrable catalytic activity. Rather than extending out across the substrate binding pocket, as in the other SULTs, loop 3 of SULT4A1 is shortened and pulled away from the active site and actually resides in the same physical space where PAPS has been shown to bind to the other SULTs (Figure 6). The “TYPKXGT” PAPS binding domain (Kakuta et al., 1998; Pedersen et al., 2002) is conserved in SULT4A1. However, a key conserved Tyr residue which has been shown to stack with the adenosine ring of PAPS in the other SULTs (Allali-Hassani et al., 2007) is substituted for a Leu residue in SULT4A1 (amino acid 60, Figure 4). Taken together, these differences between SULT4A1 and the other SULTs

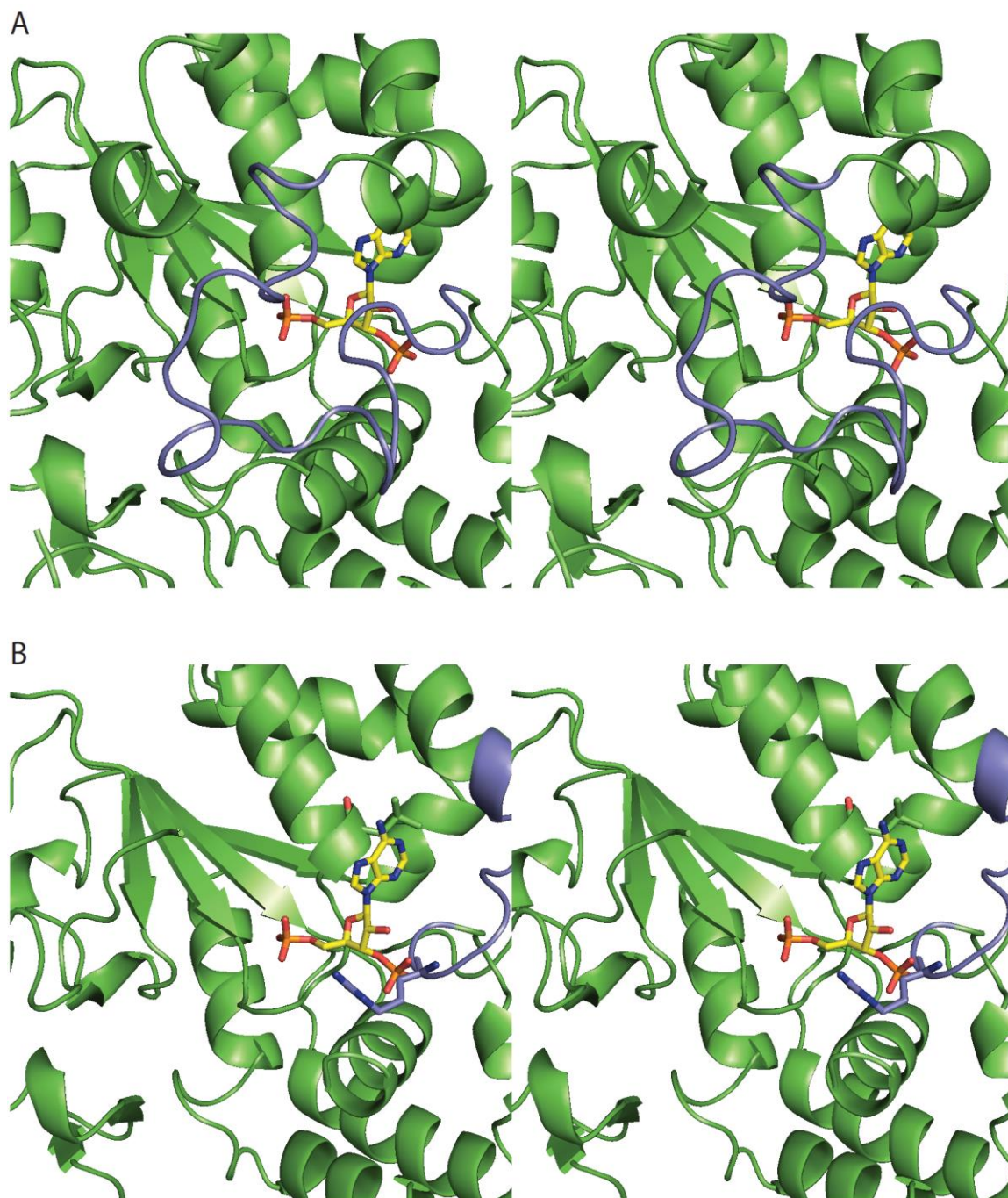


Figure 6. Stereoscopic view of PAPS binding site in SULT1B1 and SULT4A1. Human SULT1B1 (2Z5F) and SULT4A1 (1ZD1) crystal structures were aligned in PyMOL™. (A) SULT1B1 with co-crystallized PAPS (yellow). Loop three (blue) stretches out over the substrate binding pocket from the PAPS binding pocket. (B) SULT4A1 crystal structure showing steric clashing between the 3' phosphate of PAPS and R274 on the shortened loop 3 of SULT4A1.

help explain why SULT4A1 apparently does not bind the obligate donor, PAPS, and hence cannot catalyze the sulfonation of any substrates by itself.

Another result of SULT4A1's shortened loop 3 is that the putative substrate binding pocket is more open to solvent than is the case with the other SULTs (Figure 7). It is possible that another protein could be required to bind and effectively close off the active site before SULT4A1 can exhibit any activity. Several studies have been conducted in recent years to identify a binding partner. One report published in 2009 implicated peptidyl-prolyl cis/trans isomerase (Pin1) as a binding partner of SULT4A1 (Mitchell and Minchin, 2009). Pin1 is a proline isomerase thought to be involved in the regulation of mitosis that has been shown to localize to the cytoplasm and nuclei of CNS neurons in humans (Lu et al., 1996). Pin1 binding appears to be dependent upon phosphorylation of Ser/Thr-Pro motifs on the target protein, indicating that such motifs on SULT4A1 would also need to be phosphorylated for such an interaction to occur (Yaffe et al., 1997). One study demonstrated that SULT4A1 is indeed phosphorylated at Thr 11 by extracellular signal-regulated kinase1 (ERK1) and dephosphorylated by protein phosphatase 2A (PP2A) in SULT4A1 transfected HeLa cells, although this has not been demonstrated to occur in cells which endogenously express SULT4A1 (Mitchell et al., 2011).

Psychopathology

In recent years, SULT4A1 has been implicated in a number of pathological states, most notably schizophrenia (Brennan and Condra, 2005; Condra et al., 2007; Meltzer et al., 2008; Disciglio et al., 2014). The SULT4A1 gene resides in chromosome 22 (22q13.3), a region which has been linked to schizophrenia susceptibility

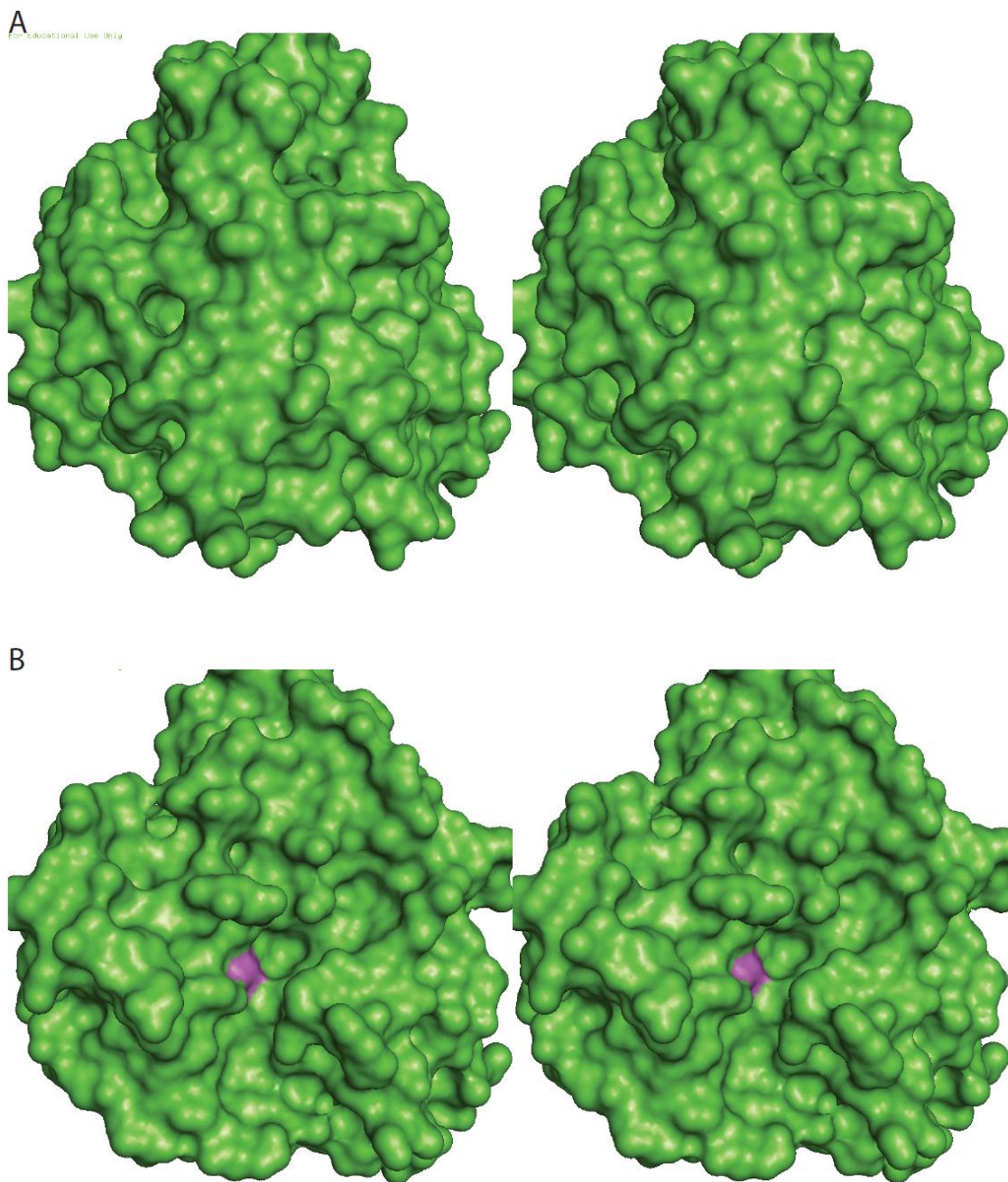


Figure 7. Stereoscopic view of a surface model of SULT4A1. (A) A surface model of SULT1B1. The active site histidine is buried within the protein. (B) A surface model of SULT4A1. The active site histidine (magenta) can be seen from the surface of the protein and is open to the solvent.

(Vallada et al., 1995; Jorgensen et al., 2002; Mowry et al., 2004). As early as 2005, a haplotype (SULT4A1-1) of polymorphisms in the 5' untranslated region (UTR) of the gene was implicated as a possible biomarker for genetic predisposition for schizophrenia (Brennan and Condra, 2005; Condra et al., 2007). The polymorphisms are non-coding and do not overlap any known promoter region. As of yet, no evidence has been published that demonstrates any decreased level of SULT4A1 expression in schizophrenic individuals who harbor this haplotype. Patients with the SULT4A1-1 haplotype have also been shown to have an increased responsiveness to the antipsychotic drug olanzapine as well as a higher baseline psychopathology (Ramsey et al., 2011; Ramsey et al., 2014). Patients with this haplotype who were treated with antipsychotics were also shown to have fewer hospitalization events than patients without the haplotype (Liu et al., 2012). Two single-nucleotide polymorphisms have been identified in the introns of the human SULT4A1 gene (Meltzer et al., 2008). Patients heterozygous for one of the SNPs were shown to have significantly more severe clinical symptoms of schizophrenia, while patients heterozygous for the other SNP performed worse during neuropsychological testing, particularly on tests of working memory. It should be noted, however, that there have not been any exonic polymorphisms identified in the SULT4A1 genes of schizophrenic patients (Lewis and Minchin, 2009).

The 22q13 gene region is also implicated in the occurrence of certain neurological developmental disorders. Deletions in this region are well described and are believed to be the cause of the Phelan-McDermid syndrome. Phelan-McDermid syndrome is characterized by global developmental delay, severe neonatal hypotonia, intellectual impairment, and minor developmental abnormalities (Phelan and Rogers, 2011; Phelan and

McDermid, 2012). Over half of Phelan-McDermid patients demonstrate autistic behavior, resulting in its classification as a form of autism spectrum disorder (ASD) (Phelan and McDermid, 2012). Typically, Phelan-McDermid syndrome is most commonly attributed to the deletion of the gene encoding the protein, SH3 and multiple ankyrin repeat domains 3 (SHANK3) (Luciani et al., 2003; Wilson et al., 2003; Bonaglia et al., 2011). SHANK3 also resides in the 22q13 gene region, just 6.8 megabase pairs (Mbp) from SULT4A1. In 2014, Disciglio *et al* reported on a new contiguous gene syndrome in patients with 22q13 deletions which did *not* involve SHANK3 (Disciglio et al., 2014). Symptoms in these patients included developmental delay, speech delay, hypotonia, autism, and dysmorphic physical features, most notably in the face, hands, and feet. The minimal deleted region in these patients included SULT4A1, implicating it as a candidate gene for the major neurological features of this syndrome.

Specific Aims

Zebrafish as a Model Organism for the Study of SULT4A1

The purpose of this study was to investigate the phenotypic effects of SULT4A1 expression deficiency as a means to gain insight into the molecular function of this protein. Given SULT4A1's implications in both schizophrenia and the 22q13 deletion syndrome described above, it could be reasonably expected that a phenotype would manifest as any one of a number of developmental, social, cognitive, or otherwise behavioral deficits. The ideal model organism for such a study would thus requisitely meet the following criteria: 1) possess a SULT4A1 gene with a high level of homology to that of the human gene, 2) easy manipulation of gene expression, and 3) the ability to conduct a variety of

behavioral tests. As is common among vertebrates, zebrafish SULT4A1 (zfSULT4A1) displays extensive homology with human SULT4A1 (hSULT4A1). The two proteins share primary sequences that are 87% identical and 92% similar, making zebrafish a suitable model organism for the study of SULT4A1 (Table 2). To date, 16 SULT genes have been identified in zebrafish, although zfSULT4A1 is the only SULT with sufficient homology to be identified as homologous to its human counterpart (Liu et al., 2010). Given the extensive homology between zfSULT4A1 and hSULT4A1, we believe that any insight gained into the role of SULT4A1 within the zebrafish nervous system will enhance our understanding of the physiological properties of the protein within the human nervous system.

Another characteristic of zebrafish that makes them well-suited for use in this and other studies is the ease with which a protein's expression can be selectively suppressed. At the transcriptional level, morpholino oligonucleotides (MOs) can be used to suppress gene expression in larval zebrafish for the first several days of development. MOs are short (usually about 25 base pair) oligonucleotides comprised of nucleic acids with modified bases. The backbones of these MOs are comprised of morpholine rings instead of ribose or deoxyribose rings, and the linkages are non-ionic phosphorodiamidate groups instead of anionic phosphodiester bonds (Summerton and Weller, 1997). These oligonucleotides can be injected into a zebrafish embryo at the one or two cell stage and prevent gene expression by binding to a complimentary strand of mRNA and either blocking splicing or blocking translation (Nasevicius and Ekker, 2000; Draper et al., 2001; Heasman, 2002; Deas et al., 2007).

Table 2: Sequence homology of SULT4A1 across different vertebrate species

Species	Total AA	AA Changed	% Identical	Similar AA	% Similar
Human (CAG30474)	284				
Rabbit (NP_001076173)	284	4	98.59	2	99.3
Rat (NP_113829)	284	6	97.89	4	98.59
Finch (NP_001232743)	284	16	94.37	7	97.54
Frog (NP_001087553)	284	31	89.08	18	93.66
Zebrafish (NP_001035334)	284	37	86.97	23	91.9

AA changed denotes the number of amino acid residues that differ from the human isoform of SULT4A1. Similar AA denotes the number of amino acid residues that differ from the human isoform of SULT4A1, but maintain the same electrochemical properties. Numbers in parentheses indicate GenBank accession number.

Note: From “Inhibition of SULT4A1 expression induces up-regulation of phototransduction gene expression in 72-hour postfertilization zebrafish larvae” by F. Crittenden, H. Thomas, C. M. Ethen, Z. L. Wu, D. Chen, T. M. Kraft, J. M. Parant, and C. N. Falany, 2014, *Drug Metabolism and Disposition*, 42, p. 947. Copyright 2014 by The American Society for Pharmacology and Experimental Therapeutics. Reprinted with permission.

While MOs are a useful tool to knockdown gene expression over a short period of time, recent advances in genomic editing technology have enabled researchers to rapidly generate heritable mutations in the zebrafish genome. One such advance utilizes transcription activator-like effector nucleases (TALENs). Identified in *Xanthomonas* bacteria, transcription activator-like effector (TALE) proteins contain a novel DNA binding motif that can be used to create DNA binding peptides that bind to highly specific sequences in the genome (Boch et al., 2009; Moscou and Bogdanove, 2009; Bogdanove and Voytas, 2011; Miller et al., 2011). By coupling them to the endonuclease FokI, researchers can use TALENs to induce double stranded breaks in the genomic DNA at specific loci (Christian et al., 2010; Miller et al., 2011). In addition to TALEN technology, a system for generating mutations has been developed which utilizes clustered, regularly interspaced, short palindromic repeats (CRISPR) system (Cong et al., 2013). The CRISPR system utilizes RNA-guided Cas9 nucleases with customizable specificities to target specific genomic loci.

Because a portion of this project calls for the monitoring of *SULT4A1* mutants for abnormal behavior, a suitable model organism would exhibit robust, quantifiable behaviors that would provide insight into a wide range of areas including, but not limited to, anxiety, cognition, activity levels, and social behaviors. Zebrafish are quickly rising in popularity as a model organism for investigating pathological behaviors (Best and Alderton, 2008; Norton and Bally-Cuif, 2010; Stewart et al., 2011) as well as modeling complex brain disorders (Miller and Gerlai, 2007; Kalueff et al., 2014; Stewart et al., 2014). The field of zebrafish behavioral analysis is currently seeing rapid advancement and characterization of social, sexual, sleep, anxiety-related, sensory, reward-seeking,

and cognitive behaviors (Kalueff et al., 2013). Much of the neuroanatomy and neurophysiology is conserved among zebrafish and mammals (Panula et al., 2006; Panula et al., 2010), justifying their use as a model organism for the study of certain behavioral paradigms. Our long term goal for this project is to characterize the physiological role of SULT4A1 within the vertebrate nervous system. We hypothesize that (1) inhibition of SULT4A1 expression by TALEN knockout or MO knockdown will impair the normal development of zebrafish larvae and will affect normal gene expression and (2) inhibition of normal SULT4A1 expression in zebrafish will result in one or more abnormal behavioral phenotypes.

The following specific aims were proposed to investigate the role of SULT4A1 in the zebrafish nervous system:

Aim 1: To characterize the effects of SULT4A1 expression deficiency on development and gene expression in larval and adult zebrafish. The objective of this aim was to investigate the potential developmental and gene expression abnormalities in SULT4A1 deficient zebrafish. Because of the extraordinary conservation of SULT4A1 and its early onset of expression, it was hypothesized that zebrafish with a mutated SULT4A1 gene or suppressed SULT4A1 expression would exhibit gross developmental or morphological abnormalities that would then provide insight into the physiological function of SULT4A1. Similarly, it was hypothesized that changes in gene expression would be observable through quantitative sequencing of the transcriptome (RNA-seq). A common belief among investigators of SULT4A1 is that the protein may act in concert with another protein or binding partner to effect its physiological function (Falany et al.,

2000; Minchin et al., 2008; Mitchell and Minchin, 2009; Mitchell et al., 2011; Crittenden et al., 2014). The intention of this aim was to identify changes in gene expression which would then provide insight into possible protein or pathway interactions of SULT4A1.

Aim 2: To analyze SULT4A1 mutants for behavioral phenotypes. Total RNA sequencing of 72 h post fertilization (hpf) control and knockdown zebrafish larvae has revealed a large number of proteins involved in phototransduction are up-regulated in SULT4A1 knockdown larvae. This, in addition to mounting evidence linking SULT4A1 polymorphisms with schizophrenia and ASD (Brennan and Condra, 2005; Condra et al., 2007; Meltzer et al., 2008; Disciglio et al., 2014), led us to hypothesize that SULT4A1 deficiency in zebrafish would lead to quantifiable changes in behavior. The objective of this aim was to determine if SULT4A1 deficiency resulted in sufficient neural dysfunction to effect quantifiable behavioral changes that could then provide insight into the role that SULT4A1 plays in the vertebrate nervous system.

Aim 3: To analyze the biochemical properties of SULT4A1. The objective of this aim was to identify a substrate, function, or protein binding partner for SULT4A1. Since its identification and cloning in 2000 by Falany et al, multiple labs have attempted and failed to identify a substrate for SULT4A1 (Falany et al., 2000; Allali-Hassani et al., 2007). Because multiple labs have been unable to identify a substrate for SULT4A1, it is conceivable that it may not be an enzyme. If such is the case, it is possible that the protein may bind in vivo with another protein in order to carry out its physiological function. In

this aim, we attempted to utilize methods including mass spectrometry metabolomics and co-immunoprecipitation to biochemically characterize SULT4A1.

CHAPTER 2

METHODS

Zebrafish Lines and Maintenance

Tubingen and AB strain zebrafish were housed in a recirculation aquaria system (Aquaneering Inc., San Diego, CA) in the UAB Zebrafish Research Facility. Light cycle was maintained at 14h light/10h dark. All animals were cared for in accordance with the guidelines set forth by the Institutional Animal Care and Use Committee of the University of Alabama at Birmingham.

Lysate Collection

Lysate was prepared from adult zebrafish brain, eye, intestine, liver, and testes as well as 72 hpf zebrafish knockdown (KD) and control embryos. Zebrafish were euthanized in ice water immediately prior to dissections. Samples were dissected and placed in sterile phosphate-buffered saline (PBS) with Complete Mini EDTA-free Protease Inhibitor Cocktail Tablets (Roche, Basel, Switzerland) and Phosphatase Inhibitor Cocktail 2 (Sigma-Aldrich, St. Louis, MO). Samples were disrupted by pipetting, shaken vigorously for 5 min at 4°C using a Vortex Genie 2™ (Thermo Fisher, Carlsbad, CA), and sonicated twice for 10 s with 30 s cooling on ice between sonications. The cycle of pipetting, vortexing, and sonicating was repeated, and lysate was collected by centrifugation at 15,000

x g for 20 min at 4°C. Lysate protein concentration was determined using a Bio-Rad protein assay and gamma-globulin standards.

Bradford Analysis of Protein Concentrations

For each protein concentration assay, a standard curve was created using a solution of gamma-globulin of known concentration (Bio-Rad, Hercules, CA). The following concentrations were used in each standard curve: 0 mg/mL, 1 mg/mL, 2 mg/mL, 5 mg/mL, and 10 mg/mL. A total of 1 μ L of each concentration as well as 1 μ L of unknown protein solution were loaded into separate test tubes. A volume of 1 mL of Bio-Rad Protein Assay Dye Reagent was added to each tube. Tubes were gently vortexed and incubated at room temperature for 5 min, then absorption at 595 nm (A_{595}) was measured for each sample on a Spectronic 601 Spectrophotometer (Milton Roy, Ivyland, PA). Standard curve measurements were plotted in Excel, and the Excel-generated trendline was used to determine protein concentrations in the unknown samples.

Trendline formula: $y = mx + b$

$y = A_{595}$ at protein concentration x mg/mL

m = slope (determined by Excel)

x = protein concentration (mg/mL)

b = y intercept (determined by Excel)

SULT4A1 Protein Expression Knockdown by Morpholino Injection

MOs (Gene Tools, LLC., Philomath, OR) were designed to target the splice donor sites of exon 1 of the SULT4A1 transcript (SULT4A1 MO, 5'-TAATGCACGCGATTGAATACCTGAT-3') (Figure 8). This results in the inclusion of intron 1 in the transcript and an in-frame premature stop codon 382 bases downstream from the translation start site. MOs were reconstituted in deionized water and diluted to a working concentration of 1.64 mM. Embryos were collected from natural matings and injected using a Harvard Apparatus PLI-100 injection system at the one or two cell stage with 0.82 pmol of either SULT4A1 MO or a standard control MO (SCM, Gene Tools). Effectiveness of KD was verified by quantitative PCR (qPCR) using TaqMan Gene Expression Assays (Life Technologies, Carlsbad, CA) and by immunoblot analysis. Zebrafish embryos injected with SULT4A1 MO and SCM were observed for gross morphological phenotype changes at 48, 72, and 120 hpf. At each time point, 10 SCM and 10 SULT4A1 MO embryos were selected at random and assessed for the development of heart, ears, eyes, circulatory system, and swim bladder.

Immunoblot Analysis

Protein samples were diluted 1:1 in 2x Laemmli sample buffer (100 mM Tris-Cl (pH 6.8), 2% SDS, 20% glycerol, 4% β -mercaptoethanol), and diluted protein samples were heated at 95°C for 3 min to denature protein. Acrylamide gels (10%) for protein electrophoresis were created by combining 4.85 mL H₂O, 2.5 mL 40% acrylamide, 2.5 mL 1.5 M Tris/SDS, 5 μ L TEMED, and 50 μ L 10% ammonium persulfate. A 5% acrylamide gel was used as a stacking gel. Samples were loaded into the 10% acrylamide



Figure 8: MO targeting of zSULT4A1 gene. The SULT41 MO was designed to target the junction of Intron 1 and Exon 1. Red: MO sequence. Black: Intron 1 sequence. Green: Exon 1 sequence. Asterisks indicate hydrogen bonding between MO nucleotides and mRNA nucleotides.

gel in a BIO-RAD Mini Trans-Blot® Cell and run at 80-160 V until blue dye reaches the bottom of the gel. Running buffer: 0.3% tris, 1.44 % glycine, 0.1% SDS. Protein was transferred onto a nitrocellulose membrane (pore size: 0.45 µm) using a BIO-RAD Trans-Blot® SD Semi-Dry Transfer Cell run at 11 V for 30 min. Transfer buffer: 48mM tris, 39 mM glycine, 20% methanol, pH 9.2. After transfer, nitrocellulose membrane was removed and allowed to dry briefly on a piece of filter paper. Membrane was blocked for 1 h at room temperature in 5% milk in Tris-buffered saline (TBS: 0.8% NaCl, 0.02% KCl, 0.3% Tris, pH 7.4). Membrane was then rinsed 3 times and stored overnight in Tween-TBS (T-TBS: 0.8% NaCl, 0.02% KCl, 0.3% Tris, 0.0005% Tween 20, pH 7.4).

Antibody solution was created by adding 200 µL blocking solution to 9.8 mL T-TBS to make 0.1% milk/T-TBS. Primary antibody was added, and membrane was incubated at room temperature in this solution for 2 h. Primary antibody solution was poured off and membrane was rinsed 3 times for 5 min each in T-TBS. Secondary antibody solution was prepared in the same manner as primary solution, and membrane was incubated at room temperature in secondary antibody solution for 1 h. Membrane was washed again 3 times in T-TBS for 5 min each. For visualization of immunoreactive bands, membranes were incubated for 5 min in SuperSignal® West Pico Chemiluminescent Substrate (Thermo Scientific, Carlsbad, CA) and developed by exposure to x-ray film.

RNA Isolation and Quantification

Tissue samples or zebrafish larvae were placed in 1 mL STAT-60 (Tel-Test, Friendswood, TX) and homogenized by repeated pipetting, then capped samples were incubated at room temperature for 5 min. A total of 200 µL chloroform was added to

each sample, and samples were vortexed for 15 s then incubated at room temperature for 3 min. Samples were centrifuged at 12,000 g for 15 min. Colorless top layer was pipetted into a fresh 1.5 mL microcentrifuge tube, and 500 μ L isopropanol added. Samples were vortexed and incubated at room temperature for 10 min, then centrifuged at 12,000 g for 10 min to precipitate RNA as a white pellet. The supernate was discarded, and 1 mL 75% EtOH added. Samples were vortexed and centrifuged for 5 min at 7,500 g. Excess EtOH was decanted, and RNA pellet was allowed to dry before re-hydrating in 100 μ L DEPC-treated water (Fisher Scientific). RNA concentration was quantified using a NanoDrop® ND-1000 spectrophotometer. RNA concentration was calculated using the following formula: $[\text{RNA}] = \text{OD}_{260} * 40 \text{ ng}/\mu\text{L}$.

Reverse Transcription of RNA

Reverse transcription of RNA to generate cDNA was carried out using SuperScript™ II Reverse Transcriptase (Invitrogen, Carlsbad, CA) according to the manufacturer's protocol. For each reaction, 200 ng of template RNA was used. Primers used in each 20 μ L reaction were either 250 ng random primers (Invitrogen) or 500 ng oligo(dT)₁₂₋₁₈ (Invitrogen).

Quantitative Real-Time PCR

qPCR reactions were carried out in 384-well clear optical reaction plates (Applied Biosystems, Carlsbad, CA) using TaqMan® Real-Time PCR Assays (Life Technologies) with an Applied Biosystems™ 7900HT Sequence Detection System. Each 15 μ L reaction contained 7.5 μ L TaqMan Master Mix, 5.75 μ L H₂O, 0.75 μ L TaqMan® assay pri-

mer/probe mix, and 1 μ L of SuperScriptTM-generated cDNA. Each reaction was carried out in triplicate. Samples were compared using the Δ Ct method, and p-values were determined using Student's t-test. Statistical significance was assumed if the p-value was less than 0.05.

RNA-Seq

Embryos injected with either SCM or SULT4A1 MO were separated into 4 groups of 15 embryos (2 SCM and 2 SULT4A1 MO). At 72 hpf, all 4 groups were sacrificed, and total RNA was isolated using STAT-60TM (Tel-Test). mRNA-sequencing was performed on an Illumina HiSeq2000 in the UAB Heflin Center for Genomic Sciences. Briefly, the quality of the total RNA was assessed using the Agilent 2100 Bioanalyzer followed by 2 rounds of polyA⁺ selection and conversion to cDNA. TruSeq library generation kits were used as per the manufacturer's instructions (Illumina, San Diego, CA). Library construction consisted of random fragmentation of the polyA⁺ mRNA followed by cDNA production using random primers. The ends of the cDNA were repaired, A-tailed, and adaptors ligated for indexing (up to 12 different barcodes per lane) during the sequencing runs. The cDNA libraries were quantitated using qPCR in a Roche Light-Cycler 480 with the Kapa Biosystems kit for library quantitation (Kapa Biosystems, Woburn, MA) prior to cluster generation. Clusters were generated to yield approximately 725K-825K clusters/mm². Cluster density and quality were determined during the run after the first base addition parameters were assessed.

The raw FASTQ files were aligned to the zebrafish reference genome (Zv9, Sanger Institute) following the workflow of the Galaxy instance installed at UAB

(<http://galaxy.uabgrid.uab.edu>). Pre-alignment was conducted to determine if trimming was needed based on reads quality score. The BAM files were generated following RNA-seq data analysis workflow of Tophat (Trapnell et al., 2009), Cufflinks, and Cuffcompare (Trapnell et al., 2010). These BAM files were loaded into Partek Genomics Suite 6.6 (Partek, Inc., Saint Louis, MO) for further statistical and functional analysis. Briefly, the reads per kilobase of exon model per million mapped reads (RPKM)-normalized reads (Mortazavi et al., 2008) were calculated and the expression levels of genes were estimated (Xing et al., 2006; Mortazavi et al., 2008; Wang et al., 2008). The differential expressions were determined by ANOVA as described in the vender user manual. A gene list was then created after false discovery rate (FDR) p-value correction using the Benjamini and Hochberg method (Benjamini and Hochberg, 1995). Further functional analysis was conducted using Ingenuity Pathway Analysis (IPA, Redwood City, CA).

Co-Immunoprecipitation of 6H-Flag-zfSULT4A1

Adding the Flag Tag

Primers were designed to amplify the zfSULT4A1 coding region with an additional Flag peptide tag (sequence: DYKDDDDK) on the carboxy terminus of the protein (forward: TCTTATCGATCGCATGGACTACAAGGACGACGATGACAAGGCGGAAAGCGAGGTGGACAC, reverse: ACTACTCGAGCTGCTTTACAGGATAAAGTC). Using these primers, the zfSULT4A1 coding region was amplified from zebrafish retina cDNA using Platinum Taq (Life Technologies) in four separate 25 μ L PCR reactions. All four reactions were combined and concentrated to 7 μ L using a DNA Clean &

Concentrator™ kit (Zymo Research, Irvine, CA). The concentrated PCR product was then blunted and ligated into pJET1.2 blunt cloning vector using a CloneJET™ PCR Cloning Kit (Fermentas, Carlsbad, CA). Following the ligation reaction, all 20 µL were transformed into Z-Competent™ *E. coli* (Zymo Research) and plated on Luria-Bertani (LB) Agar plates containing 0.1 mg/mL ampicillin. Following overnight incubation, DNA was isolated from bacteria colonies and sequenced in the Heflin sequencing core at UAB. A colony containing the correct Flag-tagged zfSULT4A1 coding region was selected and cultured, and mini preps of plasmid DNA were prepared from the culture.

Preparing the Flag-zfSULT4A1 Construct for Cloning into pPROEX Plasmid

The plasmid solutions containing Flag-tagged zfSULT4A1 were used as template DNA in Platinum Taq PCR reactions using primers designed to add an upstream NcoI restriction site as well as a downstream HindIII restriction site to the Flag-zfSULT4A1 insert (forward: TCGCATCCATGGACTACAAGGACGACGAT, reverse: ATCCCAA-GCTTGGCTC GAGCTGCTTTACAGG). The PCR product was concentrated using a DNA Clean & Concentrator™ kit, and the concentrated PCR product was then blunted and ligated into pJET1.2 blunt cloning vector using a CloneJET™ PCR Cloning Kit. The product of this ligation reaction was transformed into Z-Competent™ *E. coli* (Zymo Research) and plated on LB Agar plates containing 0.1 mg/mL ampicillin. Following overnight incubation, DNA was isolated from bacteria colonies and sequenced in the UAB Heflin sequencing core. A colony containing the correct Flag-tagged zfSULT4A1 coding region was selected and cultured, and plasmid DNA was isolated from the culture.

Ligation of Flag-zfSULT4A1 Construct into pPROEX Plasmid and Expression in BL21 E.coli

The plasmid solution containing Flag-tagged zfSULT4A1 with the correct restriction sites was digested using the restriction enzymes NcoI and HindIII and then ligated into the pPROEX expression vector. The product of this ligation reaction was then transformed into BL21 competent *E.coli* and plated on LB Agar plates containing 0.1 mg/mL ampicillin. Following overnight incubation, DNA was isolated from bacteria colonies and sequenced in the UAB Heflin sequencing core to verify correct sequence. The 6His-Flag-zfSULT4A1 construct encoded the 284 AA zfSULT4A1 protein with an N-terminal Flag-tag and a 6-histidine (6His) tag separated from the rest of the protein by a tobacco etch virus (TEV) protease cleavage site.

Purifying 6His-Flag-zfSULT4A1

BL21 *E.coli* carrying the 6His-Flag-zfSULT4A1 construct was grown in LB broth medium at 37°C to an A_{600} of 0.5 with 100 µg/ml ampicillin and 33 µg/ml chloramphenicol. Isopropyl β-D-thiogalactoside (IPTG) was then added to the culture at a final concentration of 0.3 mM to induce expression of the 6His-Flag-zfSULT4A1 protein. Cells were incubated for another 4 h with agitation at 37°C, then cell cultures were transferred to 500 mL plastic bottles and centrifuged for 30 min at 2,300xg. LB broth supernate was decanted, and cell pellets were resuspended in Ni column wash buffer (10 mM NaPO₄, 10% glycerol, 10 mM imidazole, 10 mM β-ME, 300 mM NaCl, pH 8.0) with 0.5 mM phenylmethanesulfonylfluoride (PMSF). To rupture cell membranes, cells were sonicated 6

times for 15 s with 30 s cooling on ice between each sonication. Cell lysate was then centrifuged for 15 min at 10,000xg at 4°C. The supernate was then passed over a HisPur™ Ni-NTA column (Fisher Scientific) at a rate of 1 mL/min. The column was washed with 15 bed volumes of Ni column wash buffer, and then protein was eluted with wash buffer containing 300 mM imidazole. The protein eluent was dialyzed against wash buffer containing 10 mM imidazole to remove excess imidazole.

Pulldown Phase 1 (Ni²⁺ Affinity)

Lysate was collected from adult zebrafish brain tissue, and protein concentration was determined to be 2.6 mg/mL by Bradford analysis. The zebrafish brain lysate was divided into two 3.5 mL samples named pulldown and control. A total of 200 µg 6H-Flag-zfSULT4A1 was added to the pulldown sample but not the control. Because of the relative abundance of exposed cysteine residues on the surface of SULT4A1, it was believed that an interaction between SULT4A1 and its purported binding partner could very likely involve disulfide bonding with these cysteine residues. With this possibility in mind, we endeavored to first break the putative disulfide bonds between endogenous SULT4A1 and its alleged binding partner by addition of 0.7 µL β-ME to both the control and pulldown samples. To then remove the β-ME and allow disulfide bonding to occur between the recombinant SULT4A1 bait protein and endogenous prey protein, both control and pulldown samples were then loaded onto 10 mL bed volume G-25 sephadex columns and spun at 1600 xg for 4 min. Effluent was collected, and samples were incubated with gentle agitation at 4°C for 1 h to allow binding of bait and prey protein. A volume of 100 µL Ni-NTA resin was added to each sample, and samples were incubated for 1 more

h. Control and pulldown slurries were loaded onto fresh Ni-NTA columns and washed with 15 bed volumes of Ni-NTA wash buffer *without* β -ME. Each sample was eluted with 1 mL Ni-NTA wash buffer with 200 mM imidazole and *no* β -ME. A volume of 1 μ L TEV protease was added to each sample, and samples were incubated overnight rocking at 4°C.

Pulldown Phase 2 (Flag Affinity Matrix Purification)

A 200 μ L aliquot of ANTI-FLAG M2® Affinity Gel was added to both the pull-down and control samples. Samples were incubated at 4°C for 2 h with gentle agitation. Samples were then centrifuged for 30s at 8,200 xg. Supernate was aspirated, and samples were gently resuspended in 1 mL TBS and centrifuged again for 30s at 8,200 xg. Samples were washed twice more in TBS. A solution of 3X FLAG® Peptide (Sigma, St. Louis, MO) was prepared to a final concentration of 150 ng/ μ L, and 0.5 mL of this solution was added to both the control and pulldown samples. Samples were incubated for 30 min at 4°C with gentle agitation and then centrifuged for 30s at 8,200 xg. The supernatant fractions were transferred to fresh microcentrifuge tubes and concentrated down to 30 μ L using Amicon 10 microconcentrators (EMD Millipore, Darmstadt, Germany).

SDS Gel Separation and MS/MS Analysis

Each sample was loaded onto 10% acrylamide gel and run until the dye reached the bottom of the gel. Gels were stained with SYPRO® Ruby Protein Gel Stain (Life Technologies). Mass spectrometry analysis was performed at the UAB Comprehensive Cancer Center Mass Spectrometry/Proteomics Shared Facility. Gel lanes corresponding

to control and pulldown samples were excised and equilibrated in 100 mM ammonium bicarbonate (AmBc). Gel slices were reduced, carbidomethylated, dehydrated, and digested with Trypsin Gold (Promega) as per manufacturers' instructions. Following digestion, peptides were extracted, concentrated under vacuum, and resolubilized in 0.1% formic acid prior to analysis by 1D reverse phase LC-ESI-MS2 as outlined below.

Peptide digests were injected (in duplicate) onto a Surveyor HPLC plus (Thermo Scientific) using a split flow configuration on the back end of a 100 micron I.D. x 13 cm pulled tip C-18 column (Jupiter C-18 300 Å, 5 micron, Phenomenex). This system runs in-line with a Thermo Orbitrap Velos Pro hybrid mass spectrometer, equipped with a nano-electrospray source (Thermo Scientific, San Jose CA), and all data were collected in CID mode. Peptide fractions were directly sprayed into the mass spectrometer over a 90 minute gradient set to increase from 0%-30% acetonitrile in D.I. H₂O containing 0.1% formic acid and with a flow rate of 0.3µl/min. Following each parent ion scan, fragmentation data were collected on the top most intense 18 ions. Prior to and following the analysis window, the spray voltage was set to 0.0kV and the flow rate was set at 3µl/min. During data collection, the instrument was configured as follows: spray voltage 1.9kV, capillary temperature 170°C, 1 microscan with a maximum inject time of 25ms for all modes. The fragmentation scans were obtained at 60K resolution with a minimum signal threshold of 2000 counts. The activation settings were set to charge state 3, isolation width 2.0m/z, normalized collision energy 30.0, activation Q 0.250, and activation time 25ms. For the dependent scans, charge state screening was enabled, and the dynamic exclusion was enabled with the following settings: repeat count 2, repeat duration 15.0s, exclusion list size 500, and exclusion duration 60.0s.

The XCalibur RAW files were collected in profile mode, centroided and converted to MzXML using ReAdW v. 3.5.1. The mgf files were then created using MzXML2Search (included in TPP v. 3.5) for all scans with a precursor mass between 350Da and 2,000Da. The data was searched using SEQUEST, which was set for three maximum missed cleavages, a precursor mass window of 20ppm, trypsin digestion, variable modification C at 57.0293, and M at 15.9949. For the fragment-ion mass tolerance, 0.0Da was used. Searches were performed with a species specific subset of the UniRef100 database, which included common contaminants such as digestion enzymes and human keratin, in addition to sequences specific to these experiments.

A list of peptide IDs were generated based on SEQUEST search results, which were filtered using Scaffold (Protein Sciences). Scaffold was applied in order to filter and group all of the matching peptides to generate and retain only high confidence IDs while also generating normalized spectral counts (SC) across all samples for the purpose of relative quantification. The filter cut-off values were set with peptide length (>5 AA's), no peptides with a MH+1 charge state were included, peptide probabilities were calculated and set to >90% C.I., with the number of peptides per protein set at 2 or more, and protein probabilities were set to >97% C.I., which all combined results in a list of protein IDs with >99% confidence. Scaffold incorporates the two most common methods for statistical validation of large proteome datasets, the false discovery rate (FDR) and protein probability (Keller et al., 2002; Nesvizhskii et al., 2003; Weatherly et al., 2005).

DNA Gel Electrophoresis

Agarose gels (10%) were used for DNA electrophoresis. A total of 6 g agarose (Denville Scientific, Holliston, MA) was dissolved in 60 mL TAE buffer (0.48% Tris base, 0.114% glacial acetic acid, .001 M EDTA, pH 8) with one drop of concentrated ethidium bromide (Sigma). Gels were cast, and DNA samples were loaded into this gel and run at 80 V to separate DNA. DNA bands were visualized under ultraviolet light.

Immunohistochemistry of SULT4A1 in Rat Retinas

Preparing Eye Sections

Eyes were enucleated from euthanized adult Sprague-Dawley rats and placed into ice-cold 2% paraformaldehyde fixative (0.1 M NaHPO₄, 2% paraformaldehyde, pH 7.0). After 10 min, extraocular tissue was trimmed and cornea was removed. Eyes were placed back into the fixative solution and incubated overnight at 4°C. Eyes were placed into 0.1 M phosphate buffer (0.1 M NaHPO₄) for 1 h, then transferred to a 30% sucrose solution (0.1 M NaHPO₄, 0.88 M Sucrose). Eyes were left in the sucrose solution until they sank (~5 h). Eyes were then transferred into a cyrosection mold filled with HistoPrep™ Embedding Media (Fisher Scientific) and were allowed to infiltrate with embedding media for 1 h. After 1 h, eyes were oriented in the cyrosection mold and frozen at -20°C. Using a Leica CM3000 cryostat, 10 µm sections were sliced from the center of the eye.

Staining Eye Sections

Primary antibody used in this experiment was goat α:hSULT4A1 pAb (R&D Systems). Secondary antibody used was Alexa Fluor® 488 donkey α:goat IgG (Invitrogen).

Tissue slides were placed in a solution of acetone for 3 min to dissolve embedding media. Slides were removed from acetone and placed on a 50°C slide warmer for 1 h. A Pap Pen liquid blocker was used to draw an oval around the sections on each slide. A volume of 0.3 mL of blocking solution (20% donkey serum in PBS) was applied to each section and incubated for 1 h. Blocking solution was removed, and primary antibody solution (1:20 dilution in 2% donkey serum/PBS) was applied to the slides for 5 h. Primary antibody solution was removed, and slides were washed 3 times for 5 min in 2% donkey serum/PBS. After the third wash, secondary antibody solution (1:200 dilution in 2% donkey serum/PBS) was applied to the slides. Slides were incubated for 1 h. Slides were washed 3 times as before, and a 4',6-diamidino-2-phenylindole (DAPI) solution (1:1000 dilution in PBS) was applied to each slide. Slides were incubated at room temperature for 5 min and then rinsed 3 times in PBS. Cover slips were applied to the slides using Aqua Poly/Mount (Polysciences, Inc., Warrington, PA), and slides were held at 4°C until ready to be viewed. Slides were viewed on a Zeiss Axioplan 2 Imaging microscope.

Production of pAb to zfSULT4A1

Several antibodies against hSULT4A1 are commercially available. However these antibodies exhibit substantial non-specific cross-reactivity when used on zebrafish protein samples. For this reason, it was undertaken to generate an antibody specific to zfSULT4A1. A glycerol blot of *E.coli* strain XL1-Blue containing a plasmid encoding zfSULT4A1 was used for expression. The pMAL expression vector used applied a maltose-binding protein (MBP) to N-terminus of the protein separated by a factor Xa endopeptidase recognition site. The glycerol blot was used to inoculate 1 L of LB broth con-

taining the appropriate antibodies. Culture was incubated in an orbital shaker at 37°C until it reached an A_{600} of 0.411. IPTG was then added to the culture at a final concentration of 0.3 mM to induce expression of the MBP-zfSULT4A1 protein. Cells were incubated for another 4 h under agitation at 37°C, then cell cultures were centrifuged for 20 min at 4,000xg. LB broth was decanted, and cells were resuspended in 20 mL amylose column buffer (20 mM Tris-Cl, 200 mM NaCl, 1 mM EDTA) with 0.5 mM PMSF. Cells were sonicated 6 times for 15 s with 30 s cooling on ice between sonication pulses. Cells were centrifuged at 10,000xg and 4°C for 15 min. Supernate was decanted and diluted 1:5 in amylose column buffer without PMSF, then run through a 3 mL column of amylose resin (New England Biolabs, Ipswich, MA) at a rate of 1 mL/min. Column was washed with 10 bed volumes of amylose column buffer, and protein was then eluted with column buffer containing 10 mM maltose. Fractions were collected every 1 mL, and relative protein concentrations of these fractions were determined by protein gel electrophoresis and coomassie staining. Fractions containing high concentrations of protein of the appropriate molecular size were pooled. Combined fractions were analyzed by Bradford analysis, and protein concentration was calculated to be 7.9 mg/mL. Purified protein was dialyzed against amylose column buffer without maltose. Spin-X® Centrifugal Concentrators (Corning Inc., Corning, NY) were used to concentrate protein down to 2 mL. Protein sample was loaded onto 8 separate 10% acrylamide gels and run at 100v to separate MBP from zfSULT4A1. Gels were lightly stained with coomassie, and 35 kDa bands were excised and combined. zfSULT4A1 was purified from gel bands by electro-elution using a Model 422 Electro-Eluter (Bio-Rad). The eluent fraction was concentrated to 2 mL using Amicon 10 microconcentrators, and protein purity was confirmed by acrylamide gel elec-

trophoresis and coomassie staining. Protein concentration for the purified sample was assessed by Bradford analysis to be ~ 0.5 mg/mL. To remove SDS from protein solution, 8 mL (4 volumes) of -20°C acetone was added to the protein solution, and solution was incubated for 2 h at -20°C. Sample was then centrifuged at 15,000 xg and -10°C for 10 min, and pellet was resuspended in 2 mL PBS. Protein sample was sent to Pacific Immunology (Ramona, CA) inoculation of a goat and antibody production.

Gel Filtration Chromatography of zfSULT4A1

The SULTs exist *in vivo* as homodimers (Petrotschenko et al., 2001; Weitzner et al., 2009). To determine if SULT4A1 also forms dimers, recombinant SULT4A1 was subjected to size exclusion chromatography. A 1m (length) x 16mm (diameter) Pharmacia column was packed with Pharmacia Sephadex G-100 resin (Sigma). Column was enclosed and connected to the Pharmacia AKTA-FPLC. A volume of 400 mL of enzyme buffer was pumped through the column at a rate of 0.4 mL/min to equilibrate the column. Using the same flow rate, Bio-Rad Gel Filtration Standards were injected onto the column according to manufacturer's protocol. The standards were monitored to ensure adequate separation and resolution. A UV-vis detection system was used to determine the peak elution time of each standard protein. Column was equilibrated with Ni-NTA wash buffer, and 1 mg of purified 6H-Flag-zfSULT4A1 was injected onto the column in the same manner as with the standards. Fractions were collected every 1 mL, starting the collection as the void volume was exiting the column. A UV-vis detector was used to assay the A_{595} of each fraction, and these data points were compared to the standard curve data to determine molecular weight (MW) of eluted protein.

Generation of SULT4A1 Mutant Zebrafish Using TALENs

TALEN Target Site Selection and Assembly

In order to generate heritable mutations in the SULT4A1 gene of zebrafish, TALENs were designed to target the zebrafish SULT4A1 gene. SULT4A1 gene exon sequences (GenBank Accession number: NP_001035334) were analyzed for potential TALEN targeting sites using the Old TALEN Targeter program at <https://talen.cac.cornell.edu/node/add/talen-old> (Cermak et al., 2011; Doyle et al., 2012; Thomas et al., 2014). TALEN targeting sites within the second exon were chosen with the following parameters: Left target sequence: ATTGATGAGCAGCTTCCAGT; Left repeat array sequence: NI, NG, NG, NN, NI, NG, NN, NI, NN, HD, NI, NN, HD, NG, NG, HD, HD, NI, NN, NG; Right target sequence: AGCCGGGATTGGAGATTATCC; Right repeat array sequence: NN, NN, NI, NG, NI, NI, NG, HD, NG, HD, HD, NI, NI, NG, HD, HD, HD, NN, NN, HD; spacer length: 14 nucleotides (Figure 9). Target sequences were analyzed via BLAST to ensure that no identical sequences exist in the zebrafish genome. The Golden Gate TALEN and TAL Effector Kit 2.0 was purchased from Addgene (Cambridge, MA), and TALE repeats were assembled as previously described in the Addgene protocol (Cermak et al., 2011). Briefly, the TALENs were constructed by combining the desired TAL repeat plasmids and performing several cycles of digestion and ligation. These recombined vectors were transformed into Mach1 chemically competent cells (Life Technologies) to obtain plasmids that could then be digested and ligated into TALEN expression vectors pCS2TAL3DD and pCS2TAL3RR (Dahlem et al., 2012). These plasmids contained the Tal constant region, golden gate cloning region and the left or

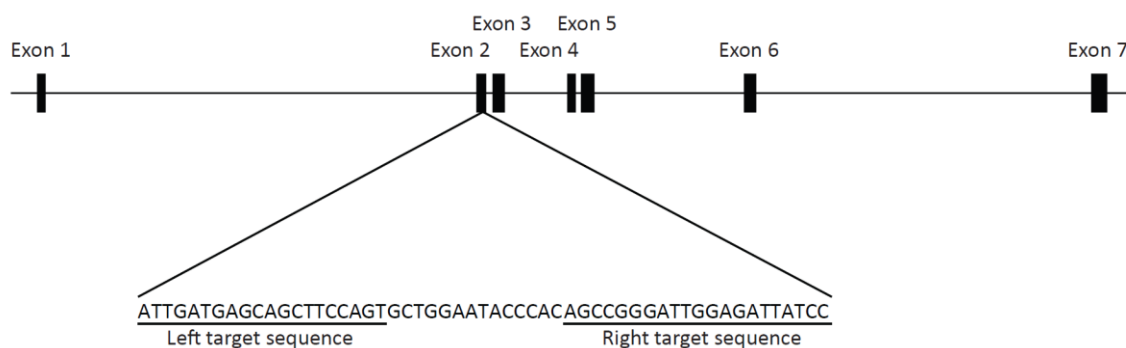


Figure 9: Schematic of the zebrafish SULT4A1 gene. Exons depicted as thick bars. Left and right TALEN target sequences within the second exon are underlined. Exon 1: 318 bp. Exon 2: 131 bp. Exon 3: 81 bp. Exon 4: 127 bp. Exon 5: 95 bp. Exon 6: 139 bp. Exon 7: 1,978 bp. Intron 1: 5,379 bp. Intron 2: 76 bp. Intron 3: 679 bp. Intron 4: 79 bp. Intron 5: 1,577 bp. Intron 6: 2,953 bp.

Note: From “Activity Suppression Behavior Phenotype in SULT4A1 Frameshift Mutant Zebrafish” by F. Crittenden, H. Thomas, J. M. Parant, and C. N. Falany, 2014, *Drug Metabolism and Disposition*, 43, p. 1037. Copyright 2015 by The American Society for Pharmacology and Experimental Therapeutics. Reprinted with permission.

right subunit of the FokI obligate heterodimer enzyme. Golden gate cloned plasmids were used for mRNA synthesis. TALEN mRNA was transcribed using the mMessage mMachine SP6 kit (Life Technologies) and purified using the RNeasy Kit (Qiagen, Venlo, Netherlands). RNA concentrations were quantified using a NanoDrop® ND-1000 spectrophotometer.

Microinjection of Zebrafish Embryos

AB strain one-cell stage embryos were collected from natural breedings, and TALEN mRNA was injected into the yolk of the embryos using a regulated air-pressure micro-injector (Harvard Apparatus, NY, model PL1-90). For TALEN mRNA injections, equal amounts of the Left and Right mRNAs were mixed to a final concentration of 100 ng/μL and injected at a volume of 0.5 nl into each embryo.

Extraction of Genomic DNA From TALEN Injected Embryos and Adult Mutant Zebrafish

TALEN injected embryos were placed into individual wells of a 96 well plate containing a solution of 95% embryo lysis buffer (ELB) (10 mM TRIS pH 8.3, 50 mM KCl, 0.3% Tween 20, 0.3% NP40) and 0.05 mg/ml proteinase K (Fisher Scientific). Embryos were incubated at 55° C overnight and the proteinase K then inactivated by incubation at 95° C for 10 min. The resultant solution was centrifuged at 2000xg for 1 min and used for subsequent high resolution melting analysis (HRMA). For extraction of DNA from adult fish, tail clippings were used in lieu of whole embryos.

Identification and Verification of SULT4A1 Mutant Zebrafish Lines

mRNA for the left and right TALENs was generated in vitro and injected into type AB zebrafish larvae at the one cell stage. This founder generation (F0) was raised to adulthood and screened for the presence of SULT4A1 mutations by HRMA (Parant et al., 2009; Dahlem et al., 2012; Thomas et al., 2014). Mutants in this founder generation were chimeric with the potential for multiple mutations. In order to isolate singular mutations, F0 fish were crossed with WT fish and the progeny (F1) were raised to adulthood and screened for SULT4A1 mutations by HRMA (Figure 10). SULT4A1 gene sequencing of these heterozygous F1 fish revealed two independent mutations. One mutation consisted of a 15 base pair (bp) deletion resulting in the removal of 5 AAs from within the putative substrate binding pocket of the protein (SULT4A1^{Δ15}) (Figure 11). The other mutation consisted of an 8 bp deletion at the TALEN targeting site (SULT4A1^{Δ8}). Deletion of these 8 nucleotides results in a frameshift at AA 89 and premature stop codon after 132 AA (Figure 12). Immunoblot analysis of brain lysate from WT, SULT4A1^{Δ15/Δ15}, and SULT4A1^{Δ8/Δ8} fish using a pAb to human SULT4A1 (Proteintech, Chicago, IL) revealed an immunoreactive band with a MW of roughly 34 kDa. This band ran at a lower MW in the SULT4A1^{Δ15/Δ15} brain lysate and was undetectable in SULT4A1^{Δ8/Δ8} lysate (Figure 13).

High Resolution Melting Analysis

In order to genotype fish, high resolution melting analysis (HRMA) was performed as described previously using digested embryos or tail clippings as the source of template DNA (Parant et al., 2009). Each 10 μl reaction contained 1 μl LC Green® Plus

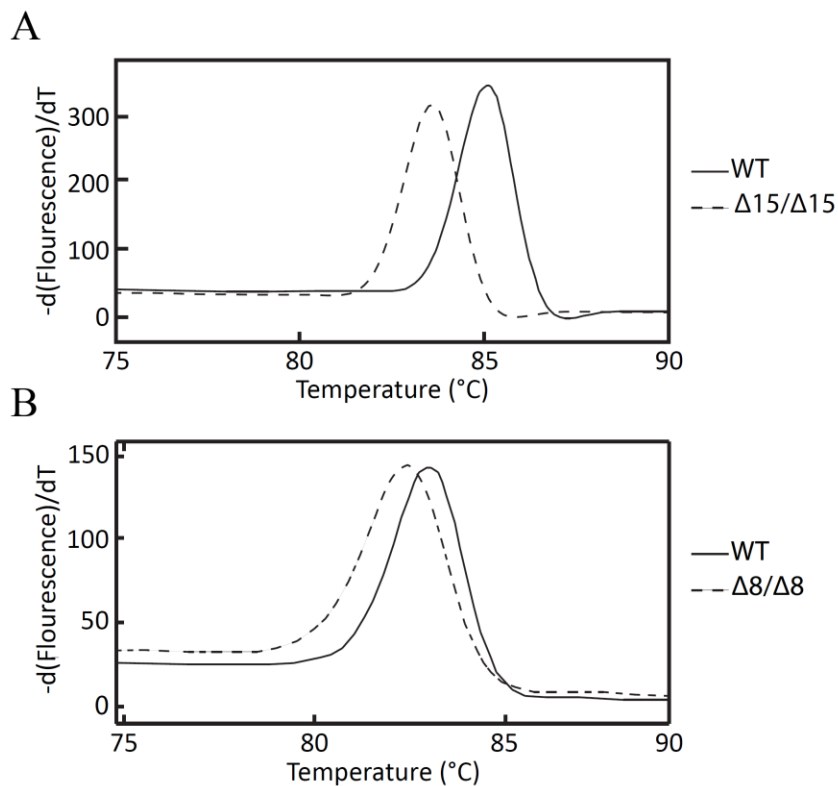


Figure 10: SULT4A1 ^{$\Delta 15/\Delta 15$} and SULT4A1 ^{$\Delta 8/\Delta 8$} screening by HRMA analysis. (A) WT and SULT4A1 ^{$\Delta 15/\Delta 15$} DNA showed a T_m difference of 1.5 $^{\circ}$ C. (B) WT and SULT4A1 ^{$\Delta 8/\Delta 8$} DNA showed a T_m difference of 0.6 $^{\circ}$ C. $\Delta 15$ primers (forward: 5'- ATGA-GATCGGGCTCATGAAT; reverse: 5'- TGCGATATGCATGTGATAAAGA). $\Delta 8$ primers (forward: 5'-TTGATGAGCAGCTTCCAGTG; reverse: 5'-TAATCTCCAATCCCGGCTGT).

Note: Adapted from “Activity Suppression Behavior Phenotype in SULT4A1 Frameshift Mutant Zebrafish” by F. Crittenden, H. Thomas, J. M. Parant, and C. N. Falany, 2014, *Drug Metabolism and Disposition*, 43, p. 1037. Copyright 2015 by The American Society for Pharmacology and Experimental Therapeutics. Reprinted with permission.

A

WT: ATTGATGAGCAGCTTCCAGTGCTGGAATACCCACAGCCGGGATTGGAGATTATCC
 $\Delta 15$: ATTGATGAGCAGCTTCCAGTGCTGG-----GATTGGAGATTATCC

B

SULT4A1^{WT} : MAESEVDTPSTPIEYESKYFEHHGVRLPPFCRGKMDEIANFSLRSSDIWI 50
 SULT4A1 ^{$\Delta 15$} : MAESEVDTPSTPIEYESKYFEHHGVRLPPFCRGKMDEIANFSLRSSDIWI 50

SULT4A1^{WT} : VTYPKSGTSLQLQEVVYLVVSQGADPDEIGLMNIDEQLPVLEYPQPLEIIQ 100
 SULT4A1 ^{$\Delta 15$} : VTYPKSGTSLQLQEVVYLVVSQGADPDEIGLMNIDEQLPVL-----GLEIIQ 95

SULT4A1^{WT} : ELTSPRLIKSHLPYRFLPSAMHNGEGKVIYMARNPKDLVVSYYQFHRSLR 150
 SULT4A1 ^{$\Delta 15$} : ELTSPRLIKSHLPYRFLPSAMHNGEGKVIYMARNPKDLVVSYYQFHRSLR 145

SULT4A1^{WT} : TMSYRGTFQEFCCRFMNDKLGYSWFEHVQEFWEHRMDSNVLFLLKYEDMY 200
 SULT4A1 ^{$\Delta 15$} : TMSYRGTFQEFCCRFMNDKLGYSWFEHVQEFWEHRMDSNVLFLLKYEDMY 195

SULT4A1^{WT} : KDLGTLVEQLARFLGVSCDKAQLESIVESSNQLIEQCCNSEALSICRGRV 250
 SULT4A1 ^{$\Delta 15$} : KDLGTLVEQLARFLGVSCDKAQLESIVESSNQLIEQCCNSEALSICRGRV 245

SULT4A1^{WT} : GLWKDVFTVSMNEKFDAIYRQKMAKSDLTFDFIL 284
 SULT4A1 ^{$\Delta 15$} : GLWKDVFTVSMNEKFDAIYRQKMAKSDLTFDFIL 279

Figure 11: SULT4A1 ^{$\Delta 15$} mutation. (A) WT and SULT4A1A ^{$\Delta 15$} DNA sequence at mutation site. Left and right TALEN target sequences are underlined. Dashes represent single nucleotide deletions. (B) WT and mutant SULT4A1 ^{$\Delta 15$} protein sequence alignment. Underlined sequence indicates divergence of SULT4A1 ^{$\Delta 15$} sequence from WT.

A

WT: ATTGATGAGCAGCTTCCAGTGCTGGAATACCCACAGCCGGGATTGGAGATTATCC
 $\Delta 8$: ATTGATGAGCAGCTTCCAGTGC-----CCACAGCCGGGATTGGAGATTATCC

B

SULT4A1^{WT}: MAESEVDTPSTPIEYESKYFEHHGVRLPPFCRGKMDEIANFSLRSSDIWI 50
 SULT4A1 ^{$\Delta 8$} : MAESEVDTPSTPIEYESKYFEHHGVRLPPFCRGKMDEIANFSLRSSDIWI 50

SULT4A1^{WT}: VTYPKSGTSLQEVVYLVSQGADPDEIGLMNIDEQLPVLEYPQPGLEIIQ 100
 SULT4A1 ^{$\Delta 8$} : VTYPKSGTSLQEVVYLVSQGADPDEIGLMNIDEQLPVPTAGIGDYPGTD 100

SULT4A1^{WT}: ELTSPRLIKSHLPYRFLPSAMHNGEGKVIYMARNPKDLVVSYYQFHRSLR 150
 SULT4A1 ^{$\Delta 8$} : IASSDQKPPAVPFSAISHAQWRROGDLYGEEP*----- 182

SULT4A1^{WT}: TMSYRGTFQEFCCRFRMNDKLGYSWFEHVQEFWEHRMDSNVLFLKYEDMY 200
 SULT4A1 ^{$\Delta 8$} : ----- 182

SULT4A1^{WT}: NSKDLGTLVEQLARFLGVSCDKAQLESLVESSNQLIEQCCEALSICRGRV 250
 SULT4A1 ^{$\Delta 8$} : ----- 182

SULT4A1^{WT}: GLWKDVFTVSMNEKFDAIYRQKMAKSDLTFDFIL* 284
 SULT4A1 ^{$\Delta 8$} : ----- 182

Figure 12: SULT4A1 ^{$\Delta 8$} mutation. (A) WT and SULT4A1A ^{$\Delta 8$} DNA sequence at mutation site. Left and right TALEN target sequences are underlined. Dashes represent single nucleotide deletions. (B) WT and mutant SULT4A1 ^{$\Delta 8$} protein sequence alignment. Underlined sequence indicates divergence of SULT4A1 ^{$\Delta 8$} sequence from WT. Asterisks indicate a stop codon.

Note: From “Activity Suppression Behavior Phenotype in SULT4A1 Frameshift Mutant Zebrafish” by F. Crittenden, H. Thomas, J. M. Parant, and C. N. Falany, 2014, *Drug Metabolism and Disposition*, 43, p. 1037. Copyright 2015 by The American Society for Pharmacology and Experimental Therapeutics. Reprinted with permission.

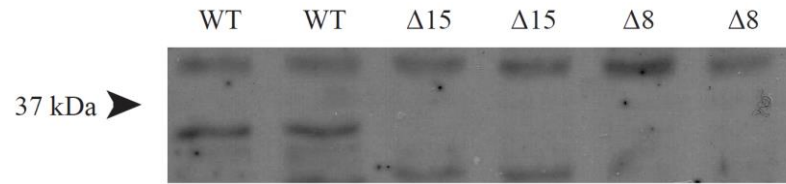


Figure 13: Immunoblot analysis of brain lysate from WT, SULT4A1^{Δ15/Δ15}, and SULT4A1^{Δ8/Δ8} fish. Lysate was collected from the brains of 2 fish of each genotype. Fish were 6 mo old at time of sacrifice. Protein concentration was determined by Bradford analysis, and 86 μg protein from each sample was loaded onto a 10% acrylamide gel. Primary Ab was a rabbit α: hSULT4A1 pAb (Proteintech), 1:1000 dilution with a 2 h incubation. Secondary Ab was a horse-radish peroxidase (HRP)-conjugated goat α: rabbit Ab (Southern Biotech), 1:8000 dilution with a 1 h incubation. Blot was developed with SuperSignal™ West Pico Chemiluminescent Substrate (Life Technologies).

(BioFire Diagnostics, Inc; Salt Lake City, UT), 0.05 μ l Ex Taq (TaKaRa; Ōtsu, Japan), 1 μ l Ex Taq buffer, 0.4 mM dNTP (0.1 mM each), 0.1 μ M forward primer, 0.1 μ M reverse primer, and 1 μ l DNA template. For screening of individual chimeric fish, the following primers were used: Forward (5'-ATGAGATCGGGCTCATGAAT) and Reverse (5'-TGCGATATGCATGTGATAAAGA). For screening of SULT4A1 ^{Δ 8/ Δ 8} individuals, the following primers designed to sequences closer to the mutation site were used: Forward (5'-TTGATGAGCAGCTTCCAGTG) and Reverse (5'-TAATCTCCAATCCCGGC-TGT). Reaction solutions were covered with 20 μ l mineral oil, and reactions were carried out in 96 well plates. After 40 PCR cycles (98°C for 10s, 59°C for 20s, 72°C for 15s), the reactions were heated to 95°C for 10 s and then cooled to 4°C. Plates were analyzed for HRMA using an HR-1 96 LightScanner™ (Idaho Technology, Inc, Salt Lake City, UT).

Dynamic Modeling of SULT4A1 ^{Δ 15} Mutant Protein

The crystal structure of SULT4A1 (pdb: 1ZD1) was imported into MOE. Using the homology model function, the cofactor-absent (open) SULT2A1 crystal structure (PDBID 1J99) was used as a template to fill in loop regions lacking resolution in the SULT4A1 crystal structure. After partial charges were calculated and corrected, these loop regions were guided into place using the Amber99 forcefield and energy minimization. The protein model was then protonated assuming an environment of pH 7.4. To create mutant isoforms, existing residue side chains were replaced or complete residues were removed, the peptide backbone reconnected, and the resulting structure was energy minimized. A water sphere (150 mM NaCl) was created around the protein with a 12 Å buffer region between the protein and the outermost edge of the sphere. Using the Nose-

Poincare-Anderson Hamiltonian equations of motion and wrapped waters, the system was equilibrated to a temperature of 310K over 100 ps followed by a 5 ns productive simulation at 310K. The resulting frames from 5 ns productive simulation were analyzed for structural differences from native SULT4A1.

Behavioral Analysis in Zebrafish

All behavioral tests were carried out between the h of 10:00 am and 2:00 pm unless stated otherwise. The water used in each apparatus was taken directly from the home aquaria system in which the fish had been housed and was changed between each trial. Each behavioral test was performed on a separate cohort of naïve fish between 6 and 8 mo of age unless stated otherwise. Adult test cohorts were an equal mix of males and females. Videos were recorded using an Ultra 720+ Resolution DSP True Day/Night Color Camera (EverFocus®, Taipei, Taiwan) with near infrared recording abilities and analyzed using EthoVision XT (Noldus, Wageningen, The Netherlands) to track fish movement and activity levels. Genetically WT siblings of the SULT4A1^{Δ8/Δ8} fish being tested were used as controls in each behavioral test.

Larval Visual-Motor Response

The visual-motor response (VMR) is a reflex in zebrafish whereby abrupt changes in light intensity are followed by rapid movement by the fish or larvae. In zebrafish, this behavior can be observed as early as 70 hpf and lasts throughout adulthood (Easter and Nicola, 1996; Emran et al., 2008). Because of the up-regulation of cone phototransduction proteins observed in SULT4A1 KD zebrafish larvae, it was hypothesized that the

KD larvae may have impaired vision and therefore a suppressed or delayed VMR as well. To test this hypothesis, we designed and built a zebrafish larvae light startle assay contraption (ZELLSAC) (Figure 14). The light source for the ZELLSAC was a Model 20520 Fiber Optic Light Source (Fostec, Inc., Siheung, South Korea). The fiber optic cables were detached from the light source and positioned 0.5 cm away so that light could still pass through, but a thin metal divider could also be placed between the light source and the fiber optic cables to effectively turn off the light entering the hood. A divider was used instead of simply switching off the light source because the latter method necessitated turning a knob to dim and subsequently turn off the light. The result of turning off the light in this manner was a slow dimming within the apparatus rather than the desired abrupt darkness. Using a divider to block the light also allowed the knob to remain in one position, meaning that the same light intensity could be maintained throughout the experiment. The lenses from the tips of the fiber optic cables were removed so that the light emanating from them was a point source rather than a focused beam. Two holes were drilled into opposite sides of the hood from an Electrophoresis Documentation and Analysis System 120 (Kodak), and the ends of the fiber optic cables were positioned within these holes. The inside of the hood was lined with white paper to reflect light from the cables and create a uniform illumination within the hood. All experiments using the ZELLSAC were recorded from a PowerShot A560 camera (Canon, Tokyo, Japan) mounted on top of the hood.

Embryos for VMR assays were collected from natural matings of AB strain zebrafish and injected at the one or two cell stage with either SULT4A1 MO or SCM. Larvae were held in E3 Blue (5 mM NaCl, 0.17 mM KCl, 0.33 mM CaCl₂, 0.33 mM

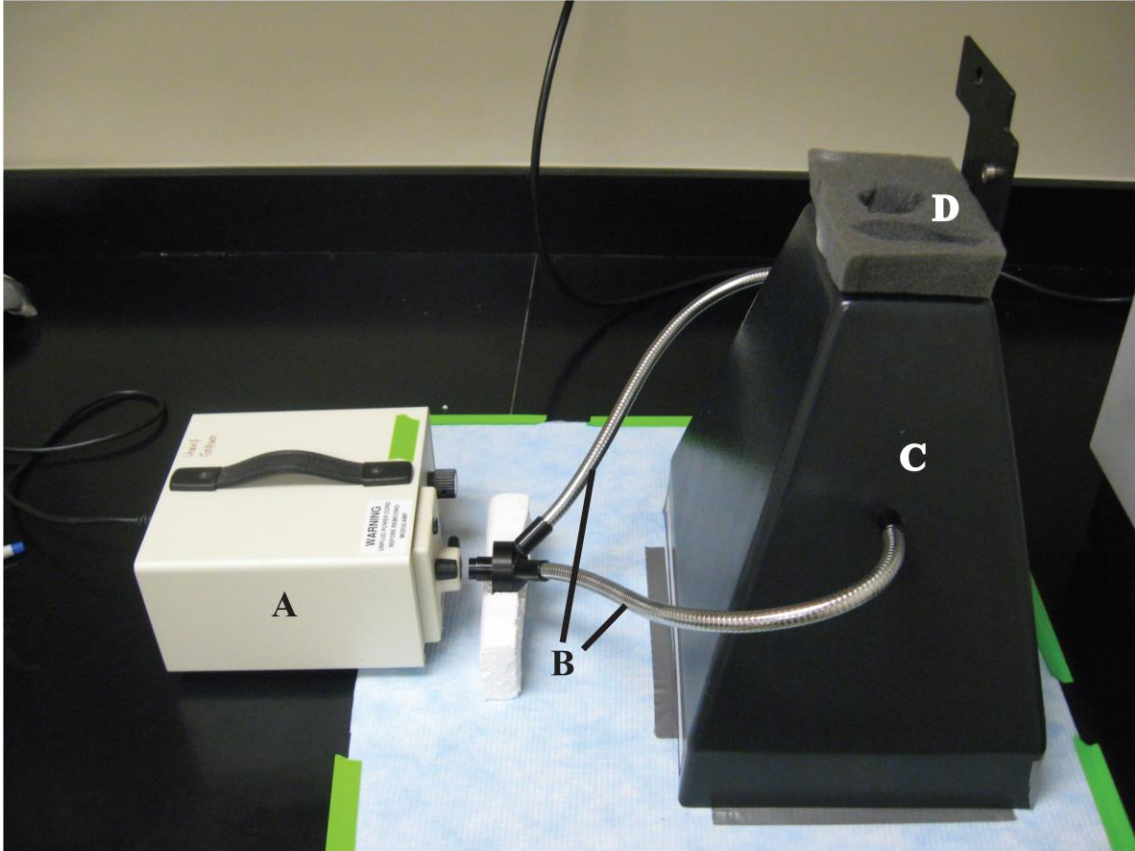


Figure 14: Zebrafish Larvae Light Startle Assay Contraption (ZELLSAC). (A) Light source. (B) Fiber optic cables. (C) Hood. (D) Camera mount.

MgSO₄, 10⁻⁵% methylene blue) at 25°C under a 14 h/10 h light/dark cycle until time of testing. Care was taken to ensure that time of fertilization was accurately recorded for all embryos with a precision of < 15 min. KD and SCM larvae were assayed for VMR according to the following protocol: one h prior to time of testing, one larva was transferred via pipet into each well of a 96 well plate. KD and SCM larvae were arranged on the plate in a checkerboard pattern so that there was an equal distribution of KD and SCM larvae on each plate. Each well was topped off with E3 Blue so that the liquid was flush with the top of the plate. The plate was then placed back into the incubator until time of assay. At the time of assay, the plate was removed from the incubator and placed underneath the ZELLSAC hood with the light on. The plate was arranged in the center of the camera's field of view, and the camera was zoomed in as far as possible without excluding any of the plate. The automatic ISO function on the camera was overridden to prevent aperture adjustment in response to light intensity changes. All VMR assays were conducted at an illuminance of 375 lx. After five min of acclimation in the testing apparatus, the test plate was exposed to five light interruption stimuli spaced 30 s apart. Stimuli were introduced by manually sliding a metal plate between the light source and the fiber optic cables for a period of one s. Individual larvae were scored as responsive if they showed any swimming movement within 2 s of the end of any one of the five light interruption stimuli.

Novel Tank Test

A standard novel tank test was used as a means to gauge stress and anxiety levels as well as locomotion in a novel tank environment (Levin et al., 2007; Bencan et al.,

2009; Egan et al., 2009). For this experiment, the novel tank used was a narrow 1.8 L polycarbonate tank (Aquaneering, San Diego, CA) which restricted lateral movement but allowed horizontal and vertical movement. The tank was filled with 1.4 L of water from the same system as the home tank of the fish being tested. Test animals were moved into the recording room 1 h prior to the beginning of testing. Fish were recorded individually in the novel tank for a total of 6 min each using a camera positioned 60 cm away. Fish movement was tracked over the course of the experiment, and the following endpoints were determined: latency to enter upper half of tank, transitions to upper half, time in upper half, distance traveled, freezing bouts, and freezing bout duration. A freezing bout was defined as a lack of movement lasting at least 2 s.

Social Preference Test

To examine zebrafish social behavior, a social preference test was used as previously described by Grossman *et al* (Grossman et al., 2010). Briefly, a clear acrylic open-top box was constructed with the following dimensions: 50 cm (length) x 10 cm (width) x 10 cm (height). The resulting 50 cm corridor was filled with home system water and divided into 5 separate, water-tight compartments through the use of 4 evenly spaced sliding doors. An unfamiliar target fish was placed in the conspecific compartment at one end of the corridor, and the compartment at the other end of the apparatus remained empty (empty compartment). To avoid lateral bias, the conspecific and empty compartments were switched between each trial for the same cohort. After acclimating the test cohorts to the recording room for one h, WT, SULT4A1^{Δ15/Δ15}, or SULT4A1^{Δ8/Δ8} fish were introduced individually into the center compartment. After a period of 30 s (to minimize han-

dling stress), the two center dividers were gently lifted to allow the test fish to swim freely along the 30 cm corridor comprised of the center zone, conspecific zone (adjacent to the conspecific compartment), and empty zone (adjacent to the empty compartment). Movement of the fish was recorded for 6 min using a camera positioned 80 cm above the tank, and the following end points were determined: empty zone entries, conspecific zone entries, time in empty zone, time in conspecific zone, and time in center zone.

Activity Analysis of SULT4A1 Mutant Zebrafish

On day one, a total of 4 fish (2 WT and 2 mutant fish) were transferred from their home tanks and individually housed in 1.8 L polycarbonate tanks on an Aquaneering model 330B stand-alone housing rack. Tanks were backlit using two 8 watt infrared (850 nm) light sources (Axton, North Salt Lake, UT). Two white, translucent, 0.4” plastic screens were placed behind the tanks to provide a uniform background and diffuse the infrared light. Two cameras were set up 75 cm from the tanks, with each camera set to record two tanks: one on top and one on bottom. Fish were allowed to habituate to the new tanks for a total of 96 h on a light/dark cycle (14 h light/10 h dark) before recordings began. After habituation was complete, 48 h recordings were initiated at zeitgeber time (ZT) 2. ZT0 corresponds to the time at which the lights come on. In the first recording, the two top tanks were occupied by WT fish, and the two bottom tanks were occupied by mutant fish. In each subsequent recording, this arrangement was reversed so that there were an equal number of videos with each arrangement. Throughout the habituation and recording period, fish were fed twice daily at ZT2 and ZT9 with dry fish food. Temperature, pH, and conductivity of the system were maintained at 28° C, 7.4, and 1380-1450

μS , respectively. Day time illuminance on the front surface of the tanks was measured at 430 lux.

For each single-fish 48-h trial, the arena was defined in EthoVision as the total area enclosed by the perimeter of the tank. The activity analysis function in EthoVision was used to determine activity levels within the arena over the course of each trial. All inactivity bouts lasting less than 1 s were excluded from analysis. Data output from the activity analysis was used to measure the following endpoints: mean activity (pixels/frame), mean activity length (s), inactive time %, inactivity bout frequency, and mean inactivity bout length (s). Data for each endpoint were grouped into 1 h time bins, and JTK_CYCLE analyses (Hughes et al., 2010) were performed on the activity, inactive time percentage, inactivity bout frequency, and inactivity bout length data for each 48 h trial to assess data rhythmicity and determine phase lag and amplitude. Period length was set at 24 h across all data series.

Due to the extremely large size of the 48 h activity analysis videos (> 60 GB), it became necessary to split the 48 h recordings into two consecutive 24 h recordings. For experiments recorded in this manner, recordings were stopped at exactly 24:05:00, and another recording was begun immediately after the end of the first.

CHAPTER 3

RESULTS

Aim 1: Characterization of the Effects of SULT4A1 Expression Deficiency on Development and Gene Expression in Larval and Adult Zebrafish

The SULT4A1 gene has been identified with remarkable sequence conservation in every vertebrate investigated to date. Because of SULT4A1's extensive conservation among vertebrates, it was reasoned that SULT4A1 has an equally conserved and important function. It was hypothesized that inhibition of SULT4A1 expression, whether by MO KD or by TALEN-induced gene mutation, would impair the development of larval zebrafish or lead to changes in gene expression that could point to a possible function for this protein. This aim was undertaken with the intention of characterizing the effects of SULT4A1 expression deficiency on developing zebrafish larvae.

SULT4A1 Expression in Brain and Eye of Adult Zebrafish

The zfSULT4A1 gene is located on chromosome 9 and consists of 7 exons separated by 6 introns (ZDB-GENE-060421-2705). When qPCR was performed on cDNA from the brain, eye, intestine, liver, and testes of adult fish using a TaqMan® assay that spans the junction of exons 2 and 3, SULT4A1 mRNA was detected in the brain, eye, and testes (Figure 15a). The findings in the brain and eye were corroborated by conventional PCR using primers to generate full-length SULT4A1. However, no SULT4A1 message

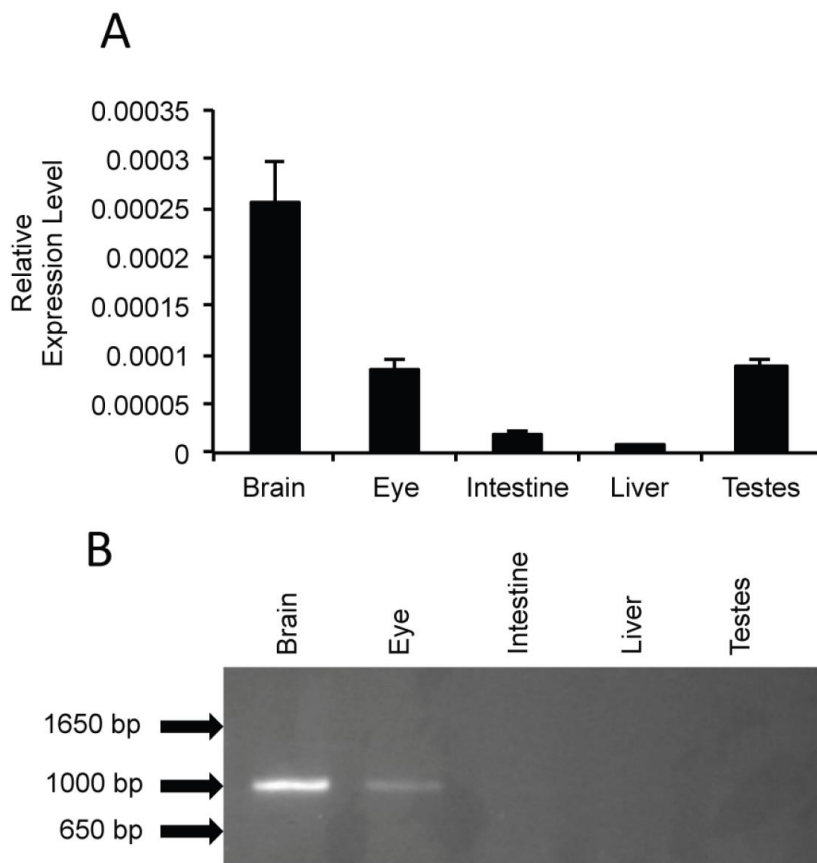


Figure 15: SULT4A1 expression in adult zebrafish tissues. A. Quantitative real-time PCR. Relative expression levels of SULT4A1 were analyzed using TaqMan expression assays for SULT4A1 (Assay ID: Dr03078008_g1) and ribosomal subunit 18s (Assay ID: Hs99999901_s1). Relative expression levels of SULT4A1 were analyzed using the ΔCt method and normalized to endogenous expression of 18s RNA. Error bars indicate standard error of the mean. Brain ($2.54\text{e-}4 \pm 4.24\text{e-}5$). Eye ($8.45\text{e-}5 \pm 1.01\text{e-}5$). Intestine ($1.75\text{e-}5 \pm 5.35\text{e-}6$). Liver ($7.7\text{e-}6 \pm 1.48\text{e-}6$). Testes ($8.69\text{e-}5 \pm 8.09\text{e-}6$). B. Qualitative PCR of SULT4A1 message in adult AB zebrafish brain, eye, intestine, liver, and testes using full-length primers (forward: 5'-atggcggaaagcgaggtgga-3'; reverse: 5'-ctgcttacaggataaagtc-3'). A total of 30 PCR cycles were carried out under the following conditions: denature at 94°C for 1 min, anneal at 55°C for 2 min, extension at 72°C for 3 min. DNA polymerase used was REDTAQ™ (Sigma).

Note: From “Inhibition of SULT4A1 expression induces up-regulation of phototransduction gene expression in 72-hour postfertilization zebrafish larvae” by F. Crittenden, H. Thomas, C. M. Ethen, Z. L. Wu, D. Chen, T. M. Kraft, J. M. Parant, and C. N. Falany, 2014, *Drug Metabolism and Disposition*, 42, p. 947. Copyright 2014 by The American Society for Pharmacology and Experimental Therapeutics. Reprinted with permission.

was detected in cDNA of the testes when analyzed by conventional PCR to generate the complete SULT4A1 coding region and agarose gel separation (Figure 15b).

After establishing that full-length SULT4A1 mRNA expression occurs in the zebrafish brain and eye, immunoblot analyses were used to demonstrate that the SULT4A1 protein is detectable in these tissues. Immunoblot analysis using a goat polyclonal antibody of human SULT4A1 detected a band at approximately 33 kDa in lysate of both the brain and eye without the optic nerve (Figure 16) corresponding to zfSULT4A1 (MW = 33 kDa).

Localization of SULT4A1 Within the Retina

Having established the expression of SULT4A1 within the retina, we next investigated the protein's localization in the retina. To determine if SULT4A1 was expressed at higher levels in the central or peripheral regions of the retina, qPCR was performed comparing SULT4A1 expression in these different regions. No significant difference was observed between SULT4A1 expression in the central or peripheral retina (Figure 17). Immunohistochemical analysis of SULT4A1 expression was performed on rat retinas to determine what specific cell type and layer express SULT4A1. Positive staining was observed in the ganglion cell layer of these retinas, although the diffuse and uniform nature of the staining suggested that it was not necessarily associated with the cell bodies of the ganglion cells (Figure 18).

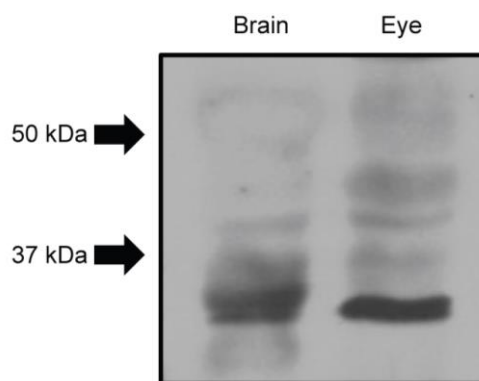


Figure 16: Immunoblot of zebrafish brain and eye lysate using anti-human SULT4A1 polyclonal antibody. Lysate was collected from the brains and eyes of adult AB strain zebrafish. Protein concentration was determined by Bradford analysis, and 396 μ g protein from each sample was loaded onto a 10% acrylamide gel. Primary Ab was a goat α : hSULT4A1 pAb (R&D Systems), 1:200 dilution with a 2.5 h incubation. Secondary Ab was a horse-radish peroxidase (HRP)-conjugated donkey α : goat Ab (Southern Biotech), 1:1000 dilution with a 1 h incubation. Blot was developed with SuperSignal™ West Pico Chemiluminescent Substrate (Life Technologies).

Note: From “Inhibition of SULT4A1 expression induces up-regulation of phototransduction gene expression in 72-hour postfertilization zebrafish larvae” by F. Crittenden, H. Thomas, C. M. Ethen, Z. L. Wu, D. Chen, T. M. Kraft, J. M. Parant, and C. N. Falany, 2014, *Drug Metabolism and Disposition*, 42, p. 947. Copyright 2014 by The American Society for Pharmacology and Experimental Therapeutics. Reprinted with permission.

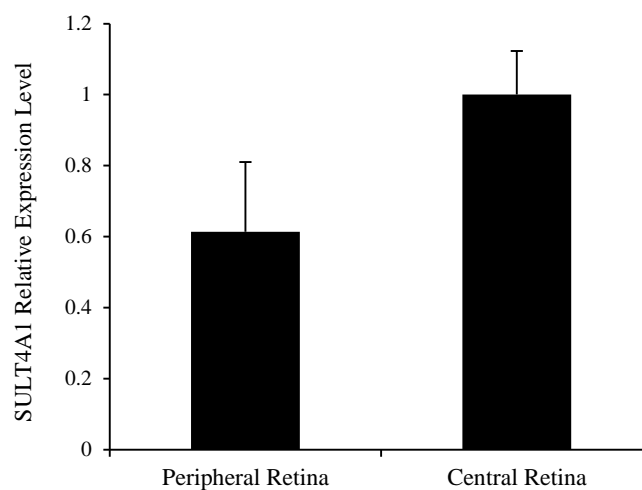


Figure 17: Relative expression level of SULT4A1 in central and peripheral retina of adult AB strain zebrafish. Eyes were enucleated, and retinas were separated from eyes. Iridectomy scissors were used to separate a portion with a diameter of roughly 1 mm from the central retina. Relative expression levels of SULT4A1 were analyzed using TaqMan expression assays for SULT4A1 (Assay ID: Dr03078008_g1) and ribosomal subunit 18s (Assay ID: Hs99999901_s1). Data were analyzed using the Δ Ct method and normalized to endogenous expression of 18s RNA. Error bars indicate standard error of the mean. Peripheral Retina (0.61 \pm 0.19). Central Retina (1 \pm 0.12). $P > 0.05$.

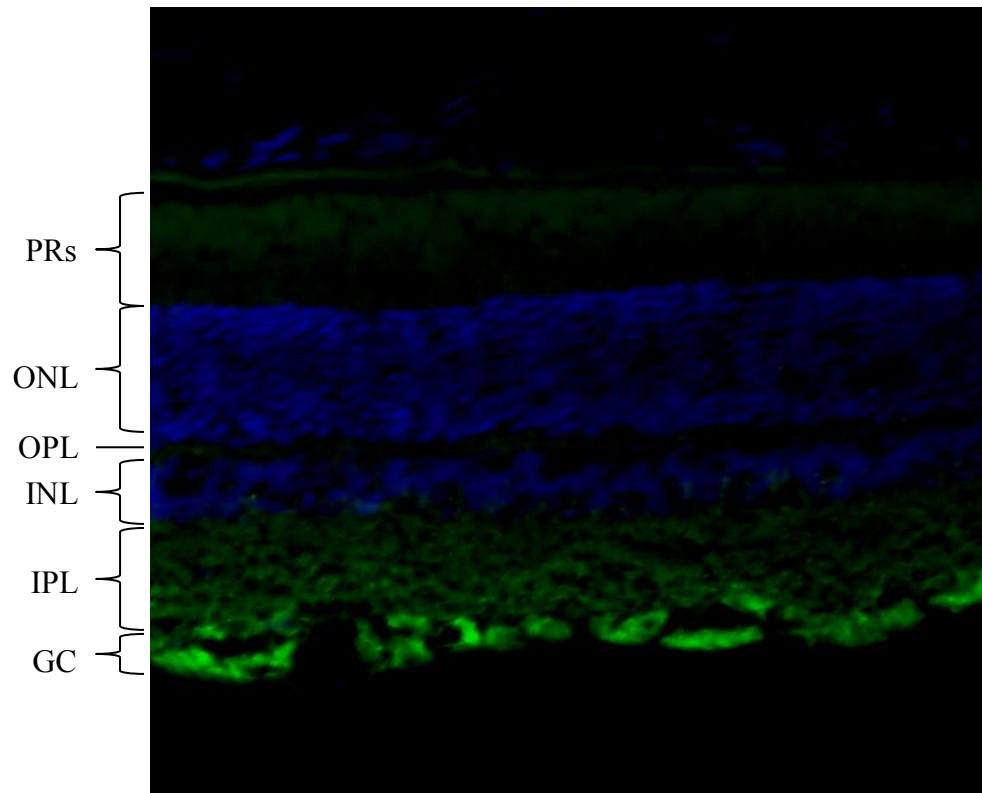


Figure 18: Immunohistochemical staining of adult rat retina for SULT4A1. Primary antibody was a goat α : hSULT4A1 pAb (R&D Systems), 1:20 dilution, 5 h incubation. Secondary antibody was donkey α : goat IgG Alexa Flour® 488 – conjugated (Life Technologies), 1:200 dilution, 1 hour incubation. Slide was counterstained with a 4',6-diamidino-2-phenylindole (DAPI) solution (1:1000 dilution in PBS) for 5 min. Slides were viewed on a Zeiss Axioplan 2 Imaging microscope. Abbreviations: Photoreceptors (PRs), outer nuclear layer (ONL), outer plexiform layer (OPL), inner nuclear layer (INL), inner plexiform layer (IPL), ganglion cells (GC).

SULT4A1 MO Effectiveness and Lack of Toxicity

The use of MOs to block translation is a well-established technique used to selectively knock down gene expression in zebrafish over the first several days of development (Morcos, 2007; Eisen and Smith, 2008; Bill et al., 2009). To investigate the effectiveness of the SULT4A1 MO as well as potential toxic effects, embryos were injected with the MO and monitored for developmental defects and SULT4A1 expression. Embryos were collected from natural matings of multiple breeding pairs of AB strain zebrafish and injected with 0.82 pmol of either the SULT4A1 MO or a standard control MO (SCM) at the one or two cell stage. To determine the effectiveness of the MO knockdown as well as when SULT4A1 is expressed in larval zebrafish, total RNA was isolated from pooled SCM as well as SULT4A1 MO larvae using STAT-60TM at 24 hpf, 48 hpf, 72 hpf, and 96 hpf. cDNA was generated using SuperScript[®] Reverse Transcriptase (Life Technologies), and SULT4A1 transcript was amplified from cDNA using REDTaq[®] DNA Polymerase (Sigma-Aldrich) and primers that amplify the full-length of the coding region of the zfSULT4A1 transcript. The PCR reaction products were separated by electrophoresis on a 10% agarose gel, and bands were stained with ethidium bromide, then visualized by UV light. In the SCM larvae, fluorescent bands representing SULT4A1 cDNA were observed at 48 hpf, 72 hpf, and 96 hpf, but not 24 hpf. In SULT4A1 MO larvae, no bands were observed at 24 or 48 hpf, and faint bands were observed at 72 and 96 hpf (Figure 19a). The SULT4A1 expression of 72 and 96 hpf SCM and SULT4A1 MO larvae was further analyzed by qPCR. Significant suppression of SULT4A1 message levels was observed at 72 hpf in the SULT4A1 MO larvae, but

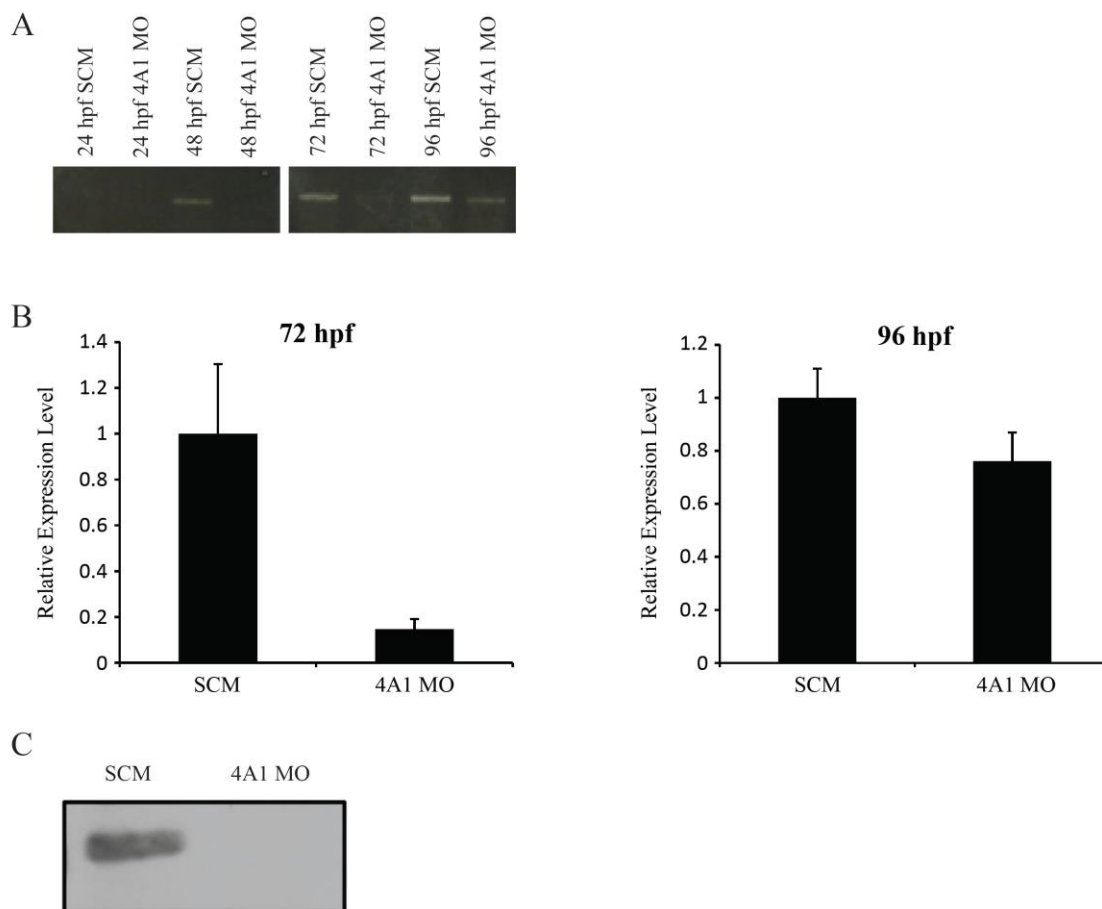


Figure 19: SULT4A1 MO effectiveness. (A) Conventional PCR of SULT4A1 transcript from SCM and 4A1 MO larvae. Total RNA was isolated from pooled SCM as well as SULT4A1 MO larvae using STAT-60™ at 24 hpf, 48 hpf, 72 hpf, and 96 hpf. cDNA was generated using SuperScript® Reverse Transcriptase (Life Technologies), and SULT4A1 transcript was amplified from cDNA using REDTaq® DNA Polymerase (Sigma-Aldrich) and primers which amplify the full-length of the coding region of the zSULT4A1 transcript (forward: 5'-CCGAGCACTCCGATTGAATACG; reverse: 5'-TCACCTTGCCTTCTCCATTGTG). PCR reactions were separated by electrophoresis on a 10% agarose gel, and bands were stained with ethidium bromide and detected by UV light. (B) qPCR of SULT4A1 mRNA from 72 and 96 hpf SCM and 4A1 MO larvae. Relative expression levels of SULT4A1 were analyzed using TaqMan expression assays for SULT4A1 (Assay ID: Dr03078008_g1) and ribosomal subunit 18s (Assay ID: Hs99999901_s1). Data were analyzed using the Δ Ct method and normalized to endogenous expression of 18s RNA. Error bars indicate standard error of the mean. (C) Immunoblot of SCM and 4A1 MO zebrafish larvae lysate at 72 hpf. Protein concentration was determined by Bradford analysis, and 173 μ g protein from each sample was loaded onto a 10% acrylamide gel. Primary Ab was a goat α : hSULT4A1 pAb (R&D Systems), 1:200 dilution with a 2.5 h incubation. Secondary Ab was a horse-radish peroxidase (HRP)-conjugated donkey α : goat Ab (Southern Biotech), 1:1000 dilution with a 1 h incubation. Blot was developed with SuperSignal™ West Pico Chemiluminescent Substrate (Life Technologies).

Note: From “Inhibition of SULT4A1 expression induces up-regulation of phototransduction gene expression in 72-hour postfertilization zebrafish larvae” by F. Crittenden, H. Thomas, C. M. Ethen, Z. L. Wu, D. Chen, T. M. Kraft, J. M. Parant, and C. N. Falany, 2014, *Drug Metabolism and Disposition*, 42, p. 947. Copyright 2014 by The American Society for Pharmacology and Experimental Therapeutics. Reprinted with permission.

expression levels had returned to normal at 96 hpf (Figure 19b). Immunoblot analysis of 72 hpf SULT4A1 MO larvae revealed no immunoreactive bands (Figure 19c).

Although the SULT4A1 MO was effective at delaying SULT4A1 expression, no gross morphological phenotype was observed in SULT4A1 MO versus SCM – injected embryos (Figure 20). At 48 hpf (Figure 20a, b), all observed SCM and KD embryos had a functional beating heart. At 72 hpf (Figure 20c, d), all observed SCM and KD embryos displayed adequate blood flow throughout the body. At 120 hpf (Figure 20e, f), all observed SCM and KD embryos had morphologically normal ears, eyes, and swim bladder.

SULT4A1 KD Induces Up-Regulation of Phototransduction Genes in 72 hpf Larvae

To investigate the effects of the inhibited expression of SULT4A1, the gene expression profile of 72 hpf embryos injected with either SCM or SULT4A1 MO was assessed using RNA-seq. RNA-seq detects transcripts over a much larger dynamic range of expression compared to microarray technology (Wang et al., 2009). Evaluation of the RNA-seq data using Ingenuity Pathway Analysis revealed a number of cellular processes to be significantly affected in the SULT4A1 KD larvae as compared to control larvae. A total of 135 messages were shown to be significantly dys-regulated by SULT4A1 KD. Of these, 47 genes were down-regulated, and 88 were up-regulated. A total of 13 genes known to be involved in phototransduction were dys-regulated by SULT4A1 KD, and all 13 of these affected genes were shown to be up-regulated (Table 3). Other pathways including LXR/RXR activation, circadian rhythm signaling, and CREB signaling in neurons were also affected by SULT4A1 KD, but none to the extent or significance of phototransduction (Table 4).

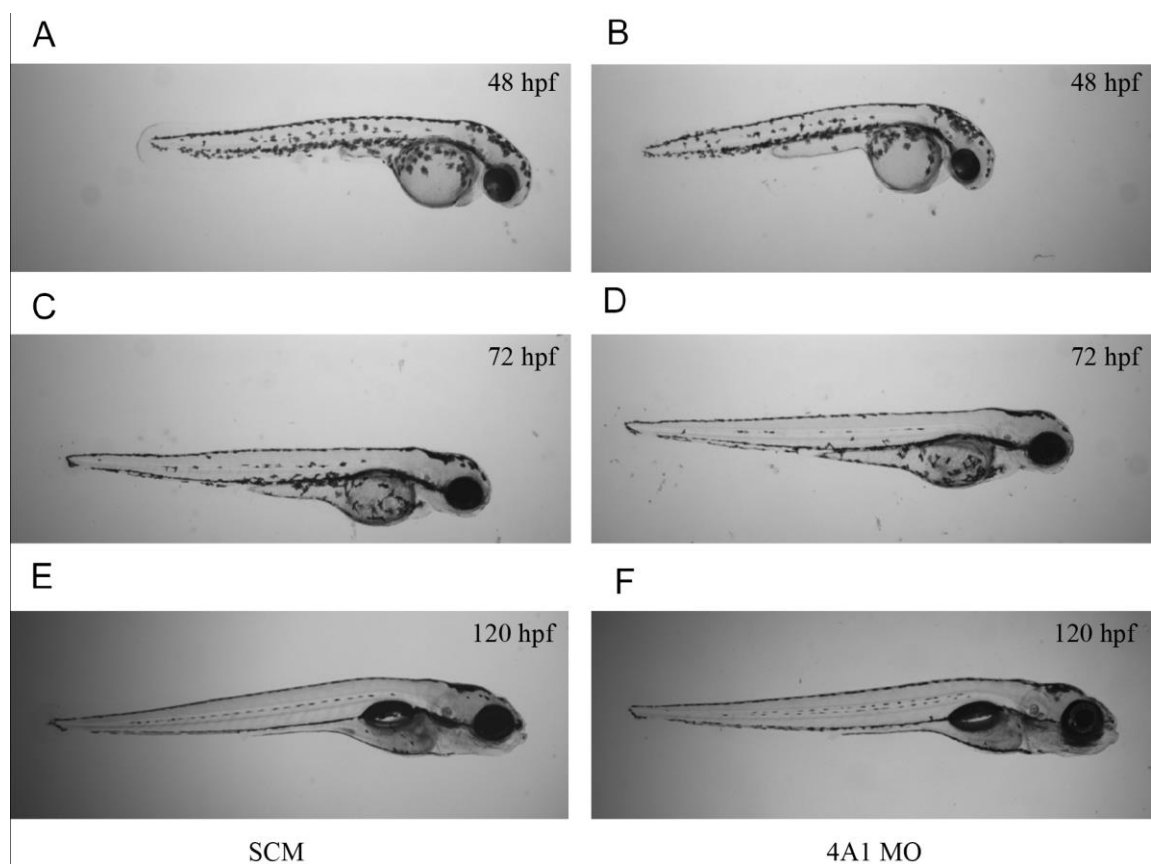


Figure 20: Normal development of SCM and 4A1 MO zebrafish larvae. Larvae were immobilized in 2% methyl cellulose and visualized using a Nikon AZ100 microscope. A. 48 hpf Control. B. 48 hpf SULT4A1 MO. C. 72 hpf Control. D. 72 hpf SULT4A1 MO. E. 120 hpf Control. F. 120 hpf SULT4A1 MO.

Note: From “Inhibition of SULT4A1 expression induces up-regulation of phototransduction gene expression in 72-hour postfertilization zebrafish larvae” by F. Crittenden, H. Thomas, C. M. Ethen, Z. L. Wu, D. Chen, T. M. Kraft, J. M. Parant, and C. N. Falany, 2014, *Drug Metabolism and Disposition*, 42, p. 947. Copyright 2014 by The American Society for Pharmacology and Experimental Therapeutics. Reprinted with permission.

Protein	Gene	Fold Change	p Value	Localization
Sulfotransferase family 4A member 1	SULT4A1	-2.15	<0.0001	
Rhodopsin	RHO	1.17	0.8233	Rod
G protein alpha transducing activity polypeptide 1	GNAT1	2.09	<0.0001	Rod
G protein alpha transducing activity polypeptide 2	GNAT2	3.35	<0.0001	Cone
G-protein-coupled receptor kinase 7a	grk7a	3.33	<0.0001	Cone
opsin 1, long-wave-sensitive, 2	OPN1LW2	2.31	<0.0001	Cone
opsin 1, medium-wave-sensitive, 2	OPN1MW1	4.56	<0.0001	Cone
opsin 1, short-wave-sensitive, 1	OPN1SW1	3.62	<0.0001	Cone
opsin 1, short-wave-sensitive, 2	OPN1SW2	3.29	<0.0001	Cone
G protein-coupled receptor kinase 1b	grk1b	4.27	<0.0001	Cone
Arrestin 3, retinal	ARR3	1.87	<0.0001	Cone
guanine nucleotide binding protein (G protein), gamma transducing activity polypeptide 2b	gngt2b	3.24	<0.0001	Both
Phosducin b	pdcb	2.76	<0.0001	Both
Guanylate cyclase activator 1e	guca1e	4.39	0.00018	Both
Cyclic nucleotide gated channel beta 1a	cngb1a	3.51	<0.0001	Both

Table 3: Summary of affected genes involved in phototransduction. Embryos injected with SCM or SULT4A1 MO were subjected to gene expression profiling using RNA-seq. P-Values were determined using ANOVA.

Note: From “Inhibition of SULT4A1 expression induces up-regulation of phototransduction gene expression in 72-hour postfertilization zebrafish larvae” by F. Crittenden, H. Thomas, C. M. Ethen, Z. L. Wu, D. Chen, T. M. Kraft, J. M. Parant, and C. N. Falany, 2014, *Drug Metabolism and Disposition*, 42, p. 947. Copyright 2014 by The American Society for Pharmacology and Experimental Therapeutics. Reprinted with permission.

Pathway	P-value	Genes
Phototransduction Pathway	2.48E-16	ARR3a, cngb1a, guca1e, GNAT1, GNAT2, gngt2b, OPN1LW2, OPN1MW1, OPN1SW1, OPN1SW2, grk1b, grk7a, pdcb
LXR/RXR Activation	4.19E-3	APOA4, CYP7A1, MMP9, CETP
Circadian Rhythm Signaling	1.42E-2	PER1, NR1D1
CREB Signaling in Neurons	1.43E-2	GNAT1, GRM1, NAT2, OPN1SW

Table 4: Gene ontology of transcripts affected by SULT4A1 knockdown. Following collection of RNA-seq data, Ingenuity Pathway Analysis was used to group affected genes into functional pathways and generate p-values.

Note: From “Inhibition of SULT4A1 expression induces up-regulation of phototransduction gene expression in 72-hour postfertilization zebrafish larvae” by F. Crittenden, H. Thomas, C. M. Ethen, Z. L. Wu, D. Chen, T. M. Kraft, J. M. Parant, and C. N. Falany, 2014, *Drug Metabolism and Disposition*, 42, p. 947. Copyright 2014 by The American Society for Pharmacology and Experimental Therapeutics. Reprinted with permission.

To validate the changes observed in the RNA-seq data, three up-regulated photo-transduction genes were selected for further analysis by qPCR. *OPN1MW1*, guanylate cyclase activator 1e (*guca1e*), and G protein-coupled receptor kinase 1b (*grk1b*) were chosen based on their relative abundance, high observed fold-change, and p-value. Pre-designed TaqMan Gene Expression Assays were used to verify the observed up-regulation of *OPN1MW1* ($p = 0.0047$) and *grk1b* ($p = 0.0392$). *Guca1e* showed an absolute increase of 1.52-fold when analyzed by qPCR, but this change was not statistically significant ($p = 0.0822$). As expected, *SULT4A1* showed a significant 7-fold decrease in expression when analyzed by qPCR ($p = 0.0253$). *Rrh* was used as a negative control since it is expressed in the retina and no change in expression levels was observed in the RNA-seq data. As expected, analysis by qPCR showed no significant change in *rrh* expression ($p = 0.3835$). (Figure 21)

Aim 2: Behavioral Analysis of *SULT4A1* KD and Mutant Zebrafish

Visual Motor Response (VMR) Assessment in SULT4A1 KD Larvae

Assay design and optimization. Because of the significant up-regulation of various photo-transduction genes observed in the 72 hpf *SULT4A1* MO-injected larvae, it was hypothesized that *SULT4A1* KD larvae would exhibit an altered visual sensitivity. To test this hypothesis, an assay was developed that would allow the quantification of larval responsiveness to increments and decrements in light intensity. In zebrafish, the VMR is a reflex wherein individual animals will initiate rapid swimming movements in response to abrupt changes in light intensity. This reflex has been observed in WT fish as early as 68 hpf and continues well into adulthood

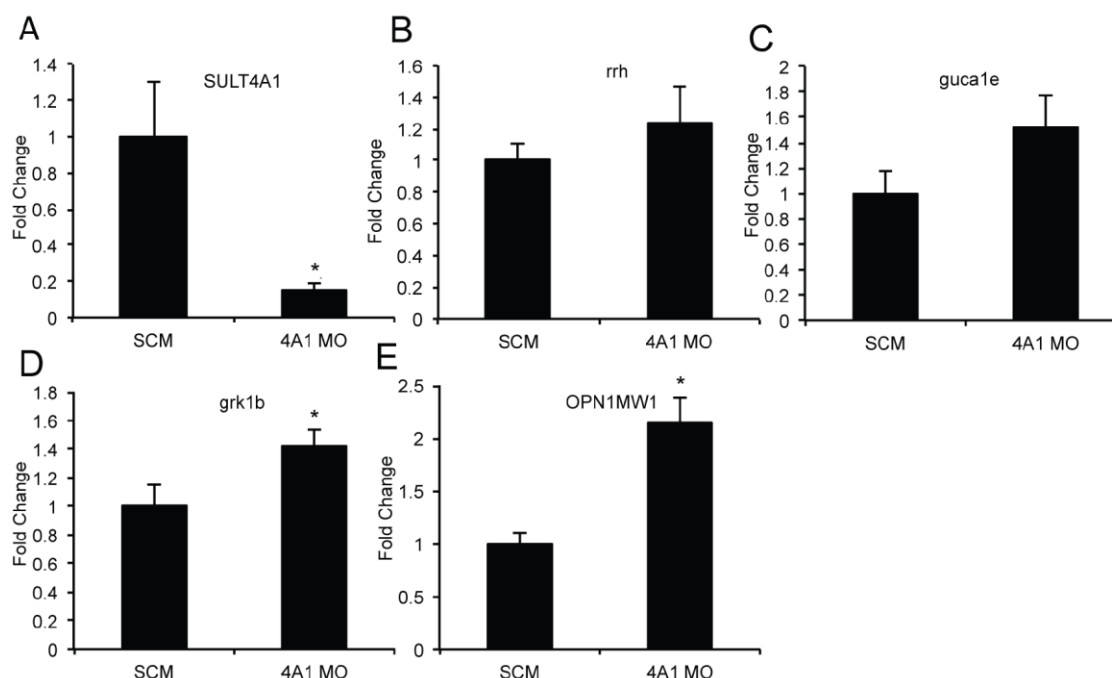


Figure 21: qPCR verification of differentially expressed phototransduction genes observed in RNA-seq data at 72 hpf. SuperScript III was used to generate cDNA from total RNA. Message level was determined on a 7900HT Sequence Detection System using pre-designed TaqMan Gene Expression Assays. Values represent average relative mRNA expression (n=3) +/- the standard error of the mean. A. SULT4A1: SCM (1.00 +/- 0.31). SULT4A1 MO (0.15 +/- 0.04). P = 0.0253. B. rh: SCM (1.00 +/- 0.12). SULT4A1 MO (1.24 +/- 0.23). P = 0.1917. C. guca1e: SCM (1.00 +/- 0.17). SULT4A1 MO (1.52 +/- 0.26). P = 0.0822. D. grk1b: SCM (1.00 +/- 0.14). SULT4A1 MO (1.43 +/- 0.11). P = 0.0392. E. OPN1MW1: SCM (1.00 +/- 0.10). SULT4A1 MO (2.15 +/- 0.22). P = 0.0047. *p<0.05 as compared to SCM-injected embryos.

Note: From “Inhibition of SULT4A1 expression induces up-regulation of phototransduction gene expression in 72-hour postfertilization zebrafish larvae” by F. Crittenden, H. Thomas, C. M. Ethen, Z. L. Wu, D. Chen, T. M. Kraft, J. M. Parant, and C. N. Falany, 2014, *Drug Metabolism and Disposition*, 42, p. 947. Copyright 2014 by The American Society for Pharmacology and Experimental Therapeutics. Reprinted with permission.

(Easter and Nicola, 1996; Kokel et al., 2010; Kokel and Peterson, 2011). Our VMR assay utilized a ZELLSAC (Figure 14) to measure the proportion of zebrafish larvae at a given time point which were responsive to the light stimulus. To optimize the lighting conditions for this assay, the assay was first performed using light intensities of 160 lx, 375 lx, 600 lx, and 800 lx. For each level of light intensity, one 96 well plate of 96 hpf larvae was subjected to 5 light interruption stimuli. Individual larvae were scored as responsive if they responded to any one of the 5 stimuli. Of the 4 light intensities used for this optimization experiment, 375 lx had the highest response rate (Figure 22).

Normal VMR development in SULT4A1 KD embryos. To determine if SULT4A1 KD larvae exhibited an impaired responsiveness to light changes, VMR was assessed at 76 hpf, 80 hpf, and 84 hpf. These time points were chosen because they are early enough that the SULT4A1 MO is still effective, but also late enough that the larvae exhibit a robust and rapidly maturing VMR. At all three time points investigated, SULT4A1 KD larvae exhibited no significant differences in VMR responsiveness when compared to SCM larvae. Both SULT4A1 KD and SCM larvae showed rapid VMR development over the course of the experiment, but the VMR in SULT4A1 KD larvae was neither advanced nor delayed (Figure 23).

Anxiety in the Novel Tank Test

Anxiety has been shown to lead to prolonged periods of inactivity in zebrafish (Egan et al., 2009). Furthermore, natural variations in anxiety levels among zebrafish populations ensure that certain strains have higher anxiety levels than others. Such is the

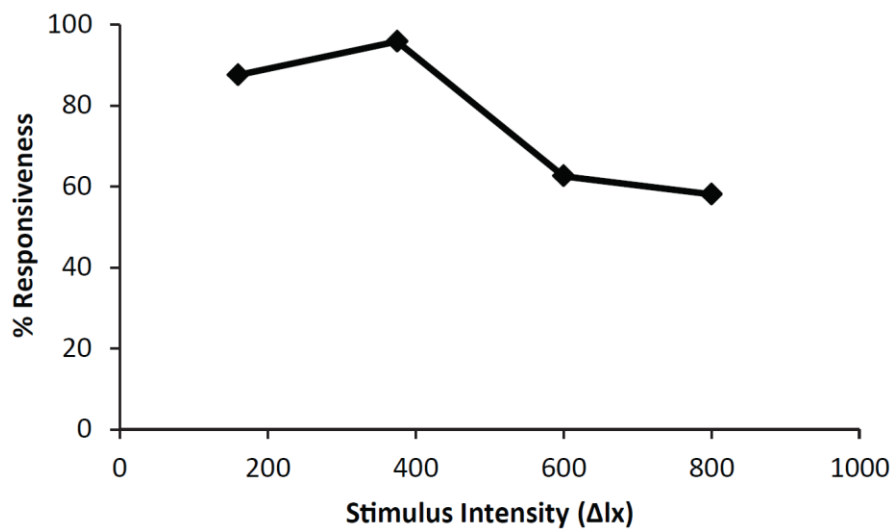


Figure 22: VMR assay light stimulus intensity optimization. For each light stimulus intensity, a total of 96 AB strain 96 hpf zebrafish larvae were subjected to 5 stimuli. Each stimulus lasted 1 s and was followed by 30 s of uninterrupted light before the next stimulus. For each individual larva, a positive response to any one of the 5 stimuli scored the individual as a positive responder. For each time point, $n = 96$.

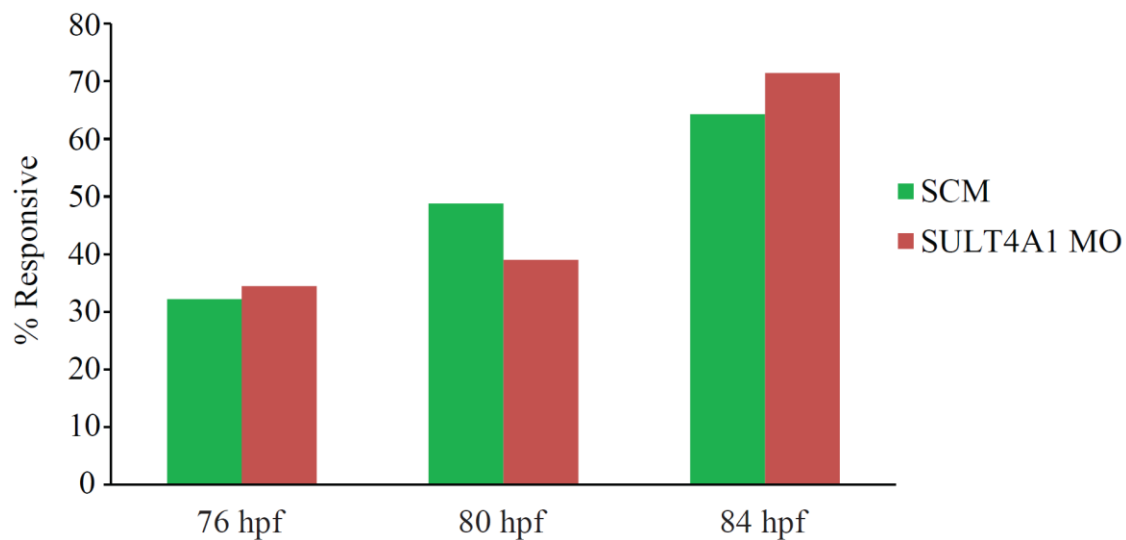


Figure 23: VMR development in 76-84 hpf SCM and SULT4A1 MO - injected larvae. No significant differences in % responsiveness of larvae were observed at any of the three time points tested. p values for each time point were determined by 2-tailed 2-sample z-test. 76 hpf: n = 87, p = 0.75. 80 hpf: n = 41, p = 0.37. 84 hpf: n = 98, p = 0.28.

case with the *leopard* skin mutant, a strain of zebrafish that presents spots instead of stripes and that also exhibits increased anxiety-like behavior (Egan et al., 2009; Cachat et al., 2011; Maximino et al., 2013). To determine whether $SULT4A1^{\Delta 8/\Delta 8}$ fish exhibited increased anxiety-like behavior, WT and mutant fish were subjected to a standard novel tank test, a test used to assess anxiety levels and locomotion in zebrafish when introduced into a novel environment (Levin et al., 2007; Bencan et al., 2009; Egan et al., 2009; Grossman et al., 2010). Over the course of the 6 min experiment, $SULT4A1^{\Delta 8/\Delta 8}$ fish did not exhibit any significant differences in latency to enter the upper half of the test chamber (Figure 24a), freezing bouts (Figure 24d), freezing duration (Figure 24e), or total distance travelled (Figure 24f). During the first 3 min of the experiment, the mutant fish displayed a decreased propensity to enter the upper half, but this did not translate into significant differences in either time in upper half or transitions to upper half (Figure 24b, c). No significant differences were observed between WT and $SULT4A1^{\Delta 15/\Delta 15}$ fish for any of these endpoints (Figure 25).

Social Preference

WT and $SULT4A1^{\Delta 8/\Delta 8}$ fish were subjected to a social preference test designed to assess social behavior and motility. The apparatus (Figure 26a) consisted of a 30 cm x 10 cm x 10 cm corridor flanked on either end by water tight compartments. One compartment (conspecific compartment) contained an unfamiliar WT fish. The other compartment (empty compartment) contained no fish. Test fish were acclimated to the center zone, and then allowed to swim freely throughout the center compartment comprised of the conspecific zone, center zone, and empty zone. In accordance with previous studies

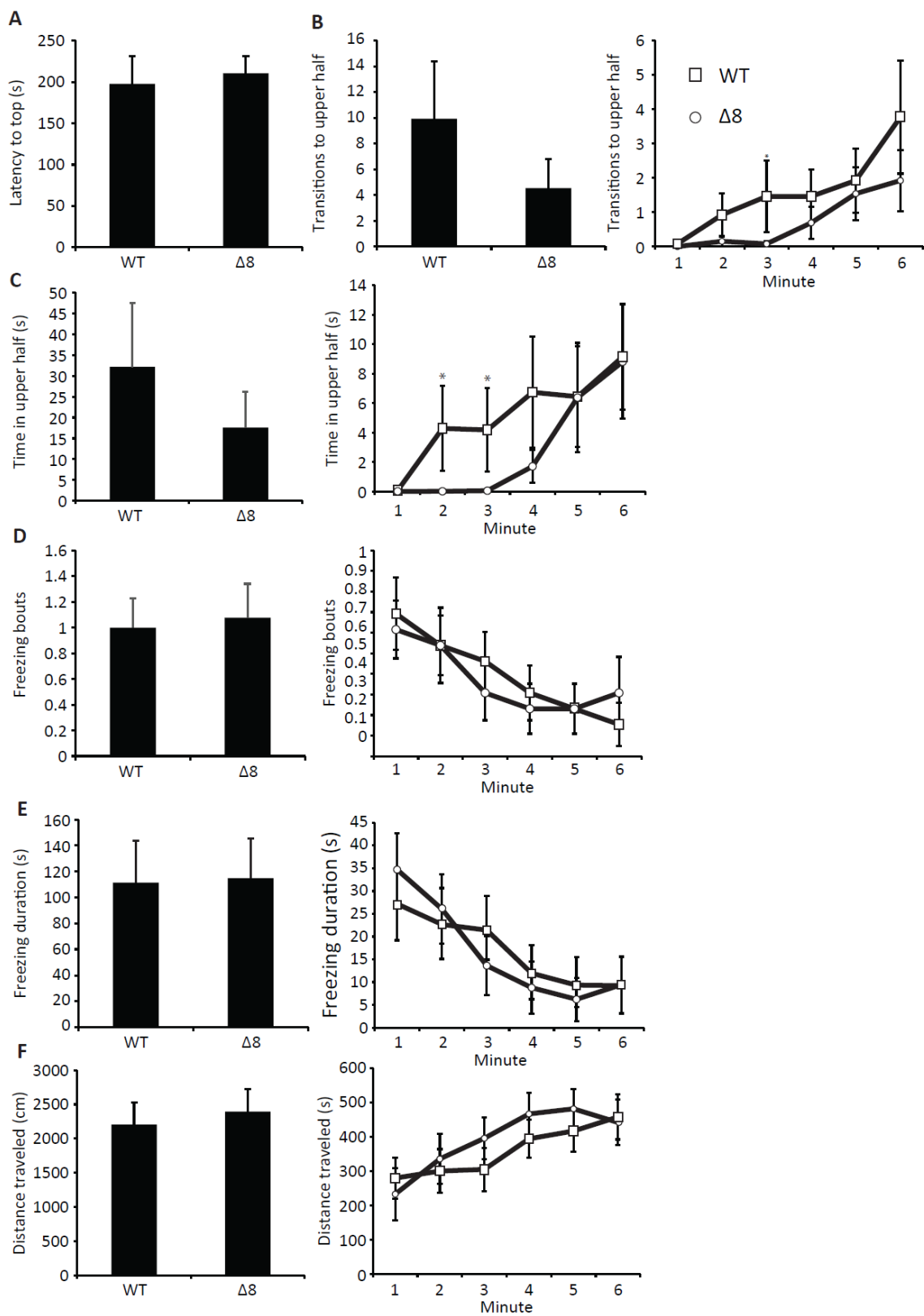


Figure 24: Standard 6 minute novel tank test in WT and SULT4A1^{Δ8/Δ8} fish. Error bars represent standard error of the mean. n = 13. Test subjects were 5 months old. (A) Latency to enter the upper half of the tank. (B) Left: total transitions to the upper half of the tank. Right: transitions to upper half per minute. (C) Left: cumulative time spent in the upper half of the tank. Right: time spent in the upper half per minute. (D) Left: total number of freezing bouts. Right: number of freezing bouts per minute. A freezing bout was defined as a total lack of movement lasting longer than 2 s. (E) Left: cumulative freezing duration. Right: freezing duration per minute. (F) Left: total distance traveled. Right: distance traveled per minute. (*P < 0.05 in Student's t test)

Note: From “Activity Suppression Behavior Phenotype in SULT4A1 Frameshift Mutant Zebrafish” by F. Crittenden, H. Thomas, J. M. Parant, and C. N. Falany, 2014, *Drug Metabolism and Disposition*, 43, p. 1037. Copyright 2015 by The American Society for Pharmacology and Experimental Therapeutics. Reprinted with permission.

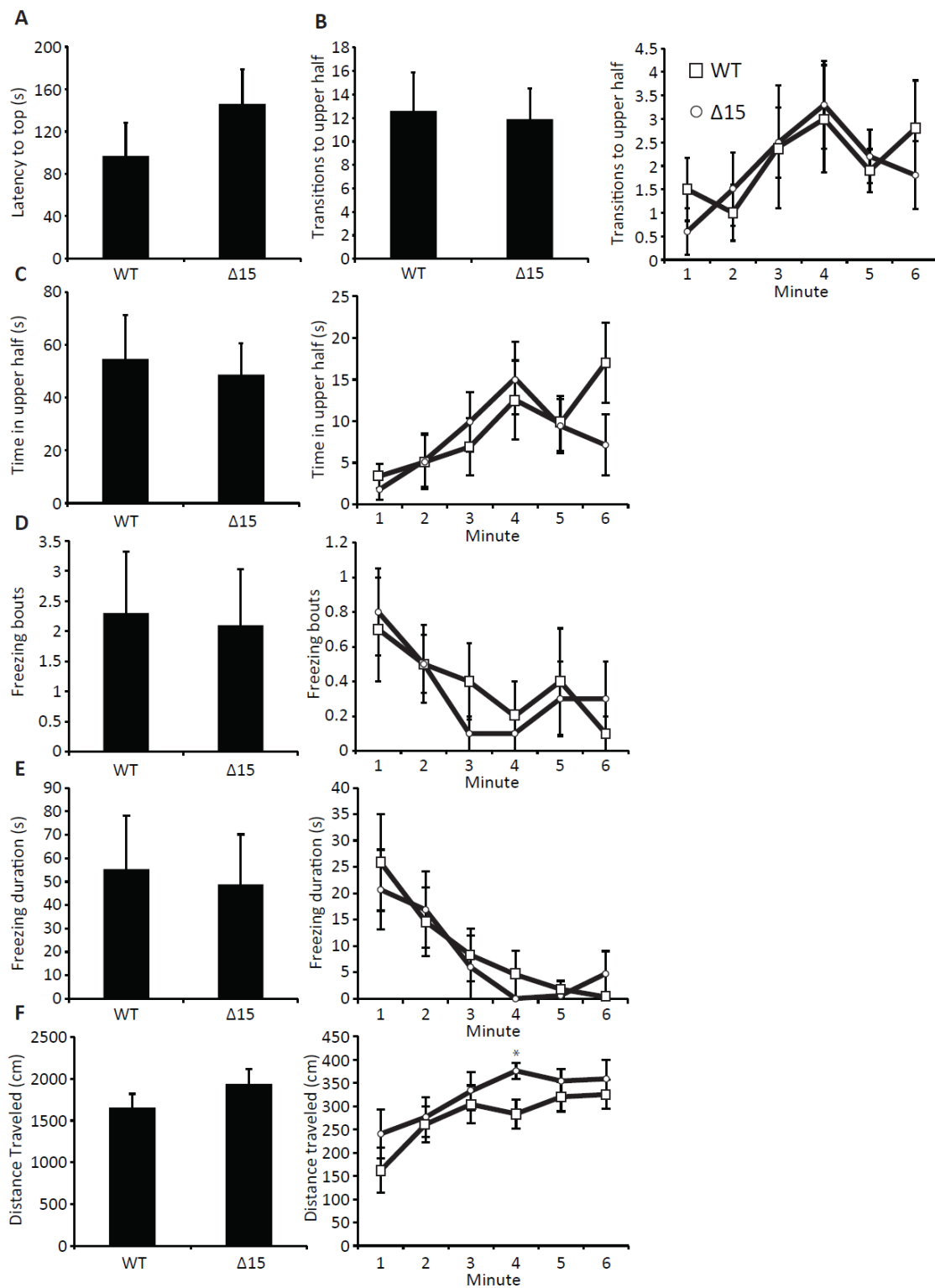


Figure 25: Standard 6 minute novel tank test in WT and SULT4A1^{Δ15/Δ15} fish. Error bars represent standard error of the mean. n = 10. Test subjects were 5 mo old. (A) Latency to enter the upper half of the tank. (B) Left: total transitions to the upper half of the tank. Right: transitions to upper half per minute. (C) Left: cumulative time spent in the upper half of the tank. Right: time spent in the upper half per minute. (D) Left: total number of freezing bouts. Right: number of freezing bouts per minute. A freezing bout was defined as a total lack of movement lasting longer than 2 s. (E) Left: cumulative freezing duration. Right: freezing duration per minute. (F) Left: total distance traveled. Right: distance traveled per minute. (*P < 0.05 in Student's t test)

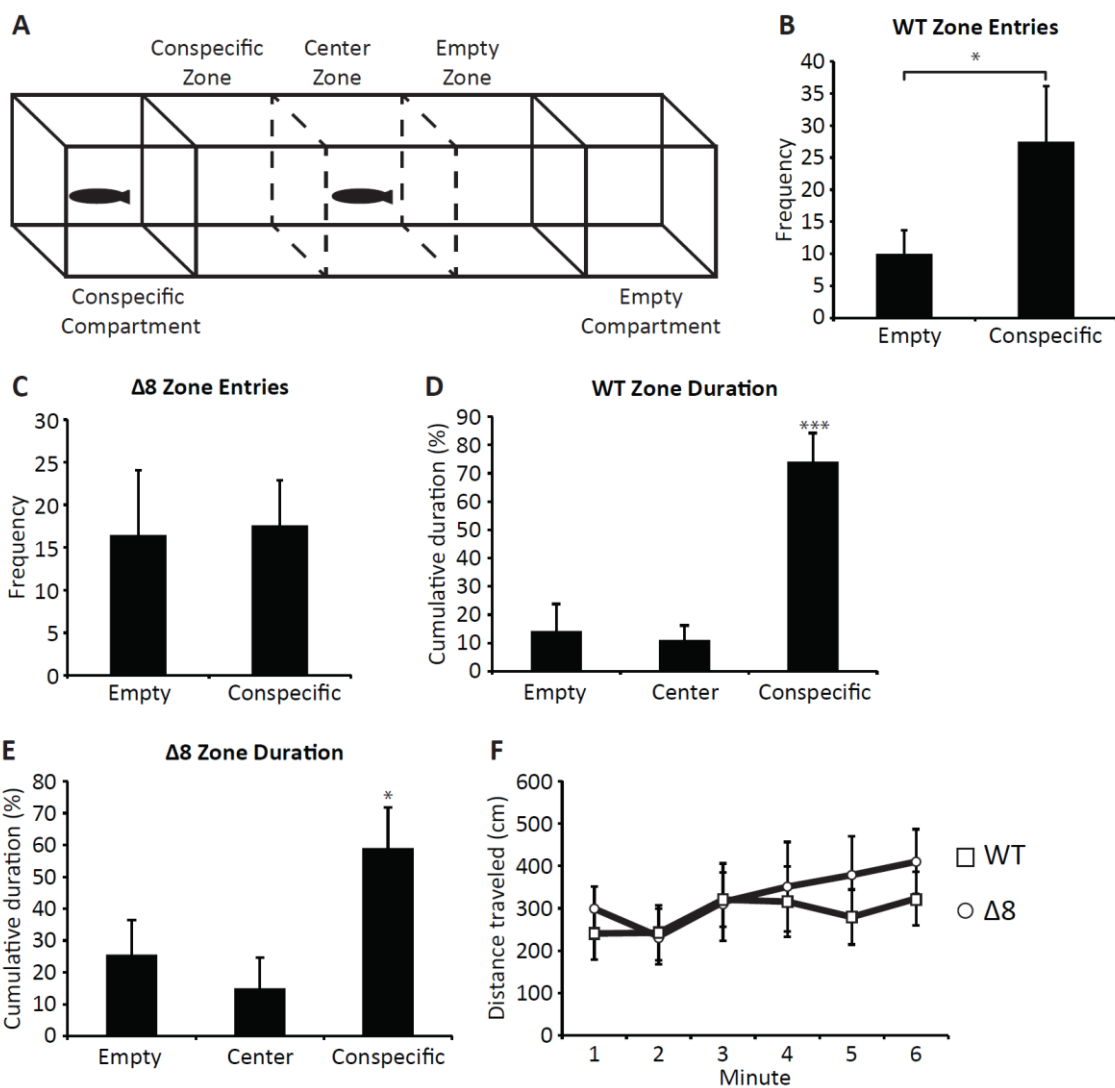


Figure 26: SULT4A1^{Δ8/Δ8} fish behavior in a social preference test. Error bars represent standard error of the mean. n = 10 (A) The apparatus consisted of a 50cm x 10cm x 10cm clear polycarbonate tank with an open top filled maximally with water. Two 10cm x 10cm x 10cm compartments at either end of the tank were separated from the rest of the tank by water tight dividers. Two more sliding dividers separated the center area into three equal-volume zones. (B) WT fish frequency of entry into the empty and conspecific zones. (C) SULT4A1^{Δ8/Δ8} fish frequency of entry into the empty and conspecific zones. (D) WT fish cumulative duration in the empty, center, and conspecific zones. (E) SULT4A1^{Δ8/Δ8} fish cumulative duration in the empty, center, and conspecific zones. (F) Distance travelled per minute. (*P < 0.05 in ANOVA)

Note: From “Activity Suppression Behavior Phenotype in SULT4A1 Frameshift Mutant Zebrafish” by F. Crittenden, H. Thomas, J. M. Parant, and C. N. Falany, 2014, *Drug Metabolism and Disposition*, 43, p. 1037. Copyright 2015 by The American Society for Pharmacology and Experimental Therapeutics. Reprinted with permission.

(Grossman et al., 2010), WT fish spent significantly more time in the conspecific zone and entered the conspecific zone more frequently than the other zones (Figure 26b, d). SULT4A1^{Δ8/Δ8} fish also spent significantly more time in the conspecific zone than both the empty and center zones (Figure 26e), but did not enter the conspecific zone more frequently (Figure 26c). No significant differences were observed in the total distance traveled by either fish throughout the experiment (Figure 26f).

Activity Analysis

Anecdotal reports of the SULT4A1 mutant fish behavior suggested that the fish were less active during daytime h. Early in the adulthood of these fish, several observers noted that the mutant zebrafish were exhibiting excessively sedentary behaviors during the day, inconsistent with published reports on diurnal activity levels and sleep in zebrafish (Zhdanova et al., 2001; Yokogawa et al., 2007; Zhdanova, 2011). Zebrafish are largely diurnal organisms which are markedly active during the day and sedentary at night during their sleep period (Yokogawa et al., 2007). Therefore, an increase in sedentary behavior during the day represents an abnormal behavior and warrants further systematic analysis. To determine whether SULT4A1^{Δ8/Δ8} fish displayed quantifiable differences in activity levels, a total of 14 WT and 14 SULT4A1^{Δ8/Δ8} fish aged 7 – 9 mo old were recorded for 48 h on a regular 14h/10h light cycle. Consistent with the anecdotal evidence, EthoVision activity analysis showed a slight decrease in activity from ZT-1 to ZT-14 with no discernible difference from ZT-15 to ZT-24 (Figure 27a). During daylight h, SULT4A1^{Δ8/Δ8} spent a larger percentage of time in an inactive state (Figure 27b) and displayed a higher inactivity bout frequency (Figure 27c). Mutant fish also displayed

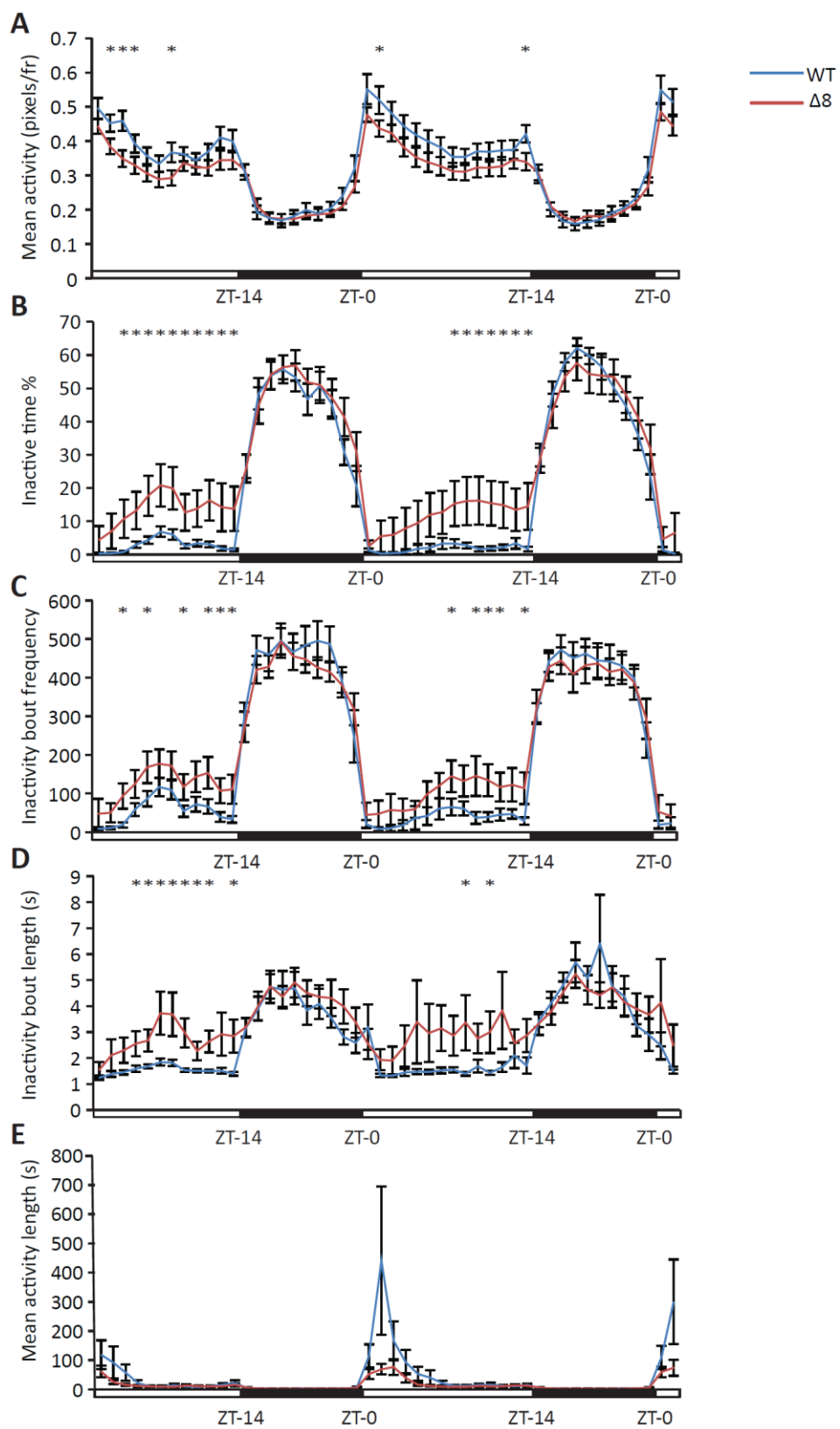


Figure 27: Suppressed activity in SULT4A1^{Δ8/Δ8} zebrafish. Error bars represent standard error of the mean. n = 14. (A) Mean activity levels. JTK_CYCLE analysis showed a significant drop in oscillatory amplitude in SULT4A1^{Δ8/Δ8} fish compared to WT fish. WT amplitude = 0.122 pixels(frame)⁻¹ +/- 0.017. SULT4A1^{Δ8/Δ8} amplitude = 0.084 pixels(frame)⁻¹ +/- 0.009. (B) Inactivity time percentage. JTK_CYCLE analysis showed a significant drop in oscillatory amplitude in SULT4A1^{Δ8/Δ8} fish compared to WT fish. WT amplitude = 11.83% +/- 2.87%. SULT4A1^{Δ8/Δ8} amplitude = 6.38% +/- 1.53%. (C) Inactivity bout frequency. JTK_CYCLE analysis did not show a significant drop in oscillatory amplitude in SULT4A1^{Δ8/Δ8} fish compared to WT fish. SULT4A1^{Δ8/Δ8} amplitude = 111.6 bouts(h)⁻¹ +/- 19.3. WT amplitude = 111.2 bouts(h)⁻¹ +/- 23.3. (D) Inactivity bout length. JTK_CYCLE analysis showed a significant drop in oscillatory amplitude in SULT4A1^{Δ8/Δ8} fish compared to WT fish. WT amplitude = 1.07s +/- 0.18s. SULT4A1^{Δ8/Δ8} amplitude = 0.65s +/- 0.09. (E) Mean activity bout length. WT peak = 256 s +/- 81.8. SULT4A1^{Δ8/Δ8} peak = 75.2 s +/- 15.3.

Note: From “Activity Suppression Behavior Phenotype in SULT4A1 Frameshift Mutant Zebrafish” by F. Crittenden, H. Thomas, J. M. Parant, and C. N. Falany, 2014, *Drug Metabolism and Disposition*, 43, p. 1037. Copyright 2015 by The American Society for Pharmacology and Experimental Therapeutics. Reprinted with permission.

increases in mean inactivity bout length during daylight h (Figure 27d). These data are summarized in Table 5. Due to the cyclic nature of these data, JTK_CYCLE analyses (Hughes et al., 2010) were used to calculate phase lag and amplitude of oscillations for each trial, and a significant decrease in the amplitude of these oscillations was observed in the mean activity level (Figure 27a) as well as inactive time % (Figure 27b) and inactivity bout length (Figure 27d) of *SULT4A1*^{Δ8/Δ8} fish. In both WT and mutant fish, a sharp spike in mean activity bout length was observed within 2 h of light onset. This peak in mean activity bout length was significantly shorter in mutant fish (Figure 27e).

Previous reports have described a sleep-like behavior in zebrafish characterized by place preference (at the top or bottom of the tank), reversible immobility, and increased arousal threshold which peak during the night-time h (Zhdanova, 2006; Yokogawa et al., 2007; Zhdanova et al., 2008; Appelbaum et al., 2009; Zhdanova, 2011). Like humans, zebrafish display diurnal sleep patterns. However, unlike the consolidated sleep bouts seen in humans, zebrafish undergo many sleep bouts throughout the night. One defining characteristic of sleep in zebrafish is an increased arousal threshold. In 2007, Yokogawa *et al* used this arousal threshold increase to define the minimum epoch of immobility to distinguish sleep from simple immobility as 6 s. Thus, if the decreased activity seen in the *SULT4A1*^{Δ8/Δ8} mutants was attributable to abnormal sleep patterns, then a selective increase in inactivity bouts greater than 6 s would be expected. However, mutant fish displayed increased daytime inactivity bout frequency for bouts lasting less than 6 s as well as those lasting greater than 6 s (Figure 28a). No changes were seen in night time or cumulative (day + night) inactivity bout frequency (Figure 28b, c)

	Light/Dark	Genotype	
		WT	$\Delta 8$
Activity (pixels/frame)	Light	0.414 +/- 0.023	0.354 +/- 0.021 *
	Dark	0.214 +/- 0.018	0.209 +/- 0.010
Inactive Time %	Light	2.27 +/- 0.19	12.15 +/- 1.13 *
	Dark	44.97 +/- 1.18	46.28 +/- 1.28
Inactivity Bout Frequency (bouts/h)	Light	45.01 +/- 17.13	106.33 +/- 36.2 *
	Dark	419.85 +/- 45.47	402.49 +/- 39.84
Inactivity Bout Length (s)	Light	1.65 +/- 0.23	2.85 +/- 0.78 *
	Dark	4.14 +/- 0.71	4.20 +/- 0.54

Table 5: Activity analysis in WT and SULT4A1 ^{$\Delta 8/\Delta 8$} fish. Asterisks indicate statistical significance in Student's *t*-test ($p < 0.05$). $n = 14$.

Note: From "Activity Suppression Behavior Phenotype in SULT4A1 Frameshift Mutant Zebrafish" by F. Crittenden, H. Thomas, J. M. Parant, and C. N. Falany, 2014, *Drug Metabolism and Disposition*, 43, p. 1037. Copyright 2015 by The American Society for Pharmacology and Experimental Therapeutics. Reprinted with permission.

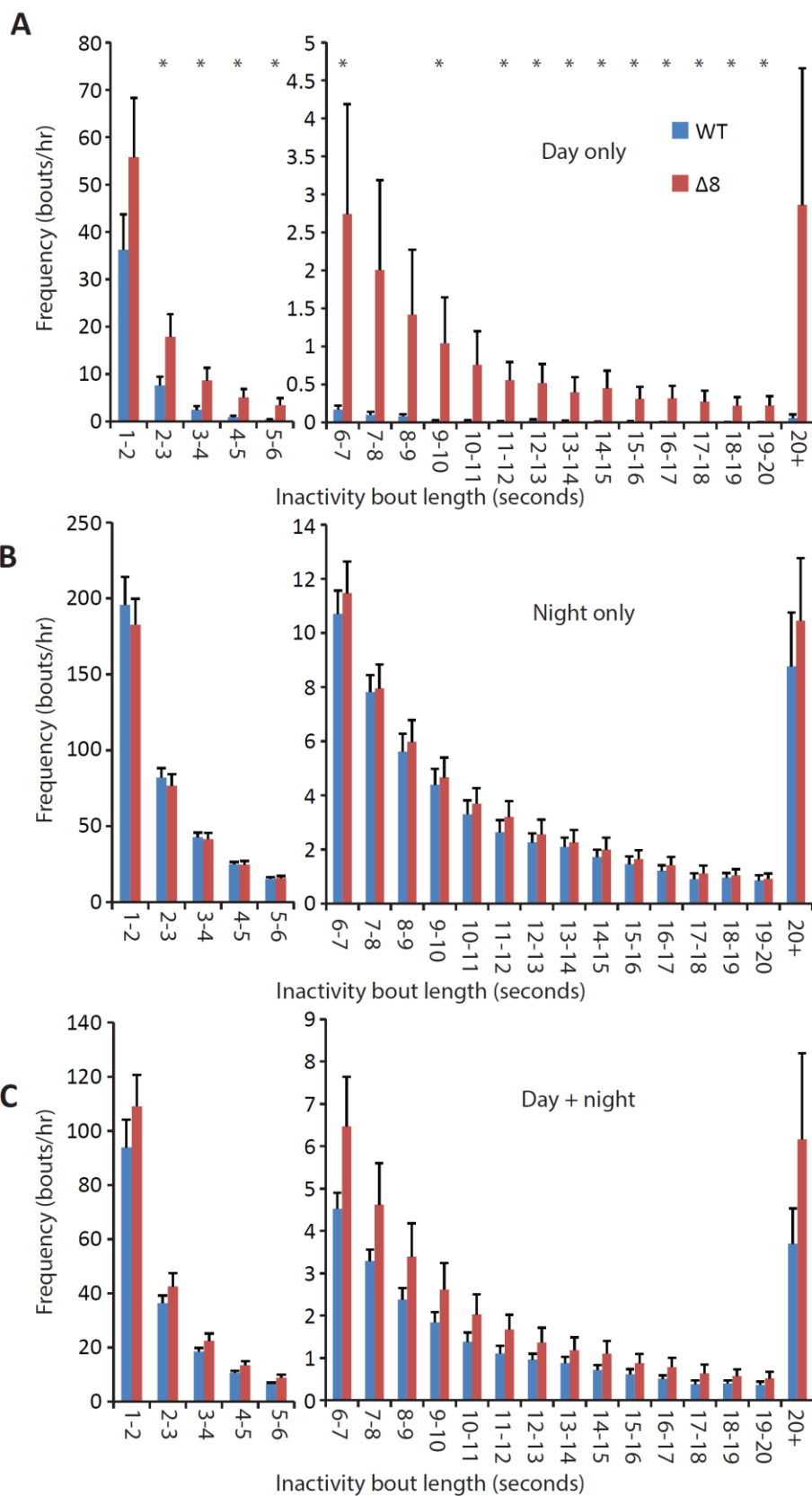


Figure 28: Frequency of different inactivity bout lengths. Error bars represent standard error of the mean. n = 14. (*P < 0.05 in Student's *t* test) (A) Day time inactivity bout frequency. (B) Night time inactivity bout frequency. (C) Cumulative (day + night) inactivity bout frequency.

Note: From “Activity Suppression Behavior Phenotype in SULT4A1 Frameshift Mutant Zebrafish” by F. Crittenden, H. Thomas, J. M. Parant, and C. N. Falany, 2014, *Drug Metabolism and Disposition*, 43, p. 1037. Copyright 2015 by The American Society for Pharmacology and Experimental Therapeutics. Reprinted with permission.

Although the SULT4A1^{Δ8/Δ8} fish did display significant differences from WT fish in the amplitude of their inactive time % and inactivity bout frequency oscillations, two SULT4A1^{Δ8/Δ8} fish had to be excluded from the JTK_CYCLE analysis for these two end points. These fish displayed no significant rhythmicity for either end point ($p > 0.05$), necessitating their exclusion from the analysis. No such arrhythmicity was observed in any of the WT fish. Representative traces of these arrhythmic fish as well as rhythmic WT fish are shown in Figure 29.

SULT4A1^{Δ15/Δ15} fish were also subjected to the same 48 h activity analysis. A total of 16 WT and 16 SULT4A1^{Δ15/Δ15} fish aged 10-12 mo were used in the experiment. Unlike the SULT4A1^{Δ8/Δ8} fish, however, SULT4A1^{Δ15/Δ15} fish did not display any differences in activity levels during the day or night (Figure 30).

Dynamic Modeling of SULT4A1^{Δ15} Mutant Protein

In contrast to the SULT4A1^{Δ8} mutation, which resulted in a frameshift at AA 89 and premature stop codon after AA 182 (Figure 12), the SULT4A1^{Δ15} mutation resulted in the deletion of 5 AA residues while leaving the rest of the protein's primary sequence still intact (Figure 11). In the only published crystal structure for SULT4A1 (1ZD1), these 5 AA residues (Glu90 – Pro94) lie within the putative substrate binding pocket directly adjacent to the “catalytic” His111. Two deleted residues, Glu90 and Tyr91, lie within 2 Å and 3.9 Å of His111, respectively (Figure 31). To investigate how the deletion of these 5 AA residues might affect the tertiary structure and stability of the SULT4A1 protein, a homology model of the SULT4A1^{Δ15} protein was created in MOE with these 5 AA residues removed. This SULT4A1^{Δ15} model as well as the native SULT4A1 model

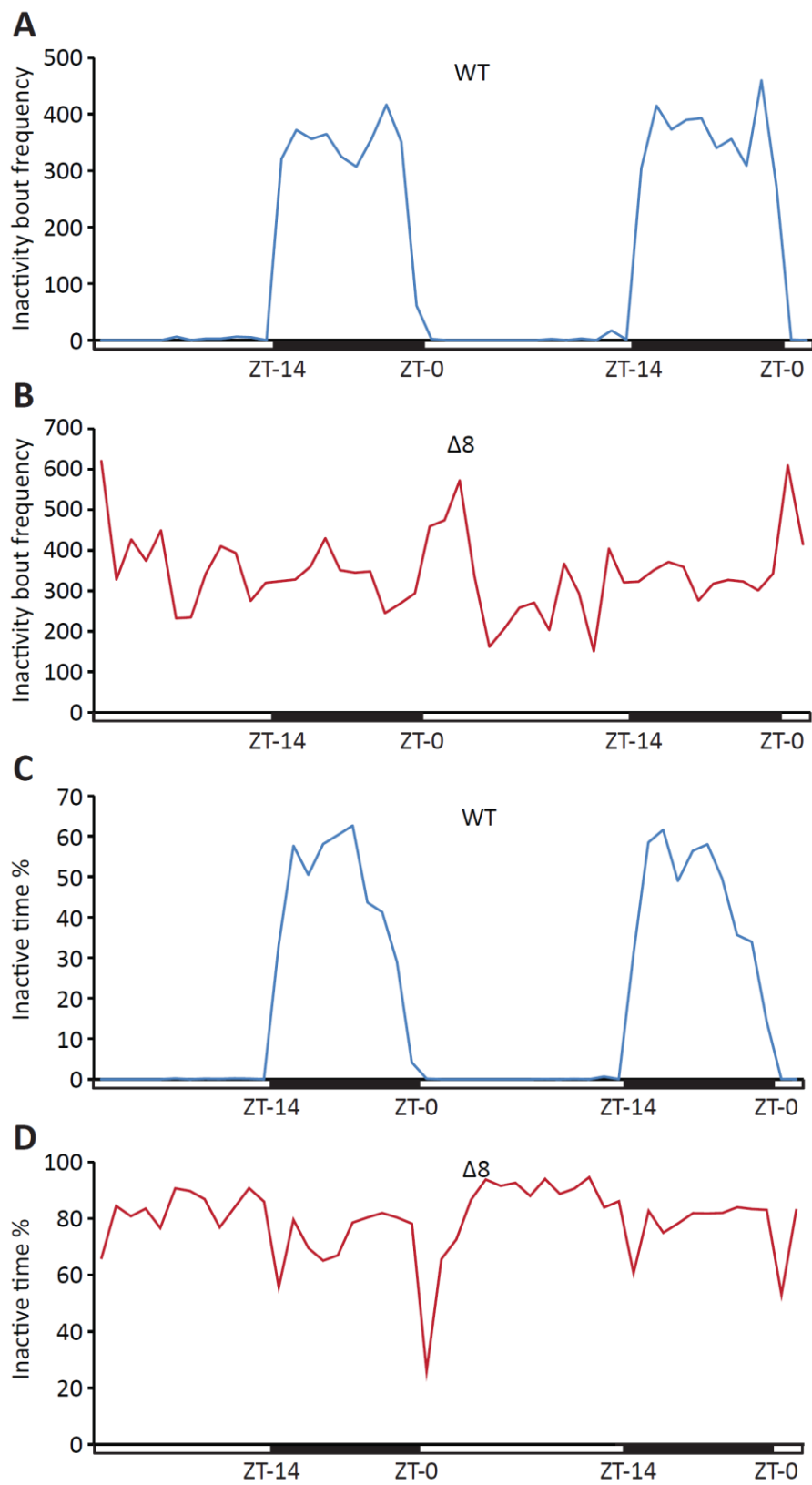


Figure 29: Arrhythmic Mutant Activity. (A) Representative inactivity frequency bout trace of a WT fish. (B) Representative inactivity bout frequency trace of an arrhythmic $SULT4A1^{\Delta 8/\Delta 8}$ fish ($p > 0.05$, JTK_CYCLE). (C) Representative inactive time % trace of a WT fish. (D) Representative inactive time % trace of an arrhythmic $SULT4A1^{\Delta 8/\Delta 8}$ fish ($p > 0.05$, JTK_CYCLE).

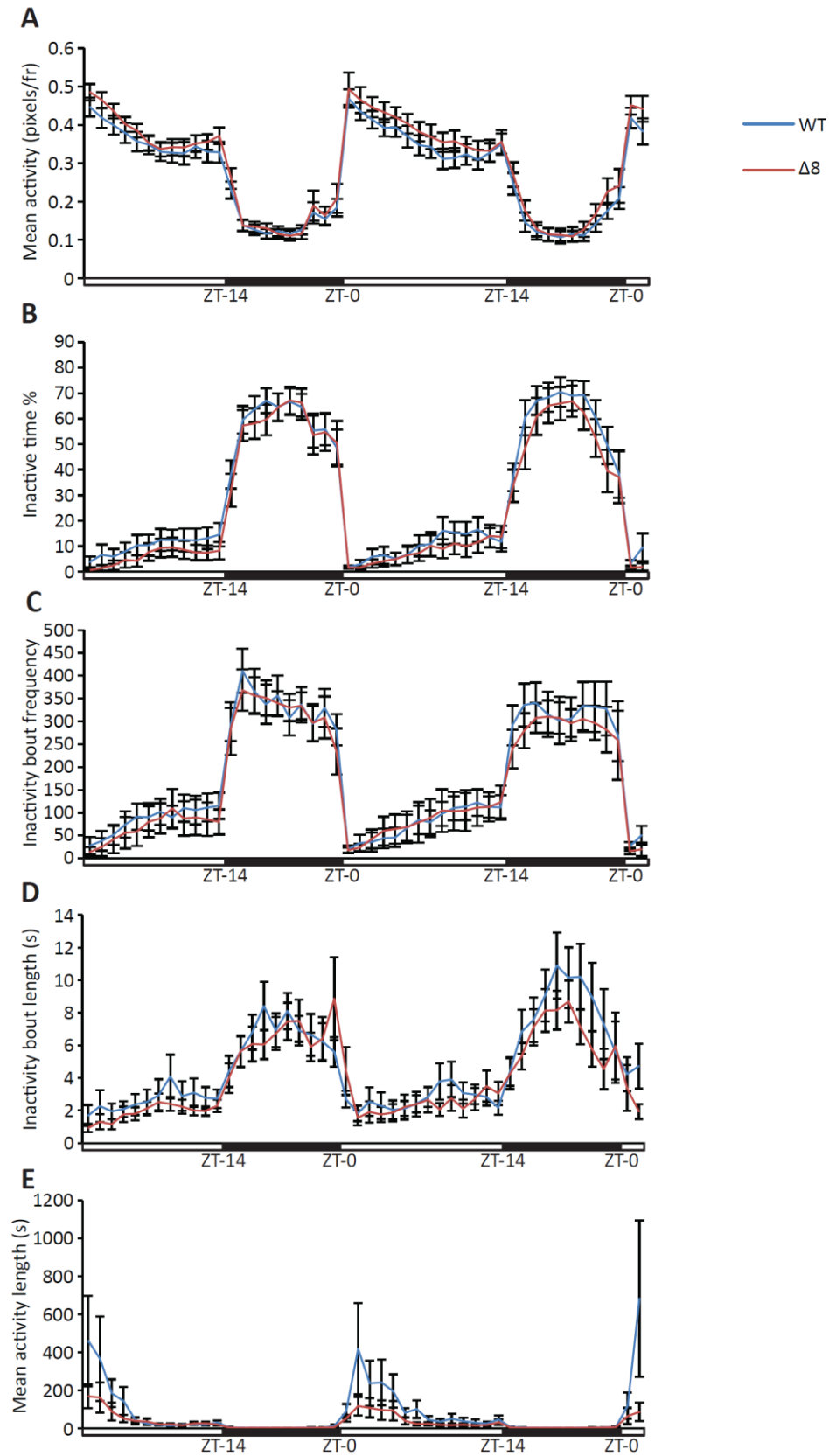


Figure 30: Unchanged activity in $SULT4A1^{\Delta 15/\Delta 15}$ zebrafish. Error bars represent standard error of the mean. $n = 16$. (A) Mean activity levels. (B) Inactivity time percentage. (C) Inactivity bout frequency. (D) Inactivity bout length. (E) Mean activity bout length.

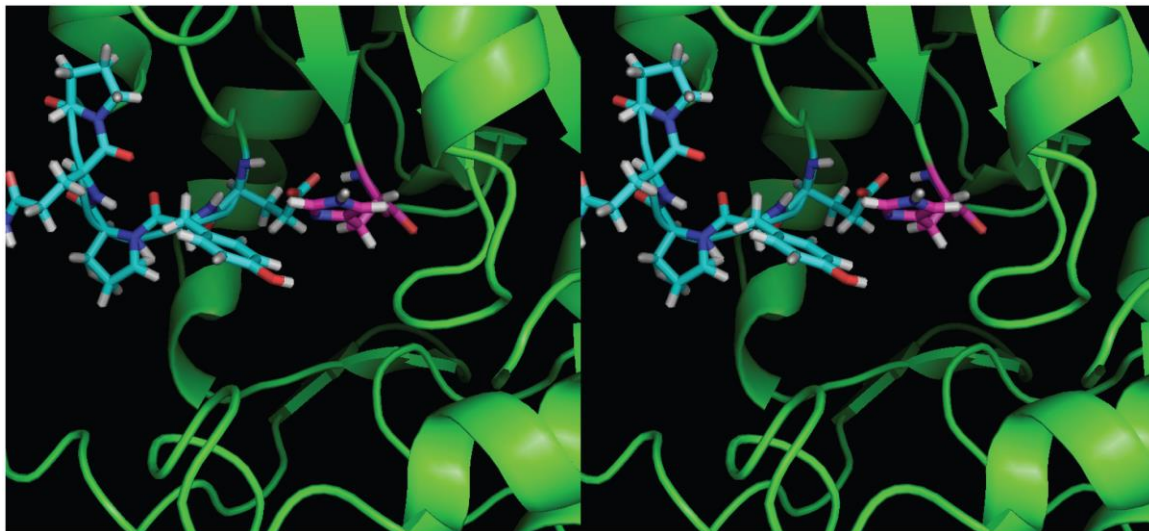


Figure 31: Stereoscopic view of the position of SULT4A1^{Δ15} deleted residues within the putative substrate binding pocket of SULT4A1. Deleted residues (blue) and “catalytic” His111 (magenta) are shown. PDB: 1ZD1

was energy minimized. Following energy minimization, the systems were equilibrated to a temperature of 310K over 100 ps followed by a 5 ns simulation at 310K.

After the 5 ns simulation, several distinct differences were observed between the WT and SULT4A1^{Δ15} proteins. These differences are depicted in Figure 32. As described earlier, the 5 AA residues deleted in the SULT4A1^{Δ15} protein lie directly adjacent to the “catalytic” His111 in the tertiary structure of the WT protein. These 5 residues are directly flanked on their amino-terminal side by Val88 and Leu89. During the simulation, these 2 residues move over to a position much closer to His111. This movement results in a 5.2 Å shift of the α -carbon atoms of both of these residues toward His111. Another notable shift takes place on the opposite side of the putative substrate binding pocket with Lys55. The α -carbon of this residue only moves 2.6 Å, but the side chain shifts 3.2 Å towards His111. The net effect of these shifts is an involution of the key residue His111 so that it is no longer accessible to the solvent.

Aim 3: Biochemical Analysis of SULT4A1

Co-Immunoprecipitation of zfSULT4A1 with YLPM1

Expression and purification of 6His-Flag-zfSULT4A1. zfSULT4A1 was expressed with a cleavable N-terminal 6His tag and Flag tag to enable a tandem co-immunoprecipitation using both a Ni²⁺-NTA affinity resin and Flag affinity matrix. The 6His-Flag-zfSULT4A1 gene construct was expressed in BL21 *E.coli* for induction and purification. Fractions from bacterial cytosol expressing this 6His-Flag-zfSULT4A1 construct were collected and analyzed by coomassie blue staining (Figure 33a) to determine relative protein concentration. Fractions exhibiting strong staining were combined, and protein

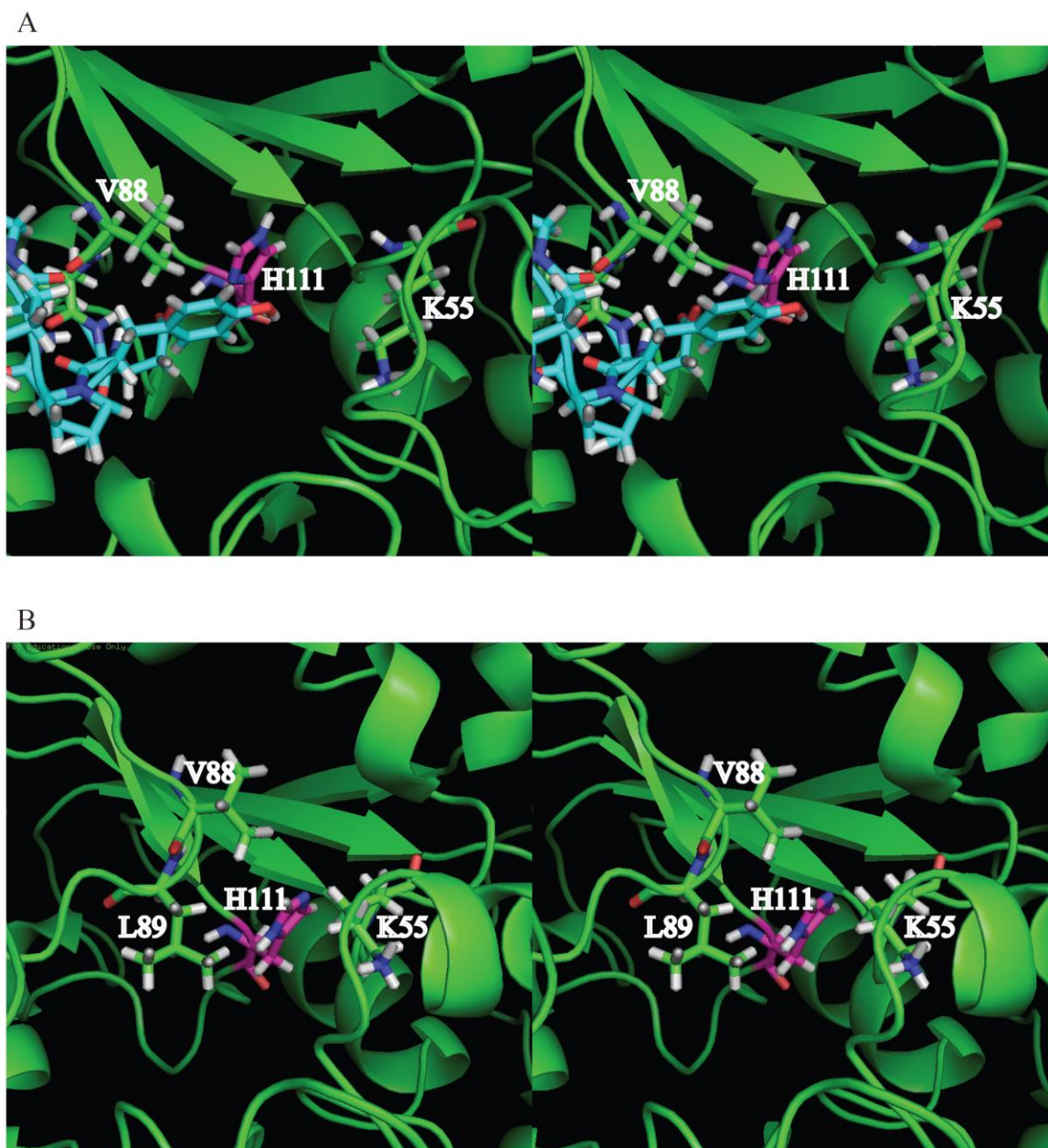


Figure 32: Stereoscopic view of the involution of His111 in SULT4A1^{Δ15} mutant protein. Molecular models of both WT SULT4A1 (A) and SULT4A1^{Δ15} (B) were subjected to a 5 ns dynamic simulation in MOE. In the SULT4A1^{Δ15} simulation, the residues Lys55, Val88, and Leu89 shifted towards the “catalytic” His111, isolating it from the solvent.

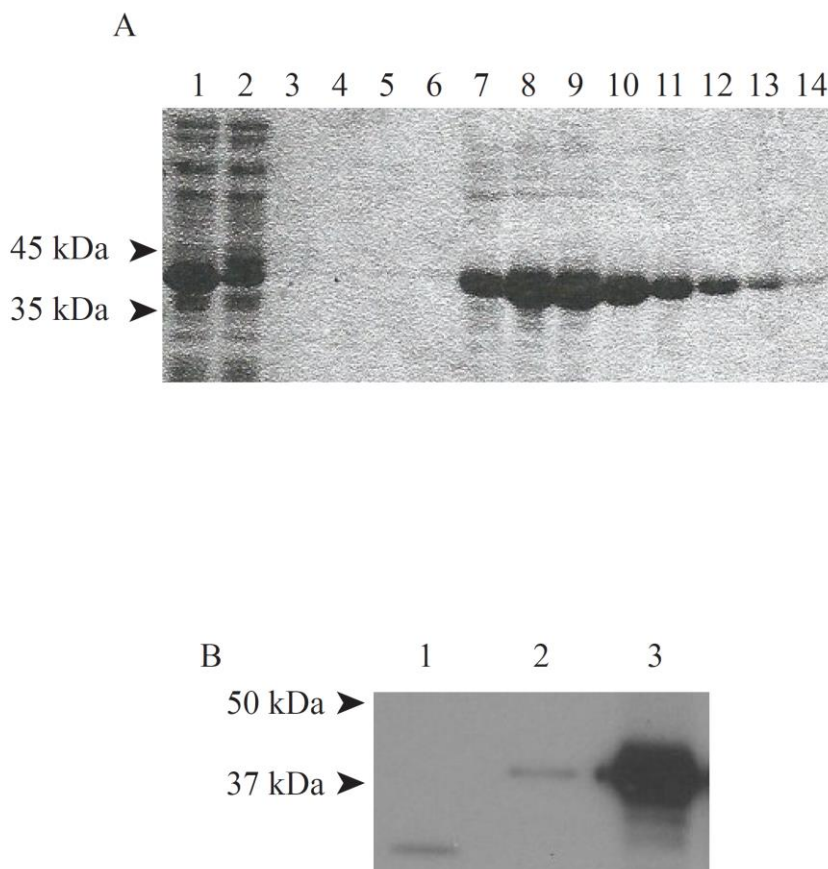


Figure 33: Expression and purification of 6His-Flag-zSULT4A1. (A) 10% acrylamide gel electrophoresis. Arrows indicate molecular weight. Lane 1: bacterial lysate after induction of 6His-Flag-zSULT4A1. Lane 2: Ni²⁺-NTA column flow through (non-bound). Lane 3: flow through after 15 bed volume wash with column buffer. After 15 bed volume wash, bound protein was eluted with 30 mL column buffer and a gradient of 10 mM imidazole to 300 mM imidazole. Fractions were collected every 1 mL. Lane 4: fraction 1. Lane 5: fraction 4. Lane 6: fraction 7. Lane 7: fraction 10. Lane 8: fraction 13. Lane 9: fraction 16. Lane 10: fraction 19. Lane 11: fraction 22. Lane 12: fraction 25. Lane 13: fraction 28. Lane 14: fraction 31. Fractions 8-17 were pooled together and dialyzed overnight against 0 mM imidazole. (B) Immunoblot of human brain lysate (lane 1), fraction 7 (lane 2), and combined fractions 8-17 (lane 3). Primary Ab was a goat α : hSULT4A1 pAb (R&D Systems), 1:200 dilution with a 2.5 h incubation. Secondary Ab was a horseradish peroxidase (HRP)-conjugated donkey α : goat Ab (Southern Biotech), 1:1000 dilution with a 1 h incubation. Blot was developed with SuperSignal™ West Pico Chemiluminescent Substrate (Life Technologies).

concentration was determined by Bradford analysis (Bradford, 1976). Immunoblot analysis of combined fractions using an anti: hSULT4A1 pAb (Protein Tech) revealed an immunoreactive band near 37 kDa (Figure 33b). The expected molecular weight of the 6His-Flag-zfSULT4A1 protein is 36.9 kDa.

Expression and purification of 6His-TEV Protease. TEV protease was expressed with an N-terminal 6His tag to enable purification. The 6His-TEV protease construct was expressed in BL21 *E.coli* and purified using a Ni²⁺-NTA affinity resin. Pooled fractions were then assayed for protease activity on the 6His-Flag-zfSULT4A1 protein construct. A total of 1 µg of 6His-TEV protease was added to 1 mg of purified 6His-Flag-zfSULT4A1 at a final concentration of 2 µg/mL. After overnight incubation at 4°C, the reaction solution was run over another Ni²⁺-NTA column to bind 6His-tagged TEV protease as well as uncut 6His-Flag-zfSULT4A1. Coomassie blue staining of both the bound and unbound fraction revealed all of the recombinant SULT4A1 to be in the unbound fractions, indicating near complete cleavage of the 6His tag (Figure 34).

Co-immunoprecipitation of YLPM1 with zfSULT4A1. To investigate whether SULT4A1 has protein binding partners in the zebrafish brain, a co-immunoprecipitation was performed using recombinant 6His-Flag-zfSULT4A1 as bait protein and zebrafish brain lysate as a prey protein source. The pulldown was carried out in conjunction with a control pulldown in which no bait protein was used, but all other conditions remained the same. After overnight incubation of zebrafish brain lysate with 6His-Flag-zfSULT4A1 bait protein, Ni²⁺-NTA affinity chromatography was used to precipitate 6His tagged bait protein

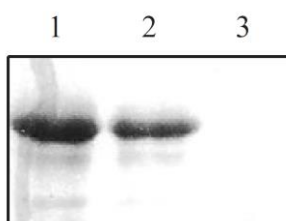


Figure 34: Activity of purified 6His-TEV Protease. Lane 1: Purified, pre-cut 6His-Flag-zSULT4A1. Lane 2: Ni²⁺-NTA column flow through after protease reaction. Lane 3: Protein bound to Ni²⁺-NTA column after protease reaction. No protein was observed in the bound fraction after the protease reaction, indicating near complete cleavage of the 6His tag.

and any bound proteins. TEV protease was used to cleave the 6His tag off of the bait protein, and then protein was further purified by Flag-affinity chromatography. Analysis of the control and pulldown samples by MS/MS revealed the presence of two peptides (Figure 35) in the pulldown sample which were unique to vertebrate YLP motif containing protein 1 (YLPM1) (Figure 36).

In-Vitro Dimerization of SULT4A1

A well-established characteristic of SULTs is their existence as homodimers *in vitro* as well as *in vivo* (Petrotchenko et al., 2001; Weitzner et al., 2009). This is facilitated through a highly conserved dimerization domain (sequence: KxxxTVxxxE) (Petrotchenko et al., 2001). Like the catalytically active SULTs, both zfSULT4A1 and hSULT4A1 contain this dimerization domain. To determine whether SULT4A1 also exists as a homodimer, purified zfSULT4A1 was subjected to size-exclusion chromatography using a Sephadex G-100 column. Fractions were collected every 1 mL after passage of the void volume, and protein concentration was determined by Bradford analysis for each fraction. Peak elution volume of zfSULT4A1 was compared to a standard curve generated using Bio-Rad Gel Filtration standards. The observed molecular weight of eluted SULT4A1 was calculated to be 61.7 kDa, in 93% agreement with the predicted dimer weight of 66.2 kDa (Figure 37).

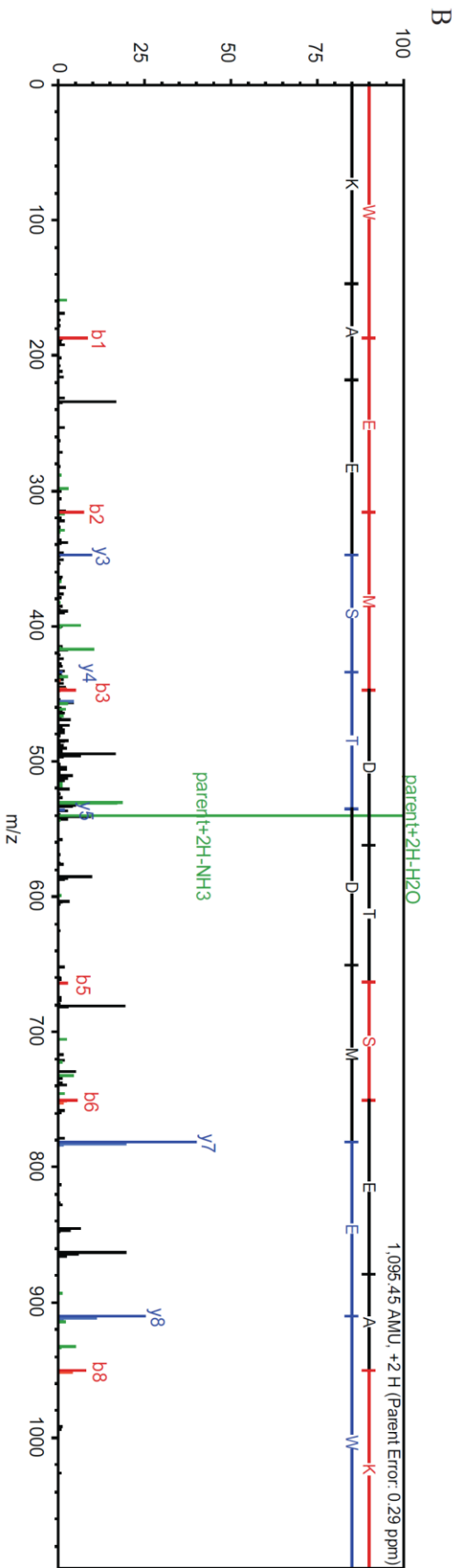
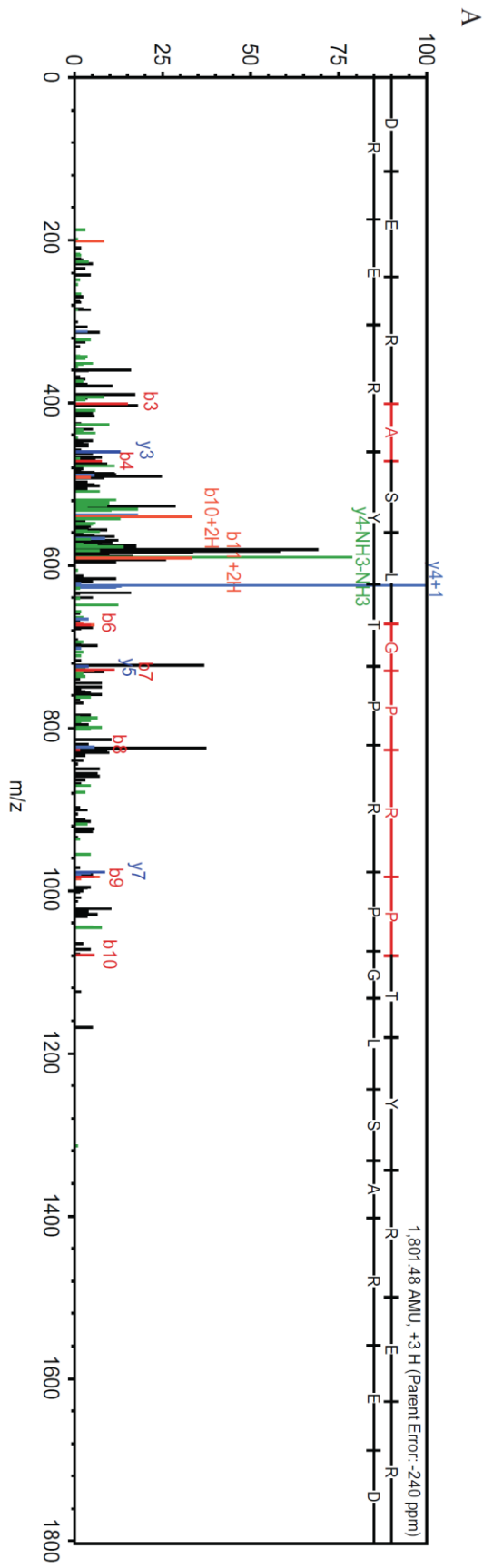


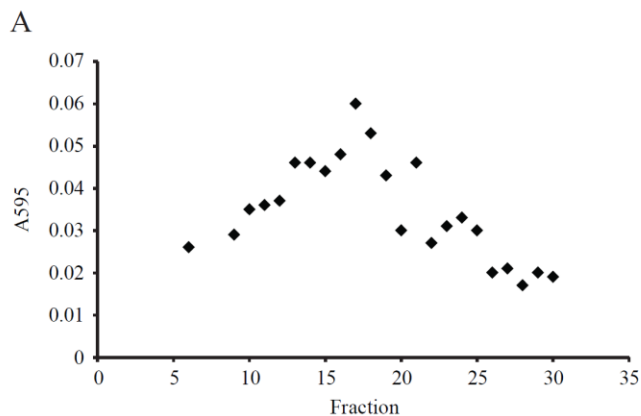
Figure 35: The MS/MS spectrum for the two unique peptides identified in the pull-down sample. (A) Sequence: DERASLGPRPTYRER. (B) Sequence: WEMDTSEAK.

```

1 MQEHAQLQQILQQYQQVIQQPAHLQTMPEMQLQHYEMQQQRFAPLYQEW 50
51 ERHFNLEWLEQFQMPYPHKDQLHDYEAQWRQWQEQMNSTSAHLQERVTTLRA 100
101 MQHQYGSSYGMMGSYGQQSPNVQMGPNMNLVGPSTPSMPPPVTMDAMP 150
151 APSTQGPSQFEGPRGPQFEQPPQQRFSGPPRFDAGQRFSPPRGNPPFFG 200
201 APARLENPPRQNTPTRFERPPVASQQGTGSGQQSSPVTGNQTKQQSAKPEA 250
251 KPVPPSYTDPDKAKSPLSQSTQKENNSSAPSMTDDLVDSDVGGFFIQSGPI 300
301 PQTKDSDKTDADSAKQDKTKEVTTKPSAPTDAPDTTNKNSNLQPPKTSHT 350
351 ANGPPQQVKPPQNKFKPDTPKETPRMLPMMNQVPPQMARGRGRGQIPMP 400
401 LRGRGRARGRGQYGGPMADPNFQREIEEDSYDHQEPGNASHGEDQDRIWR 450
451 DPSLDGPEEIDQEAPLEIWQPEEEHFPEEYPEDTHQDENWEEEPQDYWEE 500
501 EDPYWAEQRPAMRARPPFFPPGGPRRPPFFHPRFMLQGPRRPPPPGSLQHNP 550
551 LGPPPPFRPRGGVVPRFRRGLGPWGPLPRHDMMERDLRRPPAPHEIIAREP 600
601 AGPHGYEEEEIDREPAWPHPRGRGIRRPPLPPHEMGRGIRRPMPAMPRE 650
651 RWHGPPPHEEENYEEYYPYGAEDDVYRRPPHEYNEDYEHGDEYYGSREEW 700
701 DGEQPERDYPPHRPPERVREDPWLEERERSFPYEEDRYREERRGPFYPPD 750
751 PPYQDRDREPPFHSRSDWERPPPPPPPERGYSRSLSETDYEHKLDPLASL 800
801 PAPQATDSPLDESSPSATKAVLALSQRQHEIILKAAQELKMIRELQETKK 850
851 ALGEVSTTESAGLPSELPAJILGLEIPPEVKSALQATNLLSETGQTFNAG 900
901 LSSNQSTDFLSSTAPTASFIAKTVDYAHGRDGGSTVERISYGERVLLRPA 950
951 PAPSERSYEKELLGHRDPYDRSDPYAARDYDREWERDPYREKPTLDYE 1000
1001 RDRYERDRYLRDERASLGPRPTYREREREHSSRSDRELYNRPSYERS 1050
1051 YERSLEHYEHGSSSYGERRSYDERQPPPTSLPPSAPVAPPVEKKPEIKN 1100
1101 AEDILKPPGRSSRPDRIVVIMRGLPGSGKSHVAKLIRDKEVECGGAPPRV 1150
1151 LGLDDYFMTEVEKIEKDPDSGKRIKTKVLEYEYEPEMEDTYRSSMLKTFK 1200
1201 KTLDDGFFPFIILDAINDKVKYFDQFWSAAKTKGFVYLAEITTDQQTCA 1250
1251 KRNIHGRTLKDISKLSGGWESAPPHMVRDLIRSLQDAAIEDVEMEDFNP 1300
1301 SDEPKAEVKNDDDETDLGYVPKSKWEMDTSEAKLDKLDGLVGGGKRKRDA 1350
1351 GLSGMEDFLQLPDDYATRMSEPGKKRVRWADLEEQKDVDRKRAIGFVVGQ 1400
1401 TDWEKITDESGQIAQRALNRTKYF 1424

```

Figure 36: AA sequence of YPLM1. Identified peptides are highlighted yellow.



B

$$\ln(\text{MW}) = -1.735(x) + 11.75$$

$$x = \text{post void elution volume} / \text{void volume} = 17 \text{ mL} / 41 \text{ mL}$$

$$\ln(\text{MW}) = -1.735(x) + 11.75$$

$$\ln(\text{MW}) = -1.735(0.415) + 11.75$$

$$\ln(\text{MW}) = 11.02$$

$$\text{MW} = 61,696 \text{ Da}$$

Figure 37: Dimerization of zSULT4A1. (A) Elution profile of dimeric zSULT4A1 from a Sephadex G-100 column. Fractions were collected every 1 mL after passage of the void volume. Bradford analysis was used to determine relative protein concentration for each fraction. (B) Calculation of molecular weight of eluted protein. Formula was derived from elution volumes of Bio-Rad Gel Filtration Standards. MW of eluted zSULT4A1 was calculated to be 61.7 kDa.

CHAPTER 4

DISCUSSION

Effects of SULT4A1 Expression Deficiency on Development and Gene Expression in Larval and Adult Zebrafish

The use of zebrafish as a model organism provides a unique opportunity to investigate the function of SULT4A1. Advantages of the zebrafish model include the fact that large numbers of KD larvae can be generated in a very short amount of time, and the rapid onset of SULT4A1 expression and nervous system development allows generation of specimens for in vivo study of SULT4A1 more rapidly than would be possible in other vertebrate model systems. Typically, the use of zebrafish to investigate the function of human proteins would carry the disadvantage that zebrafish are more distantly related to humans than other common model organisms. However, considering the highly conserved nature of SULT4A1's sequence as well as neural localization, results from zebrafish studies may have greater relevance to the analysis of hSULT4A1 function than with less conserved proteins. Because zfSULT4A1 and hSULT4A1 are highly conserved, it is anticipated that they will have an equally conserved function.

Conventional PCR (Figure 19a), qRT-PCR (Figure 19b), immunoblot analysis (Figure 19c), and RNA-seq (Table 3) showed an effective KD of SULT4A1 expression at 72 hpf when using the SULT4A1 MO. Following fertilized egg injection, however, both the control and KD larvae developed normally, and no gross phenotypic changes could be

observed. There are a number of possible explanations for this apparent lack of a developmental phenotype. If SULT4A1 is in fact an enzyme, then an incomplete KD, as is typically achieved with MOs, may leave sufficient levels of the protein to retain its function. However, both SULT4A1^{Δ8/Δ8} and SULT4A1^{Δ15/Δ15} mutant zebrafish also develop normally, strongly indicating that SULT4A1 deficiency is not lethal.

One unexpected finding of this study was the detection of SULT4A1 mRNA in the testes via qPCR (Figure 15a). However, when full-length primers for SULT4A1 were used with cDNA from the testes, however, no amplification product was observed (Figure 15b). Likewise, no translated protein was detected in the testes by immunoblot analysis. A similar phenomenon was observed in human liver by Falany et al (2000). Hepatic expression of an incorrectly spliced and untranslatable form of hSULT4A1 mRNA was described. This type of aberrant splicing may also be occurring in the testes of zebrafish. If the included intron was of sufficient length, that could explain why no amplicon was observed after conventional PCR using full length SULT4A1 primers (Figure 15b). If intron 1 were included in the transcript, then the amplicon would increase from 860 to 6239 bases. That would be too long for amplification under the PCR conditions utilized.

Previous studies have shown the brain to be the primary site of SULT4A1 expression in humans and rats (Falany et al., 2000; Liyou et al., 2003). As expected, SULT4A1 expression was observed at high levels in the brain of adult zebrafish. Interestingly, SULT4A1 expression was also observed in the adult zebrafish eye (Figure 15a, b, Figure 16). This represents a novel finding that may provide key insights into the function of SULT4A1. If SULT4A1 does indeed prove to play an important role in vertebrate vision, then this finding further solidifies the zebrafish as a model organism to study its function.

Zebrafish have the ability to respond to light as early as 68 hpf and can track movement as early as 73 hpf (Easter and Nicola, 1996; Easter and Nicola, 1997). The strong ocular expression of SULT4A1 may also account for its relatively rapid onset of expression in zebrafish embryos, where protein was detectable by immunoblotting as early as 72 hpf (Figure 19c). This stands in contrast to rats, where significant levels of brain SULT4A1 mRNA were not detectable by Northern-blot analysis until post-natal day 21 (Falany et al., 2000). Significant retinal development occurs in rats postnatally, especially with regards to photoreceptors. Cones do not reach peak density until post-natal day 10 (Arango-Gonzalez et al., 2010). This stands in contrast to larval zebrafish vision, in which cones develop early and are the primary photoreceptor type during the first few days of eye development (Fadool and Dowling, 2008).

The ocular expression of SULT4A1 may help explain the observed up-regulation of 13 genes known to be involved in phototransduction in the MO KD study. Although adult zebrafish express higher levels of SULT4A1 in the brain than in the eye, at 72 hpf the eyes are the largest neuronal structure in the developing larvae. The immediate cause of this increase in expression remains unclear. Either SULT4A1 KD leads to an increase in the overall number of photoreceptors in the retina, or the number of photoreceptors remains the same while phototransduction protein expression increases. Given the lack of any discernible change in gross eye morphology of SULT4A1 KD larvae at 72 hpf (Figure 20), the latter seems more likely. Further investigation of the retinal histology of SULT4A1 KD and SULT4A1 mutant larvae is needed to address these possibilities.

An interesting aspect of the phototransduction up-regulation in the SULT4A1 KD larvae is that it appears to be cone-specific. Of the 13 up-regulated genes, 8 are either ex-

clusively or primarily expressed in cone photoreceptors as compared to rod photoreceptors. Four are expressed in both cones and rods, and only 1 is primarily expressed in rods. OPN1LW2, OPN1MW1, OPN1SW1, and OPN1SW2 encode the cone-specific opsin photopigments and displayed the most statistically significant up-regulation in the RNA-seq analysis. In contrast the rod-specific photopigment, rhodopsin, was not significantly dys-regulated. Arrestin 3a (*Arr3*), *grk1b*, and *grk7a* are also primarily cone genes whose expression was shown by RNA-seq to be up-regulated (Wada et al., 2006; Renninger et al., 2011). The only rod-specific gene shown to be up-regulated was the transducin alpha subunit *gnat1* (Nelson et al., 2008). The cone counterpart of *gnat1*, *gnat2*, was also up-regulated (Table 3). Larval zebrafish vision is dominated by cones (Fadool and Dowling, 2008), which may account for the disproportionate number of cone genes shown to be up-regulated in SULT4A1 KD larvae. Another possibility is that SULT4A1 KD in these embryos may somehow lead to a higher proportion of cones to rods in the developing retina. Both cells stem from the same retinal progenitor cells (Young, 1985; Wetts and Fraser, 1988; Rapaport et al., 2004), and a higher cone to rod ratio could possibly account for the cone-specific nature of the phototransduction upregulation described here. A doubling of the number of cones in the retina could be measured with a cone-specific antibody.

When the 72 hpf SULT4A1^{Δ8/Δ8} larvae were analyzed by qPCR for the same gene expression changes observed in the 72 hpf SULT4A1 KD larvae, no changes were observed. Although these results are seemingly contradictory, they are not without precedent. Numerous studies have reported instances where genetic mutation of a gene produces a profoundly different phenotype than when the same gene's expression is sup-

pressed by KD (Law and Sargent, 2014; Kok et al., 2015; Rossi et al., 2015; Stainier et al., 2015). One such example is the *EGF-like-domain, multiple 7* (*egfl7*) gene. KD of this gene has been shown to cause severe vascular tube formation defects in zebrafish, frogs, and human cells (Parker et al., 2004; Charpentier et al., 2013; Huang et al., 2014). Genetic mutation of this gene, however, causes no obvious phenotypes (Schmidt et al., 2007; Kuhnert et al., 2008). Furthermore, *egfl7* mutant zebrafish have been shown to be much less sensitive to *egfl7* MO treatment than their WT siblings, suggesting that the phenotype observed in the morphants is not due to off-target effects of the *egfl7* MO. Further investigation revealed that a separate protein, Emilin3, was upregulated in the *egfl7* mutants but not in the WT or morphant fish. Co-injection of Emilin3 mRNA with the *egfl7* MO was able to rescue the vascular phenotype seen in the morphant larvae, indicating that this was some sort of compensation mechanism that occurred in the mutants (Rossi et al., 2015). So it is possible that the lack of a phototransduction upregulation phenotype in *SULT4A1*^{Δ8/Δ8} larvae could be due to some sort of similar gene expression compensation in the mutants which does not occur in the morphants.

Despite the upregulation of phototransduction proteins observed in *SULT4A1* KD larvae, it is unlikely that *SULT4A1* plays an active role in phototransduction in the photoreceptors. Immunohistochemical analysis of *SULT4A1* in rat retinas revealed strong staining in the ganglion cell layer of the retina rather than the photoreceptor layer (Figure 18). This experiment was attempted using the same antibody in zebrafish retinas, but cross-reactivity and non-specific binding of the antibody prevented reliable analysis of the results in the fish.

The issue of non-specific binding of the SULT4A1 antibody is part of a continuing problem when using immunoaffinity to study this protein. Because SULT4A1 is so highly conserved (Table 2), all of the animals typically used to generate antibodies also express SULT4A1 with a very high level of sequence homology. As a result of this conservation, the various vertebrate SULT4A1 orthologs are not highly immunogenic. Shortly after the identification of SULT4A1, several attempts were made by our lab to generate an antibody to the human ortholog. However, because of the aforementioned immunogenicity problem, these attempts were met with little success. A suitable polyclonal antibody to hSULT4A1 was eventually made by R&D Systems using a goat as the host animal (catalog number: AF5826). This antibody is effective at detecting SULT4A1 protein in lysate prepared from neural tissue of humans, rats, and zebrafish via immunoblot and was also the primary antibody used for IHC in Figure 18. During the early stages of this project, this was the only commercially available SULT4A1 antibody. More recently, another polyclonal antibody to hSULT4A1 was developed by ProteintechTM (catalog number: 12578-1-AP) using a rabbit as the host animal. This antibody also works well against human tissue samples and is slightly better than the R&D Systems antibody at detecting SULT4A1 in immunoblots of zebrafish tissue lysate. However, there is still a substantial amount of non-specific binding when used for this purpose (Figure 13). To address this problem, we endeavored to generate a polyclonal antibody to zfSULT4A1. Recombinant zfSULT4A1 was expressed in *E.coli*, purified, and sent to Pacific Immunology (Ramona, Ca). There, it was used to inoculate a goat and raise a polyclonal antibody to zfSULT4A1. However, the serum obtained was not immunoreactive with either purified zfSULT4A1 or zebrafish brain lysate (data not shown).

Previous studies have shown that SULT4A1 does not bind the SULT cofactor product, 3', 5'-phosphoadenosine (PAP) the same way as other SULTs (Allali-Hassani et al., 2007). Our lab was also unable to show binding of ³⁵S-labeled PAPS to SULT4A1 (unpublished data). Considering this as well as the lack of detectable sulfation activity with a wide range of known SULT substrates, it is possible that SULT4A1 may act as an allosteric regulator of another protein rather than as a catalytically active SULT (Falany et al., 2000; Allali-Hassani et al., 2007). Therefore, deficits in SULT4A1 expression as seen in KD embryos could lead to dramatic changes in a cellular pathway whose activity is modulated by SULT4A1. Whether SULT4A1 is directly involved in phototransduction or some other neuronal process less specific to retinal and pineal tissue remains to be determined. However, given SULT4A1's wide distribution in the rat central nervous system (Liyou et al., 2003), the latter seems more likely. It is also possible that SULT4A1 may be expressed in the retinal ganglion cells, whose axons make up the optic nerve. While phototransduction was by far the most significantly affected cellular process in this study, this may be due to the rapid development of vision in the zebrafish larvae. Vision and the ability to react to visual stimuli play a prominent role in the development of zebrafish larvae (Easter and Nicola, 1996). Consequently, the eyes of a 72 hpf larva are disproportionately large compared to the rest of the body than those of an adult zebrafish. In contrast to KD larvae, adult SULT4A1-deficient zebrafish may present with more significant changes in different pathways such as circadian rhythm or CREB signaling in neurons (Table 4). This study is the first to identify a cellular process whose regulation appears to be associated with SULT4A1 expression. The observation that KD of SULT4A1 expression in zebrafish larvae affects expression of genes in phototransduction represents the

first possible function of this conserved orphan SULT. Characterization of visual responses and cone function in the KD larvae may identify the affected downstream visual signaling pathways.

Behavioral Abnormalities in SULT4A1 KD and Mutant Zebrafish

Because of the altered expression of phototransduction proteins observed in SULT4A1 KD larvae, it was hypothesized that these larvae would exhibit an altered responsiveness to light stimuli. To test this hypothesis, we designed and constructed an apparatus to measure the VMR of control and SULT4A1 KD mutants. During the developmental period examined, no differences in responsiveness were observed between control and SULT4A1 KD larvae. There were a number of constraints for this experiment which prevented a more thorough examination of larval VMR. First was the time frame of the KD of SULT4A1 expression. MO injection only achieves an effective suppression of gene expression for roughly 3 days (Draper et al., 2001; Morcos, 2007; Bill et al., 2009). However, the VMR response in larval zebrafish does not fully mature until day 4 or 5 post-fertilization, well after this KD window has passed. For this reason, we were only able to observe a small developmental window during which the VMR was developing and SULT4A1 expression was effectively suppressed. Observation of more mature larvae with a fully developed VMR may give different results, but this is beyond the scope of the MO KD protocol. Secondly, the capabilities of the ZELLSAC apparatus limited the type of responses we were capable of observing. Because the Canon Powershot® camera used was only capable of recording larval responses in the light, we were unable to distinguish between *lights-off* responses and *lights-on* responses. Instead, *any* movement ob-

served within the appropriate time after the end of the stimulus was scored as a positive response, whether it had initiated in response to the *lights-off* or *lights-on* portion of the stimulus.

Anecdotal reports of the SULT4A1 mutant fish behavior suggested that the fish were less active during daytime h. Early in the adulthood of these fish, several observers noted that the mutant zebrafish were exhibiting excessively sedentary behaviors during the day, inconsistent with published reports on diurnal activity levels and sleep in zebrafish (Zhdanova et al., 2001; Yokogawa et al., 2007; Zhdanova, 2011). Using the activity analysis function of EthoVision, we observed a significant decrease in daytime activity levels of adult SULT4A1^{Δ8/Δ8} zebrafish compared to WT. Interestingly, this same phenotype was not observed in SULT4A1^{Δ15/Δ15} fish. This can possibly be accounted for by the fact that the SULT4A1^{Δ8} mutation results in a frameshift and much more catastrophic mutation of the protein than the SULT4A1^{Δ15} mutation, which only results in a 5 AA deletion. This deleted portion of the SULT4A1^{Δ15} protein comprises a loop which resides within the putative active site of the protein, approximately 2 Å from the conserved catalytic His109 (Figure 31). If this lack of phenotype in SULT4A1^{Δ15/Δ15} fish proves to be reproducible, it may be because the mutated area of the protein is not as important for its function as we once thought. Another possible explanation is the differences in age between the fish used in the SULT4A1^{Δ15/Δ15} and SULT4A1^{Δ8/Δ8} experiments. The SULT4A1^{Δ8/Δ8} fish were between 7 and 9 mo old, while the SULT4A1^{Δ15/Δ15} fish were between 10 and 12 mo old. This age difference was obviously not ideal, but technical difficulties during recording delayed the SULT4A1^{Δ15/Δ15} experiment. Like

most other animals, zebrafish become gradually less active with age. This could have a masking effect on an activity phenotype that may have shown up at an earlier age.

One possible explanation for the suppressed activity observed in *SULT4A1*^{Δ8/Δ8} fish is the disruption of normal sleep cycles. Zebrafish are diurnal animals whose sleep is markedly inhibited by light (Yokogawa et al., 2007). If sleep cycle dysregulation is responsible for the suppressed daytime activity seen in the mutant fish, this would provide a unique opportunity to elucidate *SULT4A1*'s biological function. Much of the molecular machinery and effector molecules of sleep regulation, such as hypocretin and melatonin, are conserved among vertebrates (Chen et al., 2014). Zebrafish, however, are unique from most other vertebrates in that their circadian clock is decentralized (Whitmore et al., 1998; Cermakian et al., 2000). Most vertebrates (including humans) possess a small population of “pacemaker cells” within the suprachiasmatic nucleus (SCN) that are responsible for maintaining diurnal rhythms (Mistlberger, 2005). Zebrafish possess an SCN, but evidence suggests that it is not required for the normal development of circadian rhythms (Noche et al., 2011). Instead, the zebrafish brain has been shown to be globally rhythmic and light-sensitive (Whitmore et al., 1998; Moore and Whitmore, 2014). Given the diffuse nature of *SULT4A1* expression in the retina and brain outside the SCN and pineal gland in mammals (Liyou et al., 2003), it is unlikely that *SULT4A1* is involved in the maintenance of diurnal rhythms. However, it is possible that *SULT4A1* may be involved in regulating the neuronal response to circadian input from effector molecules such as hypocretins or melatonin. As in other diurnal vertebrates, hypocretins and melatonin play a central role in the regulation of sleep and wakefulness in zebrafish (Appelbaum et al., 2009; Mieda et al., 2013). Furthermore, hypocretin deficiency has

been shown to cause narcolepsy in nocturnal as well as diurnal animals, including humans (Chemelli et al., 1999; Lin et al., 1999; Peyron et al., 2000; Thannickal et al., 2000). If SULT4A1 is involved in the regulation of hypocretin signaling at the post-synaptic level, then that may help explain an increase in sleep-like behavior during the day. In order for the observed inactivity bouts to be conclusively characterized as sleep, an increase in arousal threshold will need to be demonstrated during the inactivity bouts. In zebrafish, this is typically done via electric shock. Live video tracking equipment will continuously monitor fish movement, and when movement stops for a few s, a mild electric shock is automatically delivered to the holding tank. This shock steadily increases in intensity until the fish begins to move again, and increases in the voltage required to reanimate the fish are used to distinguish sleep bouts from simple inactivity (Zhdanova, 2006; Yokogawa et al., 2007; Zhdanova, 2011). Due to the brevity and unpredictable timing of the inactivity bouts observed in SULT4A1^{Δ8/Δ8} fish, demonstrating an increased arousal threshold is exceedingly difficult. So at this point, the possibility of sleep dysregulation remains.

The identification of the SULT4A1^{Δ8/Δ8} fish which displayed no significant rhythmicity in their inactivity bout frequency and inactive time % was an unexpected and interesting finding. No SULT4A1^{Δ15/Δ15} fish and no WT fish from either the SULT4A1^{Δ8/Δ8} or SULT4A1^{Δ15/Δ15} experiments exhibited this type of arrhythmicity. These pronounced phenotypes were confirmed upon re-screening of the SULT4A1^{Δ8/Δ8} fish used in the experiment, and the arrhythmic fish have been kept for further evaluation. It is possible that these fish possess a genotype which compounds with the SULT4A1

frameshift mutation to produce a much more pronounced phenotype. That possibility remains to be explored.

Previous studies have shown that anxiety in zebrafish can lead to increased inactivity bouts (Egan et al., 2009; Cachat et al., 2010; Grossman et al., 2010; Cachat et al., 2011). However, the results of this study suggest that the increase in inactivity bouts are most likely not attributable to anxiety. In the novel tank test designed to induce and analyze anxiety in zebrafish, *SULT4A1*^{Δ15/Δ15} and *SULT4A1*^{Δ8/Δ8} fish did not show any increase over WT fish in freezing bout frequency, freezing duration, or total distance travelled. *SULT4A1*^{Δ8/Δ8} fish did show a decreased propensity to enter the upper half of the tank in the novel tank test, but only during the second and third min of the experiment, after which they did not behave differently from WT fish (Figure 24).

In 2014, our laboratory reported an upregulation of several cone-specific phototransduction genes in *SULT4A1* knockdown zebrafish larvae (Crittenden et al., 2014). This dysregulation of cone genes was observed at 72 h post fertilization and was not accompanied by any overt morphological or developmental defects. It is possible that the dysregulation of cone phototransduction genes may carry over into adulthood in the *SULT4A1* mutant fish. If such is the case, however, it does not appear as though this results in blindness in the fish. *SULT4A1*^{Δ8/Δ8} fish were able to see and identify the conspecific fish in a social preference test. Given the water-tight nature of the boundary between the center and conspecific compartments in the test, this preference is more likely attributable to vision than another social stimulus such as olfaction. Although the *SULT4A1*^{Δ8/Δ8} fish are most likely not blind, the possibility that they may have altered or impaired color vision remains to be investigated.

Elucidation of SULT4A1's role in activity regulation will require a comprehensive inquiry into the biochemical activity of SULT4A1 within the CNS. Recent work has described the post-translational modification of SULT4A1 via phosphorylation/dephosphorylation as well as a possible interaction with the peptidyl-prolyl cis-trans isomerase, Pin1 (Mitchell and Minchin, 2009; Mitchell et al., 2011). Yet little is known about the exact biological function that SULT4A1 plays on a molecular level, and understanding its role in the regulation of activity will require extensive work. Although it does not resolve address the question of the enzymatic activity or biochemical function of SULT4A1, these findings represent a major step forward in the search for this protein's function in its identification of a behavioral phenotype associated with SULT4A1 mutation.

Biochemical Analysis of SULT4A1

One of the long-term goals for this project is to identify the physiological function of SULT4A1 and to understand the role that it plays in the vertebrate nervous system. With previous studies failing to identify a substrate (Allali-Hassani et al., 2007; Minchin et al., 2008), it was hypothesized that SULT4A1 may not in fact be a catalytically active SULT. This possibility is bolstered by the observation that SULT4A1 does not bind the SULT cofactor, PAPS, likely due to the positioning of loop 3 blocking the PAPS binding site (Allali-Hassani et al., 2007).

One possibility is that SULT4A1 must first bind to another protein before it can carry out its function. This hypothesis is based in part on the observation that the putative substrate binding pocket in the crystal structure of SULT4A1 is much more open to the

solvent than it is in the catalytically active SULTs (Figure 7). Whereas in the other SULTs, loop 3 stretches out across the substrate binding pocket and effectively forms a lid over the active site, loop 3 in SULT4A1 is pulled away from the substrate binding pocket (Figure 5). SULT4A1 is the only SULT isoform which has been shown to display this loop 3 arrangement (Allali-Hassani et al., 2007), and the effect is that the conserved catalytic His residue of SULT4A1 is open to the cytosol (Figure 7). This is in contrast to the other SULTs, whose catalytic His residues are fully enclosed in the proteins' structures (Allali-Hassani et al., 2007). Given the relatively large size of the putative substrate binding pocket of SULT4A1, it is likely that the substrate (if one exists) is larger than the typical SULT substrate. The size and openness of the putative substrate binding pocket of SULT4A1 could potentially allow the binding of peptides or even whole proteins. In 2009, Mitchell and Minchin used a yeast two-hybrid screen to demonstrate an interaction between SULT4A1 and the proline isomerase Pin1 in HeLa cells (Mitchell and Minchin, 2009). This interaction was shown to have a destabilizing effect on SULT4A1. Although the interaction was confirmed by co-immunoprecipitation, these experiments were carried out in a cell line (HeLa) which does not endogenously express SULT4A1.

For this project, the co-immunoprecipitation was carried out using zebrafish brain lysate as a source of prey protein and 6His-Flag-zfSULT4A1 as bait protein. After tandem Ni²⁺-NTA affinity and α :Flag purification, MS/MS analysis revealed 2 unique peptides in the pulldown but not control samples which were shown to belong to *YLP motif containing 1* (YLPM1). Also known as ZAP3, YLPM1 was identified first by Misawa *et al* (Misawa et al., 2000) and subsequently by Sutherland *et al* (Sutherland et al., 2001). YLPM1 is a large protein (240 kDa) which has been shown to localize to the nucleus

(Sutherland et al., 2001). The exact physiological function of YLPM1 remains unclear. In 2004, Armstrong *et al* reported a role for YLPM1 as a transcription factor regulating the activity of telomerase in embryonic stem cells (Armstrong et al., 2004). A more recent report demonstrates that it complexes with 5 other nuclear proteins and suggested that it may also have a role as a nucleotide kinase (Ulke-Lemee et al., 2007).

Whether SULT4A1 and YLPM1 are true binding partners is unclear. YLPM1 is a nuclear protein (Sutherland et al., 2001). Conversely, the only published study on the localization of SULT4A1 suggests a cytosolic and in certain cases interstitial, but never nuclear, localization (Liyou et al., 2003). If SULT4A1 and YLPM1 are, in fact, binding partners, it raises interesting possibilities. Both YLPM1 and SULT4A1 are essentially orphan enzymes. SULT4A1 was identified as a putative SULT based on sequence homology to other known SULTs (Falany et al., 2000). Further investigation demonstrated an ability to bind various small molecules but failed to demonstrate any catalytic activity, likely due to an inability to bind the nucleotide cofactor, PAPS (Allali-Hassani et al., 2007). Similarly, YLPM1 was identified as a putative nucleotide kinase based on sequence homology to other known nucleotide kinases. Further investigation demonstrated an ability to bind various nucleotides, but failed to demonstrate any kinase activity (Ulke-Lemee et al., 2007). It is possible that SULT4A1 and YLPM1, two proteins with no catalytic activity by themselves, could interact in such a way that SULT4A1 binds a substrate molecule and presents it so that YLPM1 can bind and provide the nucleotide sulfate/phosphate donor. The carboxy-terminal portion of YLPM1 which contains the putative kinase domain is highly conserved in all higher eukaryotes except for fungi and worms (Ulke-Lemee et al., 2007). This indicates that if SULT4A1 and YLPM1 interact in

the zebrafish CNS, they could interact in other vertebrates as well. When the pulldown was repeated in human brain lysate, however, these results proved to be irreproducible. There are a number of ways in which the protocol could be modified to produce more reproducible results. One likely explanation for the lack of reproducibility in human brain tissue is the manner in which the brain tissue was obtained. Better control is needed over the tissue preparation and procurement process to ensure that the tissue is not fixed before lysate can be prepared from it. Also, the β -ME removal step may be superfluous and may need to be omitted in future pulldown experiments.

Any proposed model for a multi enzyme complex or other protein-protein interaction involving SULT4A1 must take into account the natural tendency for SULT4A1 to form homodimers. The KxxxTVxxxE dimerization domain is one of the most highly conserved sequences in the SULTs and is one of the distinguishing characteristics that influenced the classification of SULT4A1 as a member of the SULT gene family (Falany et al., 2000). As expected, SULT4A1 had an apparent molecular weight of 61.7 kDa when analyzed by size-exclusion chromatography. This is roughly twice the size of monomeric SULT4A1 and indicates that SULT4A1 exists as a dimer. This finding is supported by a recent study which also demonstrated homodimerization of SULT4A1 (Sidharthan et al., 2014) as well as another study which reported the crystallization of SULT4A1 with the exact same dimer interface as all of the other reported SULT crystal structures (Weitzner et al., 2009).

As noted earlier, the deleted sequence in SULT4A1 ^{Δ 15} is in a highly conserved region (Figure 38) that lies in close proximity to His109 in the tertiary structure of the protein (Figure 31, 32). It was believed that these characteristics made this region an ideal

Human	1	MAESEAETPSTPGEFESKYFEFHG-VRLPPFCRGKMEEIANFPVRPSDVW	49
Chimpanzee	1	MAESEAETPSTPGEFESKYFEFHG-VRLPPFCRGKMEEIANFPVRPSDVW	49
Rat	1	MAESEAETPSTPGEFESKYFEFHG-VRLPPFCRGKMEIDIA ^D FPVRPSDVW	49
Chicken	1	MAESEAETPSTPGEFESKYFEYKHKI ^V SPDL ^C CRHK ^G E ^E IGNFV ^V SPS ⁻ W	48
Finch	1	MAESEAETPSTPCE ^F FESKYFEYNG-VRLPPFCRGKMEEIANFPVR ^D SDVW	49
Xenopus	1	MAESEAETPSTPCE ^F FESKYFEYNG-IRLPPFCRGKMEEIS ^D DFPVRKNDI ^W	49
Zebrafish	1	MAESEVD ^T TPSTPTE ^Y ESKYFEHHG-VRLPPFCRGKME ^D EIANF ^S LRSSDI ^W	49

Human	50	IVTYPKSGT ^S LLQEVVYLV ^S QGADPDEI ^G LMNIDEQ ^L PLVLEYPQ ^F GLDII	99
Chimpanzee	50	IVTYPKSGT ^S LLQEVVYLV ^S QGADPDEI ^G LMNIDEQ ^L PLVLEYPQ ^F GLDII	99
Rat	50	IVTYPKSGT ^S LLQEVVYLV ^S QGADPDEI ^G LMNIDEQ ^L PLVLEYPQ ^F GLDII	99
Chicken	49	VICK ^A QA ^A GT ^G LLQEVVYLV ^S QGADPDEI ^G LMNIDEQ ^L PLVLEYPQ ^F GLDII	98
Finch	50	IVTYPKSGT ^S LLQEVVYLV ^S QGADPDEI ^G LMNIDEQ ^L PLVLEYPQ ^F GLDII	99
Xenopus	50	IVTYPKSGT ^S LLQEVVYLV ^S QGADPDEI ^G LMNIDEQ ^L PLVLEYPQ ^F GLDII	99
Zebrafish	50	IVTYPKSGT ^S LLQEVVYLV ^S QGADPDEI ^G LMNIDEQ ^L PLVLEYPQ ^F GL ^E II	99

PAPS binding domain **SULT4A1^{A15} deletion**

Human	100	KELTS ^P RLIKSH ^L PYRFLPS ^D LNHGDSKVI ^Y MARNPKDLV ^S SYQ ^F H ^R SL	149
Chimpanzee	100	KELTS ^P RLIKSH ^L PYRFLPS ^D LNHGDSKVI ^Y MARNPKDLV ^S SYQ ^F H ^R SL	149
Rat	100	KELTS ^P RLIKSH ^L PYRFLPS ^D LNHGDSKVI ^Y MARNPKDLV ^S SYQ ^F H ^R SL	149
Chicken	99	KELTS ^P RLIKSH ^L PYRFLPS ^D LNHGNS ^K VI ^Y MARNPKDLV ^S SYQ ^F H ^R SL	148
Finch	100	KELTS ^P RLIKSH ^L PYRFLPS ^D LNHGNS ^K VI ^Y MARNPKDLV ^S SYQ ^F H ^R SL	149
Xenopus	100	KELTS ^P RLIKSH ^L PYRFLPS ^D LNHGNS ^K VI ^Y MARNPKDLV ^S SYQ ^F H ^R SL	149
Zebrafish	100	QELTS ^P RLIKSH ^L PYRFLPS ^A MHN ^G EG ^K VI ^Y MARNPKDLV ^S SYQ ^F H ^R SL	149

His109

Human	150	RTMSYRGT ^F Q ^E FCRRFMNDK ^L GYGSWF ^E HVQ ^E FWEHRMDS ^N VLFLKYEDM	199
Chimpanzee	150	RTMSYRGT ^F Q ^E FCRRFMNDK ^L GYGSWF ^E HVQ ^E FWEHRMDS ^N MLFLKYEDM	199
Rat	150	RTMSYRGT ^F Q ^E FCRRFMNDK ^L GYGSWF ^E HVQ ^E FWEHRMD ^A NVLFLKYEDM	199
Chicken	149	RTMSYRGT ^F Q ^E FCRRFMNDK ^L GYGSWF ^E HVQ ^E FWEH ^H MDANVLFLKYEDM	198
Finch	150	RTMSYRGT ^F Q ^E FCRRFMNDK ^L GYGSWF ^E HVQ ^E FWEH ^H MDANVLFLKYEDM	199
Xenopus	150	RTMSYRGT ^F Q ^E FCRRFMNDK ^L GYGSWF ^D HVQ ^E FW ^D HRL ^D SNVLFLKYEDM	199
Zebrafish	150	RTMSYRGT ^F Q ^E FCRRFMNDK ^L GYGSWF ^E HVQ ^E FWEHRMDS ^N VLFLKYEDM	199

Human	200	HRDLVTMVEQLARFLGV ^S CDKAQLE ^A LTE ^H CHQLV ^D QCCNAEALPVGRGR	249
Chimpanzee	200	HRDLVTMVEQLARFLGV ^S CDKAQLE ^A LTE ^H CHQLV ^D QCCNAEALPVGRGR	249
Rat	200	HRDLVTMVEQLARFLGV ^S CDKAQLES ^L IE ^H CHQLV ^D QCCNAEALPVGRGR	249
Chicken	199	HKDLATMVEQLV ^R FLGVSYD ^K AQLES ^M VEHCHQLID ^Q CCNAEALPVGRGR	248
Finch	200	HKDLATMVEQLV ^R FLGVSYD ^K AQLES ^M VEHCHQLID ^Q CCNAEALPVGRGR	249
Xenopus	200	HKDLGTMVEQLV ^R FLGVSYD ^K AQLES ^T IE ^H CH ^L LLID ^Q CCNAEALP ^I GRGR	249
Zebrafish	200	YKDLGTLVEQLARFLGV ^S CDKAQLES ^L VESS ^N QLIE ^Q CCNS ^E ALS ^I CRGR	249

Loop 3

Human	250	VGLWKDIFTVSMNEKFDLVYKQKMGKCDLTFDFYL	284
Chimpanzee	250	VGLWKDIFTVSMNEKFDLVYKQKMGKCDLTFDFYL	284
Rat	250	VGLWKDIFTVSMNEKFDLVYKQKMGKCDLTFDFYL	284
Chicken	249	VGLWKDIFTVSMNEKFDLVYKQKMGKCDLTFDFYL	283
Finch	250	VGLWKDIFTVSMNEKFDLVYKQKMGKCDLTFDFYL	284
Xenopus	250	VGLWKDIFTVSMNEKFDLVYK ^Q RMG ^S DLTFE ^F SL	284
Zebrafish	250	VGLWKDV ^F FTVSMNEKFD ^A IY ^R QKMA ^A KS ^D LTDFD ^I L	284

Dimerization domain

Figure 38: SULT4A1 species alignments. AA sequences for human (*Homo sapiens*), chimpanzee (*Pan troglodytes*), rat (*Rattus norvegicus*), chicken (*Gallus gallus*), finch (*Taeniopygia guttata*), xenopus (*Xenopus tropicalis*), and zebrafish (*Danio rerio*) SULT4A1 were aligned in MacVector. Green sequence indicates agreement with the consensus SULT4A1 sequence. Yellow sequence indicates a deviation from hSULT4A1 sequence that still maintains the same biochemical properties. Red sequence indicates a deviation from hSULT4A1 that results in a change in type of AA. Canonical PAPS binding domain, catalytic His residue, SULT4A1^{Δ15} deleted region, loop 3, and SULT dimerization domain are denoted by black boxes.

site for a deletion that would result in a loss of function and an easily identifiable phenotype. However, given the lack of any observed phenotype in the *SULT4A1*^{Δ15/Δ15} fish in the behavioral assays (Figure 25, 30), it is possible that this region is not as important as was once believed. Figure 38 compares the *SULT4A1* sequences of 7 different species. The His109 residue responsible for coordinating the sulfonate transfer in the catalytic *SULTs* is conserved in all of these species, indicating that *SULT4A1* may yet serve a catalytic function. However, it is unlikely that such a catalytic function involves a sulfonate transfer from PAPS to a substrate, given the inability of *SULT4A1* to bind PAPS (Allal-Hassani et al., 2007). Despite the high level of overall sequence similarity between the orthologs of *SULT4A1* in Figure 38, one ortholog, that belonging to chickens, has a PAPS binding domain which shares less than 29% homology with the canonical PAPS binding domain and the other *SULT4A1* orthologs. Similar to the other *SULTs*, the dimerization domain of *SULT4A1* is highly conserved across the species represented in Figure 38. This conservation is reflected in the fact that *SULT4A1* has been shown to form dimers in this study (Figure 37) as well as a previous study (Sidharthan et al., 2014). The Loop 3 region, which sets *SULT4A1* apart from the other *SULTs*, is also highly conserved amongst the different orthologs represented in Figure 38. This is notable because of the observation that Loop 3 imparts a great deal of substrate specificity in the other *SULTs* (Cook et al., 2013a; Cook et al., 2013b; Cook et al., 2013c) and also because Loop 3 physically occludes the PAPS binding site in *SULT4A1* (Figure 6)

Future Directions

This study represents a substantial step forward in its identification of a behavioral phenotype associated with SULT4A1 mutation in zebrafish, although it doesn't address the underlying molecular function of SULT4A1 within the vertebrate nervous system. Future studies conducted by our lab will endeavor to uncover the specific function that this protein plays, and identification of that function will allow pharmacologic intervention to study SULT4A1's pathway in the future.

One question that has not been conclusively addressed in the scientific literature is whether or not SULT4A1 is post-translationally modified, and if so what specific modifications take place. The post-translational modification of SULT4A1 is a distinct possibility, and may be required before SULT4A1 displays any enzymatic activity (if it is, in fact, an enzyme). Previous studies have demonstrated that Thr11 on hSULT4A1 is phosphorylated by ERK1 in HeLa cells transfected with a Flag-tagged hSULT4A1 construct (Mitchell et al., 2011). This phosphorylation of SULT4A1 is then followed by binding to and destabilization by the peptidyl prolyl *cis-trans* isomerase Pin1 (Mitchell and Minchin, 2009). However all of this was demonstrated in HeLa cells, a cell line which does not express SULT4A1 naturally. Whether or not SULT4A1 is post-translationally modified in the cells of the CNS has yet to be determined. In order to answer this question, we propose to conduct a 2D gel immunoblot of human brain lysate spiked with purified bacterially-expressed SULT4A1. If SULT4A1 is phosphorylated or otherwise post-translationally modified in brain tissue, we would expect to see a shift in the isoelectric point (the first dimension) of SULT4A1 on the 2D gel. Phosphorylation at only one site on a protein has been shown to have the potential to shift the isoelectric point of the mod-

ified protein by several pH points on a 2D-gel (Zhu et al., 2005). If a shift of SULT4A1 is observed, then the spot on the 2D-gel can then be excised and analyzed by MS/MS to determine the nature of the post-translational modification.

Another possibility which has not been explored here is the potential for an obligatory ordered reaction mechanism where the substrate binds first before the sulfate donor, PAPS, can bind. Such an ordered reaction mechanism is unlikely but not without precedent. One bile acid sulfotransferase in the rhesus monkey liver only exhibits sulfotransferase activity if it binds to its substrate, glycolithocholate, first (Barnes et al., 1986). SULT4A1 has been shown to be capable of binding to apomorphine, epinephrine, and norepinephrine, albeit without any demonstrable catalytic activity (Allali-Hassani et al., 2007). It is possible that SULT4A1 must first bind to its substrate or another cofactor before PAPS can bind.

The methods used in this study to monitor the development of the VMR response in SCM and SULT4A1 KD larvae were reasonably effective at detecting movement at the onset of light at the end of the stimulus. But due to the manual scoring required during analysis, the results were restricted to a simple binary output. Either the individual larvae responded, or they didn't. However, larval zebrafish respond to light in a much more intricate and complex manner than can be assayed with such binary methods. Allwardt *et al* have described a mutant zebrafish called *no optokinetic response c* (*nrc*) which does not exhibit an optokinetic response (Allwardt et al., 2001). These larval *nrc* mutants exhibit a normal *off*-VMR and a suppressed *on*-VMR which is also delayed by as much as 15 s (Emran et al., 2007). These studies were carried out with more sophisticated recording and tracking equipment than what was available to us, and our methods and

apparatus were designed to emulate the capabilities of the more sophisticated larva recording equipment such as DanioVision™ (Noldus). Another reflex which will be assessed in mutant and WT fish is the optomotor response (OMR). The OMR describes the tendency for zebrafish to turn and swim in the direction of a perceived motion when presented with a whole-field moving stimulus (Maaswinkel and Li, 2003; Portugues and Engert, 2009). Similarly, the optokinetic response (OKR) describes the tendency of vertebrates to track a whole-field moving stimulus with a slow eye movement in the direction of the perceived motion followed by a quick return saccade. The OKR functions to stabilize the visual image on the retina and allows high visual resolution (Huang and Neuhaus, 2008). The OMR and OKR responses will be analyzed in WT and mutant zebrafish using a modified OptoMotry® apparatus (CerebralMechanics, Lethbridge, AB, Canada) as has been utilized by Tappeiner *et al* (Tappeiner et al., 2012). Improvement of our methods and equipment will allow a much more robust investigation into larval mutant responses to visual cues than has been possible up to this point.

Initially, it was hypothesized that the excessive inactivity bouts observed during the day in the SULT4A1^{Δ8/Δ8} fish were due to sleep. As discussed earlier, however, reporting these behaviors as sleep would require demonstrating an increased arousal threshold. Given the sporadic nature of the daytime inactivity bouts observed in SULT4A1^{Δ8/Δ8} fish, demonstrating an increased arousal threshold during these periods would be exceedingly difficult. However, the SULT4A1^{Δ8/Δ8} fish which displayed arrhythmic activity patterns were inactive upwards of 80% of the time during the day (Figure 29). These fish were identified and then bred with the intention of screening the progeny for a similar exaggerated phenotype. If this trait proves to be heritable, then demon-

strating an increased arousal threshold in these fish would be much more feasible due to the much higher frequency of inactivity bouts displayed by these fish.

Another possible future use for these arrhythmic fish is the potential identification of a compounding genotype which combines with the *SULT4A1*^{Δ8/Δ8} genotype to produce the exaggerated phenotype described here. If the progeny do, in fact, exhibit the same arrhythmic phenotype and excessive daytime inactivity, then that would strongly indicate that there is another genotype or gene interaction causing the phenotype in conjunction with *SULT4A1*^{Δ8/Δ8}. Identification of this hypothetical genotype would be difficult, but not impossible, given the rapidly advancing nature of the fields of genomics and transcriptomics. Identification of such a genotype could potentially point to a protein which interacts directly with *SULT4A1* or another protein in the same pathway. These arrhythmic fish should also be subjected to proteomic analysis using 2D gel electrophoresis to determine what changes in protein expression could account for the pronounced phenotype.

The 72 hpf *SULT4A1* morphant larvae exhibited a phenotype characterized by an upregulation of cone-specific phototransduction genes (Table 3). The 72 hpf *SULT4A1*^{Δ8/Δ8} larvae did not. As discussed earlier, this is likely due to a genetic compensation that occurs in the mutants but not in the morphants, but it also raises the possibility that the morphant phenotype may be caused by off-target effects of the *SULT4A1* MO. To address this possibility, *SULT4A1*^{Δ8/Δ8} embryos could be injected with the *SULT4A1* MO and assessed for the phototransduction phenotype. If the *SULT4A1*^{Δ8/Δ8} larvae are less sensitive than the WT larvae, this would argue against the possibility of off-target effects accounting for the phototransduction phenotype.

Future studies will endeavor to determine the cause of the cone-specific nature of the phototransduction upregulation. A number of hypotheses will be tested. One possibility is that SULT4A1 KD leads to a higher ratio of cone photoreceptors to rod photoreceptors in the developing retina. The retina forms early during larval zebrafish development with all cells in the retina stemming from a population of stem cells known as retinal progenitor cells (RPC) (Young, 1985; Rapaport et al., 2004). The various cell types of the retina differentiate at varying stages of retinal development. Cell fate is thought to be determined via a complex combination of intrinsic and extrinsic cues as well as stochastic mechanisms (Cepko, 2014). Therefore, it is conceivable that changes in gene expression brought about by suppression of SULT4A1 during retinal development could then lead to changes in cell fate determination and a larger population of one cell type (*e.g.*, cones) than would normally be expected. Cones typically comprise only a small proportion of the total number of photoreceptors, and the use of cone-specific antibodies can be used to quantify the proportion of cones (Clark and Kraft, 2012). Through analysis of mutant, WT, and morphant retinal histology, we will seek to quantify potential changes in cone prevalence as well as any other morphological changes brought on by SULT4A1 deficiency.

When stimulated by light, the retina produces a characteristic electrical response known as an electroretinogram (ERG). ERG recordings are a well-established tool used for investigating retinal electrophysiology (Granit, 1933; Marmor et al., 2009). Under dim lighting conditions, weak stimuli will activate rod photoreceptors, and use of sufficient background lighting will effectively bleach rods and allow the study of cone-driven responses. Combined with pharmacological block of retinal synapses, this allows research-

ers to isolate populations of rod or cone photoreceptors as isolated elements within the ERG and will facilitate the investigation of cone function in the SULT4A1 morphants as well as mutants (Korenbrodt et al., 2013). This will also allow the investigation of the possibility that the upregulation of cone genes is due to cone gene expression in rod photoreceptors, a phenomenon which has been demonstrated in *Nr1h3*^{-/-} mice (Daniele et al., 2005) and *rd7* mice (Corbo and Cepko, 2005). A hybrid rod expressing the OPN1MW1 gene, which was upregulated in 72 hpf SULT4A1 morphants, would have increased sensitivity to mid-long wavelength light. Similarly, a rod expressing abnormally high levels of GNAT2 and/or *grk7a* would likely display faster phototransduction inactivation and thus a higher sensitivity to temporal frequency of light intensity changes.

Aside from the phototransduction pathway, one of the pathways affected by SULT4A1 KD as determined by RNA seq was the circadian clock (Table 4). Two genes from this pathway, *Per1* and *NR1D1*, were found to be upregulated in the KD larvae at 72 hpf. *Per1* is one of four highly conserved proteins that drive the oscillations of the circadian clock in vertebrates (Fukada and Okano, 2002; Ishikawa et al., 2002; Yamajuku et al., 2010). The other three central proteins in this transcriptional regulation feedback loop, *BMAL1*, *CLOCK*, and *CRY* were not affected by SULT4A1 KD. In zebrafish, *Per1* mRNA expression peaks near ZT3 (Laranjeiro and Whitmore, 2014), roughly 2 h after the upregulation observed in the KD larvae. *NR1D1* is a transcription factor which regulates the transcription of several circadian clock genes including *BMAL1* (Wang et al., 2006). While *Per1* and *NR1D1* were the only two canonical circadian clock genes identified in the RNA seq results, recent reports have shown a large number of cone-specific

phototransduction genes to fall under circadian control, including several which were up-regulated by SULT4A1 KD (Laranjeiro and Whitmore, 2014).

Given its broad expression within the CNS, it is unlikely that SULT4A1 plays a role in maintaining circadian rhythms. It is possible, however, that SULT4A1 may mediate a peripheral cellular response to circadian stimulation from the hypothalamus. Hypocretin is produced in the hypothalamus by a small population of neurons that make up the SCN (Sakurai et al., 1998). These neurons, which are responsible for maintaining the circadian clock in vertebrates, have axons which project throughout the CNS and retina and use the neuropeptide, hypocretin, as one of their primary neurotransmitters (Mistlberger, 2005; Richardson, 2005). This allows the neurons of the SCN to maintain a centralized circadian clock while still exerting control over gene expression in neurons throughout the CNS and retina. If SULT4A1 is involved in mediating the peripheral neuronal response to hypocretin, this could potentially explain the observed dysregulation of the cone-specific phototransduction genes which fall under circadian control. This hypothesis could be tested by overexpressing hypocretin in the WT and SULT4A1^{Δ8/Δ8} fish and observing the changes in activity levels of the larvae using DanioVision™. Transgenic and pharmacological impairment of hypocretin signaling has implicated this neuropeptide in the promotion of wakefulness and arousal (Nishino, 2007), and overexpression of hypocretin has been shown to promote an insomnia-like state in zebrafish larvae (Prober et al., 2006).

Given the exceptional conservation of SULT4A1 across all vertebrates, there is little doubt that this protein plays an important and conserved role within the vertebrate nervous system. However, this runs counter to our observation that the SULT4A1 mutant

fish survive well into adulthood and have little difficulty breeding. Furthermore, the SULT4A1 mutants appear to behave normally aside from a slight, but significant, decrease in daytime activity levels. A logical conclusion from this would be that SULT4A1 does not play as important of a role as was once thought. However, we do not believe this to be the truth. Clearly, the forces of natural selection favor individuals with an unaltered SULT4A1 gene sequence. If the decreased activity levels seen in SULT4A1^{Δ8/Δ8} fish are also seen in other species with SULT4A1 mutations, this may help explain why there are so few SULT4A1 polymorphisms. In a controlled laboratory setting, where food is plentiful and matings are deliberately arranged, these less active fish survive and propagate with ease. In the wild, however, these individuals would be at a distinct disadvantage.

In summary, this study demonstrates that KD of SULT4A1 expression using a SULT4A1 MO results in an up-regulation of cone-specific phototransduction proteins in 72 hpf zebrafish larvae. These morphant larvae survived well into adulthood and did not display any gross developmental defects. Despite the apparent dysregulation of phototransduction, these morphant zebrafish larvae were still able to respond to light stimuli with a normal VMR. The SULT4A1 mutant zebrafish generated using TALENs also survived well into adulthood without any gross developmental defects, and did not show the same phototransduction dysregulation phenotype as the morphant larvae. Analysis of activity levels over 48 h in the SULT4A1^{Δ8/Δ8} fish demonstrated a significant drop in activity during the day. The exact cause of this drop in daytime activity levels remains unclear. Although it does not resolve the question of the enzymatic activity or biochemical function of SULT4A1, this study represents a major step forward in the search for this pro-

tein's function in its identification of a behavioral phenotype associated with SULT4A1 mutation.

REFERENCES

- Allali-Hassani A, Pan PW, Dombrovski L, Najmanovich R, Tempel W, Dong A, Loppnau P, Martin F, Thornton J, Edwards AM, Bochkarev A, Plotnikov AN, Vedadi M, and Arrowsmith CH (2007) Structural and chemical profiling of the human cytosolic sulfotransferases. *PLoS biology* 5:e97.
- Allwardt BA, Lall AB, Brockerhoff SE, and Dowling JE (2001) Synapse formation is arrested in retinal photoreceptors of the zebrafish *nrc* mutant. *The Journal of neuroscience : the official journal of the Society for Neuroscience* 21:2330-2342.
- Alnouti Y, and Klaassen CD (2006) Tissue distribution and ontogeny of sulfotransferase enzymes in mice. *Toxicological sciences : an official journal of the Society of Toxicology* 93:242-255.
- Appelbaum L, Wang GX, Maro GS, Mori R, Tovin A, Marin W, Yokogawa T, Kawakami K, Smith SJ, Gothilf Y, Mignot E, and Mourrain P (2009) Sleep-wake regulation and hypocretin-melatonin interaction in zebrafish. *Proceedings of the National Academy of Sciences of the United States of America* 106:21942-21947.
- Arango-Gonzalez B, Szabo A, Pinzon-Duarte G, Lukats A, Guenther E, and Kohler K (2010) In vivo and in vitro development of S- and M-cones in rat retina. *Investigative ophthalmology & visual science* 51:5320-5327.
- Armstrong L, Lako M, van Herpe I, Evans J, Saretzki G, and Hole N (2004) A role for nucleoprotein Zap3 in the reduction of telomerase activity during embryonic stem cell differentiation. *Mechanisms of development* 121:1509-1522.
- Armstrong RN (1991) Glutathione S-transferases: reaction mechanism, structure, and function. *Chemical research in toxicology* 4:131-140.
- Barnes S, Waldrop R, Crenshaw J, King RJ, and Taylor KB (1986) Evidence for an ordered reaction mechanism for bile salt: 3'phosphoadenosine-5'-phosphosulfate: sulfotransferase from rhesus monkey liver that catalyzes the sulfation of the hepatotoxin glycolithocholate. *Journal of lipid research* 27:1111-1123.
- Bencan Z, Sledge D, and Levin ED (2009) Buspirone, chlordiazepoxide and diazepam effects in a zebrafish model of anxiety. *Pharmacology, biochemistry, and behavior* 94:75-80.
- Benjamini Y, and Hochberg Y (1995) controlling the false discovery rate: a practical and powerful approach to multiple testing. *J Roy Statist Soc Ser B* 57:289-300.
- Best JD, and Alderton WK (2008) Zebrafish: An in vivo model for the study of neurological diseases. *Neuropsychiatric disease and treatment* 4:567-576.
- Bill BR, Petzold AM, Clark KJ, Schimmenti LA, and Ekker SC (2009) A primer for morpholino use in zebrafish. *Zebrafish* 6:69-77.

- Blanchard RL, Freimuth RR, Buck J, Weinshilboum RM, and Coughtrie MW (2004) A proposed nomenclature system for the cytosolic sulfotransferase (SULT) superfamily. *Pharmacogenetics* 14:199-211.
- Boch J, Scholze H, Schornack S, Landgraf A, Hahn S, Kay S, Lahaye T, Nickstadt A, and Bonas U (2009) Breaking the code of DNA binding specificity of TAL-type III effectors. *Science (New York, NY)* 326:1509-1512.
- Bogdanove AJ, and Voytas DF (2011) TAL effectors: customizable proteins for DNA targeting. *Science (New York, NY)* 333:1843-1846.
- Bonaglia MC, Giorda R, Beri S, De Agostini C, Novara F, Fichera M, Grillo L, Galesi O, Vetro A, Ciccone R, Bonati MT, Giglio S, Guerrini R, Osimani S, Marelli S, Zucca C, Grasso R, Borgatti R, Mani E, Motta C, Molteni M, Romano C, Greco D, Reitano S, Baroncini A, Lapi E, Cecconi A, Arrigo G, Patricelli MG, Pantaleoni C, D'Arrigo S, Riva D, Sciacca F, Dalla Bernardina B, Zoccante L, Darra F, Termine C, Maserati E, Bigoni S, Priolo E, Bottani A, Gimelli S, Bena F, Brusco A, di Gregorio E, Bagnasco I, Giussani U, Nitsch L, Politi P, Martinez-Frias ML, Martinez-Fernandez ML, Martinez Guardia N, Bremer A, Anderlid BM, and Zuffardi O (2011) Molecular mechanisms generating and stabilizing terminal 22q13 deletions in 44 subjects with Phelan/McDermid syndrome. *PLoS genetics* 7:e1002173.
- Bradford MM (1976) A rapid and sensitive method for the quantitation of microgram quantities of protein utilizing the principle of protein-dye binding. *Analytical biochemistry* 72:248-254.
- Brennan MD, and Condra J (2005) Transmission disequilibrium suggests a role for the sulfotransferase-4A1 gene in schizophrenia. *American journal of medical genetics Part B, Neuropsychiatric genetics : the official publication of the International Society of Psychiatric Genetics* 139b:69-72.
- Butcher NJ, Mitchell DJ, Burow R, and Minchin RF (2010) Regulation of mouse brain-selective sulfotransferase *sult4a1* by cAMP response element-binding protein and activating transcription factor-2. *Molecular pharmacology* 78:503-510.
- Cachat J, Stewart A, Grossman L, Gaikwad S, Kadri F, Chung KM, Wu N, Wong K, Roy S, Suciuc C, Goodspeed J, Elegante M, Bartels B, Elkhayat S, Tien D, Tan J, Denmark A, Gilder T, Kyzar E, Dileo J, Frank K, Chang K, Utterback E, Hart P, and Kalueff AV (2010) Measuring behavioral and endocrine responses to novelty stress in adult zebrafish. *Nature protocols* 5:1786-1799.
- Cachat J, Stewart A, Utterback E, Hart P, Gaikwad S, Wong K, Kyzar E, Wu N, and Kalueff AV (2011) Three-dimensional neurophenotyping of adult zebrafish behavior. *PloS one* 6:e17597.
- Cepko C (2014) Intrinsically different retinal progenitor cells produce specific types of progeny. *Nature reviews Neuroscience* 15:615-627.
- Cermak T, Doyle EL, Christian M, Wang L, Zhang Y, Schmidt C, Baller JA, Somia NV, Bogdanove AJ, and Voytas DF (2011) Efficient design and assembly of custom TALEN and other TAL effector-based constructs for DNA targeting. *Nucleic acids research* 39:e82.
- Cermakian N, Whitmore D, Foulkes NS, and Sassone-Corsi P (2000) Asynchronous oscillations of two zebrafish CLOCK partners reveal differential clock control and

- function. *Proceedings of the National Academy of Sciences of the United States of America* 97:4339-4344.
- Charpentier MS, Christine KS, Amin NM, Dorr KM, Kushner EJ, Bautch VL, Taylor JM, and Conlon FL (2013) CASZ1 promotes vascular assembly and morphogenesis through the direct regulation of an EGFL7/RhoA-mediated pathway. *Developmental cell* 25:132-143.
- Chemelli RM, Willie JT, Sinton CM, Elmquist JK, Scammell T, Lee C, Richardson JA, Williams SC, Xiong Y, Kisanuki Y, Fitch TE, Nakazato M, Hammer RE, Saper CB, and Yanagisawa M (1999) Narcolepsy in orexin knockout mice: molecular genetics of sleep regulation. *Cell* 98:437-451.
- Chen Q, de Lecea L, Hu Z, and Gao D (2014) The Hypocretin/Orexin System: An Increasingly Important Role in Neuropsychiatry. *Medicinal research reviews*.
- Christian M, Cermak T, Doyle EL, Schmidt C, Zhang F, Hummel A, Bogdanove AJ, and Voytas DF (2010) Targeting DNA double-strand breaks with TAL effector nucleases. *Genetics* 186:757-761.
- Clark ME, and Kraft TW (2012) Measuring rodent electroretinograms to assess retinal function. *Methods in molecular biology (Clifton, NJ)* 884:265-276.
- Condra JA, Neibergs H, Wei W, and Brennan MD (2007) Evidence for two schizophrenia susceptibility genes on chromosome 22q13. *Psychiatric genetics* 17:292-298.
- Cong L, Ran FA, Cox D, Lin S, Barretto R, Habib N, Hsu PD, Wu X, Jiang W, Marraffini LA, and Zhang F (2013) Multiplex genome engineering using CRISPR/Cas systems. *Science (New York, NY)* 339:819-823.
- Cook I, Wang T, Almo SC, Kim J, Falany CN, and Leyh TS (2013a) The gate that governs sulfotransferase selectivity. *Biochemistry* 52:415-424.
- Cook I, Wang T, Almo SC, Kim J, Falany CN, and Leyh TS (2013b) Testing the sulfotransferase molecular pore hypothesis. *The Journal of biological chemistry* 288:8619-8626.
- Cook I, Wang T, Falany CN, and Leyh TS (2013c) High accuracy in silico sulfotransferase models. *The Journal of biological chemistry* 288:34494-34501.
- Cook IT, Leyh TS, Kadlubar SA, and Falany CN (2010) Structural rearrangement of SULT2A1: effects on dehydroepiandrosterone and raloxifene sulfation. *Hormone molecular biology and clinical investigation* 1:81-87.
- Corbo JC, and Cepko CL (2005) A hybrid photoreceptor expressing both rod and cone genes in a mouse model of enhanced S-cone syndrome. *PLoS genetics* 1:e11.
- Coughtrie MW (2002) Sulfation through the looking glass--recent advances in sulfotransferase research for the curious. *The pharmacogenomics journal* 2:297-308.
- Crittenden F, Thomas H, Ethen CM, Wu ZL, Chen D, Kraft TW, Parant JM, and Falany CN (2014) Inhibition of SULT4A1 expression induces up-regulation of phototransduction gene expression in 72-hour postfertilization zebrafish larvae. *Drug metabolism and disposition: the biological fate of chemicals* 42:947-953.
- Dahlem TJ, Hoshijima K, Jurynek MJ, Gunther D, Starker CG, Locke AS, Weis AM, Voytas DF, and Grunwald DJ (2012) Simple methods for generating and detecting locus-specific mutations induced with TALENs in the zebrafish genome. *PLoS genetics* 8:e1002861.

- Daniele LL, Lillo C, Lyubarsky AL, Nikonov SS, Philp N, Mears AJ, Swaroop A, Williams DS, and Pugh EN, Jr. (2005) Cone-like morphological, molecular, and electrophysiological features of the photoreceptors of the Nrl knockout mouse. *Investigative ophthalmology & visual science* 46:2156-2167.
- Danielson PB (2002) The cytochrome P450 superfamily: biochemistry, evolution and drug metabolism in humans. *Current drug metabolism* 3:561-597.
- Deas TS, Bennett CJ, Jones SA, Tilgner M, Ren P, Behr MJ, Stein DA, Iversen PL, Kramer LD, Bernard KA, and Shi PY (2007) In vitro resistance selection and in vivo efficacy of morpholino oligomers against West Nile virus. *Antimicrobial agents and chemotherapy* 51:2470-2482.
- Diao X, Pang X, Xie C, Guo Z, Zhong D, and Chen X (2014) Bioactivation of 3-n-butylphthalide via sulfation of its major metabolite 3-hydroxy-NBP: mediated mainly by sulfotransferase 1A1. *Drug metabolism and disposition: the biological fate of chemicals* 42:774-781.
- Disciglio V, Lo Rizzo C, Mencarelli MA, Mucciolo M, Marozza A, Di Marco C, Massarelli A, Canocchi V, Baldassarri M, Ndoni E, Frullanti E, Amabile S, Anderlid BM, Metcalfe K, Le Caignec C, David A, Fryer A, Boute O, Joris A, Greco D, Pecile V, Battini R, Novelli A, Fichera M, Romano C, Mari F, and Renieri A (2014) Interstitial 22q13 deletions not involving SHANK3 gene: a new contiguous gene syndrome. *American journal of medical genetics Part A* 164:1666-1676.
- Dong D, Ako R, and Wu B (2012) Crystal structures of human sulfotransferases: insights into the mechanisms of action and substrate selectivity. *Expert opinion on drug metabolism & toxicology* 8:635-646.
- Doyle EL, Booher NJ, Standage DS, Voytas DF, Brendel VP, Vandyk JK, and Bogdanove AJ (2012) TAL Effector-Nucleotide Targeter (TALE-NT) 2.0: tools for TAL effector design and target prediction. *Nucleic acids research* 40:W117-122.
- Draper BW, Morcos PA, and Kimmel CB (2001) Inhibition of zebrafish fgf8 pre-mRNA splicing with morpholino oligos: a quantifiable method for gene knockdown. *Genesis (New York, NY : 2000)* 30:154-156.
- Easter SS, Jr., and Nicola GN (1996) The development of vision in the zebrafish (*Danio rerio*). *Developmental biology* 180:646-663.
- Easter SS, Jr., and Nicola GN (1997) The development of eye movements in the zebrafish (*Danio rerio*). *Developmental psychobiology* 31:267-276.
- Edmondson DE, Mattevi A, Binda C, Li M, and Hubalek F (2004) Structure and mechanism of monoamine oxidase. *Current medicinal chemistry* 11:1983-1993.
- Egan RJ, Bergner CL, Hart PC, Cachat JM, Canavello PR, Elegante MF, Elkhayat SI, Bartels BK, Tien AK, Tien DH, Mohnot S, Beeson E, Glasgow E, Amri H, Zukowska Z, and Kalueff AV (2009) Understanding behavioral and physiological phenotypes of stress and anxiety in zebrafish. *Behavioural brain research* 205:38-44.
- Eisen JS, and Smith JC (2008) Controlling morpholino experiments: don't stop making antisense. *Development (Cambridge, England)* 135:1735-1743.

- Emran F, Rihel J, Adolph AR, Wong KY, Kraves S, and Dowling JE (2007) OFF ganglion cells cannot drive the optokinetic reflex in zebrafish. *Proceedings of the National Academy of Sciences of the United States of America* 104:19126-19131.
- Emran F, Rihel J, and Dowling JE (2008) A behavioral assay to measure responsiveness of zebrafish to changes in light intensities. *Journal of visualized experiments : JoVE*.
- Evans WE, and Relling MV (1999) Pharmacogenomics: translating functional genomics into rational therapeutics. *Science (New York, NY)* 286:487-491.
- Fadool JM, and Dowling JE (2008) Zebrafish: a model system for the study of eye genetics. *Progress in retinal and eye research* 27:89-110.
- Falany CN, Xie X, Wang J, Ferrer J, and Falany JL (2000) Molecular cloning and expression of novel sulphotransferase-like cDNAs from human and rat brain. *The Biochemical journal* 346 Pt 3:857-864.
- Fukada Y, and Okano T (2002) Circadian clock system in the pineal gland. *Molecular neurobiology* 25:19-30.
- Glatt H, Boeing H, Engelke CE, Ma L, Kuhlow A, Pabel U, Pomplun D, Teubner W, and Meinel W (2001) Human cytosolic sulphotransferases: genetics, characteristics, toxicological aspects. *Mutation research* 482:27-40.
- Granit R (1933) The components of the retinal action potential in mammals and their relation to the discharge in the optic nerve. *The Journal of physiology* 77:207-239.
- Gregus Z, Fekete T, Varga F, and Klaassen CD (1993) Dependence of glycine conjugation on availability of glycine: role of the glycine cleavage system. *Xenobiotica; the fate of foreign compounds in biological systems* 23:141-153.
- Grossman L, Utterback E, Stewart A, Gaikwad S, Chung KM, Suciuc C, Wong K, Elegante M, Elkhayat S, Tan J, Gilder T, Wu N, Dileo J, Cachat J, and Kalueff AV (2010) Characterization of behavioral and endocrine effects of LSD on zebrafish. *Behavioural brain research* 214:277-284.
- Gulseth MP, Grice GR, and Dager WE (2009) Pharmacogenomics of warfarin: uncovering a piece of the warfarin mystery. *American journal of health-system pharmacy : AJHP : official journal of the American Society of Health-System Pharmacists* 66:123-133.
- Harayama S, Kok M, and Neidle EL (1992) Functional and evolutionary relationships among diverse oxygenases. *Annual review of microbiology* 46:565-601.
- He D, and Falany CN (2006) Characterization of proline-serine-rich carboxyl terminus in human sulfotransferase 2B1b: immunogenicity, subcellular localization, kinetic properties, and phosphorylation. *Drug metabolism and disposition: the biological fate of chemicals* 34:1749-1755.
- He D, Meloche CA, Dumas NA, Frost AR, and Falany CN (2004) Different subcellular localization of sulphotransferase 2B1b in human placenta and prostate. *The Biochemical journal* 379:533-540.
- Heasman J (2002) Morpholino oligos: making sense of antisense? *Developmental biology* 243:209-214.
- Her C, Kaur GP, Athwal RS, and Weinshilboum RM (1997) Human sulfotransferase SULT1C1: cDNA cloning, tissue-specific expression, and chromosomal localization. *Genomics* 41:467-470.

- Higashi Y, Fuda H, Yanai H, Lee Y, Fukushige T, Kanzaki T, and Strott CA (2004) Expression of cholesterol sulfotransferase (SULT2B1b) in human skin and primary cultures of human epidermal keratinocytes. *The Journal of investigative dermatology* 122:1207-1213.
- Hildebrandt MA, Carrington DP, Thomae BA, Eckloff BW, Schaid DJ, Yee VC, Weinshilboum RM, and Wieben ED (2007) Genetic diversity and function in the human cytosolic sulfotransferases. *The pharmacogenomics journal* 7:133-143.
- Huang C, Yuan X, Li Z, Tian Z, Zhan X, Zhang J, and Li X (2014) VE-statin/Egfl7 siRNA inhibits angiogenesis in malignant glioma in vitro. *International journal of clinical and experimental pathology* 7:1077-1084.
- Huang YY, and Neuhauss SC (2008) The optokinetic response in zebrafish and its applications. *Frontiers in bioscience : a journal and virtual library* 13:1899-1916.
- Hughes ME, Hogenesch JB, and Kornacker K (2010) JTK_CYCLE: an efficient nonparametric algorithm for detecting rhythmic components in genome-scale data sets. *Journal of biological rhythms* 25:372-380.
- Ishikawa T, Hirayama J, Kobayashi Y, and Todo T (2002) Zebrafish CRY represses transcription mediated by CLOCK-BMAL heterodimer without inhibiting its binding to DNA. *Genes to cells : devoted to molecular & cellular mechanisms* 7:1073-1086.
- Jorgensen TH, Borglum AD, Mors O, Wang AG, Pinaud M, Flint TJ, Dahl HA, Vang M, Kruse TA, and Ewald H (2002) Search for common haplotypes on chromosome 22q in patients with schizophrenia or bipolar disorder from the Faroe Islands. *American journal of medical genetics* 114:245-252.
- Kakuta Y, Petrotchenko EV, Pedersen LC, and Negishi M (1998) The sulfuryl transfer mechanism. Crystal structure of a vanadate complex of estrogen sulfotransferase and mutational analysis. *The Journal of biological chemistry* 273:27325-27330.
- Kalueff AV, Gebhardt M, Stewart AM, Cachat JM, Brimmer M, Chawla JS, Craddock C, Kyzar EJ, Roth A, Landsman S, Gaikwad S, Robinson K, Baatrup E, Tierney K, Shamchuk A, Norton W, Miller N, Nicolson T, Braubach O, Gilman CP, Pittman J, Rosemberg DB, Gerlai R, Echevarria D, Lamb E, Neuhauss SC, Weng W, Bally-Cuif L, and Schneider H (2013) Towards a comprehensive catalog of zebrafish behavior 1.0 and beyond. *Zebrafish* 10:70-86.
- Kalueff AV, Stewart AM, and Gerlai R (2014) Zebrafish as an emerging model for studying complex brain disorders. *Trends in pharmacological sciences* 35:63-75.
- Keller A, Nesvizhskii AI, Kolker E, and Aebersold R (2002) Empirical statistical model to estimate the accuracy of peptide identifications made by MS/MS and database search. *Analytical chemistry* 74:5383-5392.
- King CD, Green MD, Rios GR, Coffman BL, Owens IS, Bishop WP, and Tephly TR (1996) The glucuronidation of exogenous and endogenous compounds by stably expressed rat and human UDP-glucuronosyltransferase 1.1. *Archives of biochemistry and biophysics* 332:92-100.
- King CD, Rios GR, Green MD, and Tephly TR (2000) UDP-glucuronosyltransferases. *Current drug metabolism* 1:143-161.
- Knights KM, Sykes MJ, and Miners JO (2007) Amino acid conjugation: contribution to the metabolism and toxicity of xenobiotic carboxylic acids. *Expert opinion on drug metabolism & toxicology* 3:159-168.

- Kok FO, Shin M, Ni CW, Gupta A, Grosse AS, van Impel A, Kirchmaier BC, Peterson-Maduro J, Kourkoulis G, Male I, DeSantis DF, Sheppard-Tindell S, Ebarasi L, Betsholtz C, Schulte-Merker S, Wolfe SA, and Lawson ND (2015) Reverse genetic screening reveals poor correlation between morpholino-induced and mutant phenotypes in zebrafish. *Developmental cell* 32:97-108.
- Kokel D, Bryan J, Laggner C, White R, Cheung CY, Mateus R, Healey D, Kim S, Werdich AA, Haggarty SJ, Macrae CA, Shoichet B, and Peterson RT (2010) Rapid behavior-based identification of neuroactive small molecules in the zebrafish. *Nature chemical biology* 6:231-237.
- Kokel D, and Peterson RT (2011) Using the zebrafish photomotor response for psychotropic drug screening. *Methods in cell biology* 105:517-524.
- Korenbrot JI, Mehta M, Tserentsoodol N, Postlethwait JH, and Rebrik TI (2013) EML1 (CNG-modulin) controls light sensitivity in darkness and under continuous illumination in zebrafish retinal cone photoreceptors. *The Journal of neuroscience : the official journal of the Society for Neuroscience* 33:17763-17776.
- Kuhnert F, Mancuso MR, Hampton J, Stankunas K, Asano T, Chen CZ, and Kuo CJ (2008) Attribution of vascular phenotypes of the murine *Egfl7* locus to the microRNA miR-126. *Development (Cambridge, England)* 135:3989-3993.
- Kurogi K, Chen M, Lee Y, Shi B, Yan T, Liu MY, Sakakibara Y, Suiko M, and Liu MC (2012) Sulfation of buprenorphine, pentazocine, and naloxone by human cytosolic sulfotransferases. *Drug metabolism letters* 6:109-115.
- Kurogi K, Liu TA, Sakakibara Y, Suiko M, and Liu MC (2013) The use of zebrafish as a model system for investigating the role of the SULTs in the metabolism of endogenous compounds and xenobiotics. *Drug metabolism reviews* 45:431-440.
- Lambeth JD, McCaslin DR, and Kamin H (1976) Adrenodoxin reductase-adrenodoxin complex. *The Journal of biological chemistry* 251:7545-7550.
- Langouet S, Paehler A, Welti DH, Kerriguy N, Guillouzo A, and Turesky RJ (2002) Differential metabolism of 2-amino-1-methyl-6-phenylimidazo[4,5-b]pyridine in rat and human hepatocytes. *Carcinogenesis* 23:115-122.
- Laranjeiro R, and Whitmore D (2014) Transcription factors involved in retinogenesis are co-opted by the circadian clock following photoreceptor differentiation. *Development (Cambridge, England)* 141:2644-2656.
- Law SH, and Sargent TD (2014) The serine-threonine protein kinase PAK4 is dispensable in zebrafish: identification of a morpholino-generated pseudophenotype. *PloS one* 9:e100268.
- Levin ED, Bencan Z, and Cerutti DT (2007) Anxiolytic effects of nicotine in zebrafish. *Physiology & behavior* 90:54-58.
- Levy G, and Tsuchiya T (1972) Salicylate accumulation kinetics in man. *The New England journal of medicine* 287:430-432.
- Lewis AG, and Minchin RF (2009) Lack of exonic sulfotransferase 4A1 mutations in controls and schizophrenia cases. *Psychiatric genetics* 19:53-55.
- Lin L, Faraco J, Li R, Kadotani H, Rogers W, Lin X, Qiu X, de Jong PJ, Nishino S, and Mignot E (1999) The sleep disorder canine narcolepsy is caused by a mutation in the hypocretin (orexin) receptor 2 gene. *Cell* 98:365-376.
- Liu Q, Ramsey TL, Meltzer HY, Massey BW, Padmanabhan S, and Brennan MD (2012) Sulfotransferase 4A1 Haplotype 1 (SULT4A1-1) Is Associated With Decreased

- Hospitalization Events in Antipsychotic-Treated Patients With Schizophrenia. The primary care companion to CNS disorders 14.
- Liu TA, Bhuiyan S, Liu MY, Sugahara T, Sakakibara Y, Suiko M, Yasuda S, Kakuta Y, Kimura M, Williams FE, and Liu MC (2010) Zebrafish as a model for the study of the phase II cytosolic sulfotransferases. *Current drug metabolism* 11:538-546.
- Liu XG, and Feng YP (1995) [Protective effect of dl-3-n-butylphthalide on ischemic neurological damage and abnormal behavior in rats subjected to focal ischemia]. *Yao xue xue bao = Acta pharmaceutica Sinica* 30:896-903.
- Liyou NE, Buller KM, Tresillian MJ, Elvin CM, Scott HL, Dodd PR, Tannenberg AE, and McManus ME (2003) Localization of a brain sulfotransferase, SULT4A1, in the human and rat brain: an immunohistochemical study. *The journal of histochemistry and cytochemistry : official journal of the Histochemistry Society* 51:1655-1664.
- Lu KP, Hanes SD, and Hunter T (1996) A human peptidyl-prolyl isomerase essential for regulation of mitosis. *Nature* 380:544-547.
- Luciani JJ, de Mas P, Depetris D, Mignon-Ravix C, Bottani A, Prieur M, Jonveaux P, Philippe A, Bourrouillou G, de Martinville B, Delobel B, Vallee L, Croquette MF, and Mattei MG (2003) Telomeric 22q13 deletions resulting from rings, simple deletions, and translocations: cytogenetic, molecular, and clinical analyses of 32 new observations. *Journal of medical genetics* 40:690-696.
- Maaswinkel H, and Li L (2003) Spatio-temporal frequency characteristics of the optomotor response in zebrafish. *Vision research* 43:21-30.
- Marchitti SA, Brocker C, Stagos D, and Vasiliou V (2008) Non-P450 aldehyde oxidizing enzymes: the aldehyde dehydrogenase superfamily. *Expert opinion on drug metabolism & toxicology* 4:697-720.
- Marmor MF, Fulton AB, Holder GE, Miyake Y, Brigell M, and Bach M (2009) ISCEV Standard for full-field clinical electroretinography (2008 update). *Documenta ophthalmologica Advances in ophthalmology* 118:69-77.
- Maximino C, Puty B, Matos Oliveira KR, and Herculano AM (2013) Behavioral and neurochemical changes in the zebrafish leopard strain. *Genes, brain, and behavior* 12:576-582.
- Meltzer HY, Brennan MD, Woodward ND, and Jayathilake K (2008) Association of Sult4A1 SNPs with psychopathology and cognition in patients with schizophrenia or schizoaffective disorder. *Schizophrenia research* 106:258-264.
- Meunier B, de Visser SP, and Shaik S (2004) Mechanism of oxidation reactions catalyzed by cytochrome p450 enzymes. *Chemical reviews* 104:3947-3980.
- Mieda M, Tsujino N, and Sakurai T (2013) Differential roles of orexin receptors in the regulation of sleep/wakefulness. *Frontiers in endocrinology* 4:57.
- Miller JC, Tan S, Qiao G, Barlow KA, Wang J, Xia DF, Meng X, Paschon DE, Leung E, Hinkley SJ, Dulay GP, Hua KL, Ankoudinova I, Cost GJ, Urnov FD, Zhang HS, Holmes MC, Zhang L, Gregory PD, and Rebar EJ (2011) A TALE nuclease architecture for efficient genome editing. *Nature biotechnology* 29:143-148.
- Miller N, and Gerlai R (2007) Quantification of shoaling behaviour in zebrafish (*Danio rerio*). *Behavioural brain research* 184:157-166.

- Minchin RF, Lewis A, Mitchell D, Kadlubar FF, and McManus ME (2008) Sulfotransferase 4A1. *The international journal of biochemistry & cell biology* 40:2686-2691.
- Misawa K, Nosaka T, Morita S, Kaneko A, Nakahata T, Asano S, and Kitamura T (2000) A method to identify cDNAs based on localization of green fluorescent protein fusion products. *Proceedings of the National Academy of Sciences of the United States of America* 97:3062-3066.
- Mistlberger RE (2005) Circadian regulation of sleep in mammals: role of the suprachiasmatic nucleus. *Brain research Brain research reviews* 49:429-454.
- Mistry M, and Houston JB (1987) Glucuronidation in vitro and in vivo. Comparison of intestinal and hepatic conjugation of morphine, naloxone, and buprenorphine. *Drug metabolism and disposition: the biological fate of chemicals* 15:710-717.
- Mitchell DJ, Butcher NJ, and Minchin RF (2011) Phosphorylation/dephosphorylation of human SULT4A1: role of Erk1 and PP2A. *Biochimica et biophysica acta* 1813:231-237.
- Mitchell DJ, and Minchin RF (2009) Cytosolic Aryl sulfotransferase 4A1 interacts with the peptidyl prolyl cis-trans isomerase Pin1. *Molecular pharmacology* 76:388-395.
- Moore HA, and Whitmore D (2014) Circadian rhythmicity and light sensitivity of the zebrafish brain. *PloS one* 9:e86176.
- Morcos PA (2007) Achieving targeted and quantifiable alteration of mRNA splicing with Morpholino oligos. *Biochemical and biophysical research communications* 358:521-527.
- Mortazavi A, Williams BA, McCue K, Schaeffer L, and Wold B (2008) Mapping and quantifying mammalian transcriptomes by RNA-Seq. *Nature methods* 5:621-628.
- Moscou MJ, and Bogdanove AJ (2009) A simple cipher governs DNA recognition by TAL effectors. *Science (New York, NY)* 326:1501.
- Mowry BJ, Holmans PA, Pulver AE, Gejman PV, Riley B, Williams NM, Laurent C, Schwab SG, Wildenauer DB, Bauche S, Owen MJ, Wormley B, Sanders AR, Nestadt G, Liang KY, Duan J, Ribble R, Norton N, Soubigou S, Maier W, Ewen-White KR, DeMarchi N, Carpenter B, Walsh D, Williams H, Jay M, Albus M, Nertney DA, Papadimitriou G, O'Neill A, O'Donovan MC, Deleuze JF, Lerer FB, Dikeos D, Kendler KS, Mallet J, Silverman JM, Crowe RR, and Levinson DF (2004) Multicenter linkage study of schizophrenia loci on chromosome 22q. *Molecular psychiatry* 9:784-795.
- Nasevicius A, and Ekker SC (2000) Effective targeted gene 'knockdown' in zebrafish. *Nature genetics* 26:216-220.
- Nelson DR (2003) Comparison of P450s from human and fugu: 420 million years of vertebrate P450 evolution. *Archives of biochemistry and biophysics* 409:18-24.
- Nelson SM, Frey RA, Wardwell SL, and Stenkamp DL (2008) The developmental sequence of gene expression within the rod photoreceptor lineage in embryonic zebrafish. *Developmental dynamics : an official publication of the American Association of Anatomists* 237:2903-2917.
- Nesvizhskii AI, Keller A, Kolker E, and Aebersold R (2003) A statistical model for identifying proteins by tandem mass spectrometry. *Analytical chemistry* 75:4646-4658.

- Nishino S (2007) The hypothalamic peptidergic system, hypocretin/orexin and vigilance control. *Neuropeptides* 41:117-133.
- Noche RR, Lu PN, Goldstein-Kral L, Glasgow E, and Liang JO (2011) Circadian rhythms in the pineal organ persist in zebrafish larvae that lack ventral brain. *BMC neuroscience* 12:7.
- Norton W, and Bally-Cuif L (2010) Adult zebrafish as a model organism for behavioural genetics. *BMC neuroscience* 11:90.
- Ong E, Yeh JC, Ding Y, Hindsgaul O, Pedersen LC, Negishi M, and Fukuda M (1999) Structure and function of HNK-1 sulfotransferase. Identification of donor and acceptor binding sites by site-directed mutagenesis. *The Journal of biological chemistry* 274:25608-25612.
- Panula P, Chen YC, Priyadarshini M, Kudo H, Semenova S, Sundvik M, and Sallinen V (2010) The comparative neuroanatomy and neurochemistry of zebrafish CNS systems of relevance to human neuropsychiatric diseases. *Neurobiology of disease* 40:46-57.
- Panula P, Sallinen V, Sundvik M, Kolehmainen J, Torkko V, Tiittula A, Moshnyakov M, and Podlasz P (2006) Modulatory neurotransmitter systems and behavior: towards zebrafish models of neurodegenerative diseases. *Zebrafish* 3:235-247.
- Parant JM, George SA, Pryor R, Wittwer CT, and Yost HJ (2009) A rapid and efficient method of genotyping zebrafish mutants. *Developmental dynamics : an official publication of the American Association of Anatomists* 238:3168-3174.
- Parker LH, Schmidt M, Jin SW, Gray AM, Beis D, Pham T, Frantz G, Palmieri S, Hillan K, Stainier DY, De Sauvage FJ, and Ye W (2004) The endothelial-cell-derived secreted factor Egl7 regulates vascular tube formation. *Nature* 428:754-758.
- Parkinson A (1996) *Biotransformation of xenobiotics*. McGraw-Hill, New York.
- Pedersen LC, Petrotchenko E, Shevtsov S, and Negishi M (2002) Crystal structure of the human estrogen sulfotransferase-PAPS complex: evidence for catalytic role of Ser137 in the sulfuryl transfer reaction. *The Journal of biological chemistry* 277:17928-17932.
- Petrotchenko EV, Pedersen LC, Borchers CH, Tomer KB, and Negishi M (2001) The dimerization motif of cytosolic sulfotransferases. *FEBS letters* 490:39-43.
- Peyron C, Faraco J, Rogers W, Ripley B, Overeem S, Charnay Y, Nevsimalova S, Aldrich M, Reynolds D, Albin R, Li R, Hungs M, Pedrazzoli M, Padigaru M, Kucherlapati M, Fan J, Maki R, Lammers GJ, Bouras C, Kucherlapati R, Nishino S, and Mignot E (2000) A mutation in a case of early onset narcolepsy and a generalized absence of hypocretin peptides in human narcoleptic brains. *Nature medicine* 6:991-997.
- Phelan K, and McDermid HE (2012) The 22q13.3 Deletion Syndrome (Phelan-McDermid Syndrome). *Molecular syndromology* 2:186-201.
- Phelan K, and Rogers RC (2011) Phelan-McDermid Syndrome. In *GeneReviews(R)*, RA Pagon, MP Adam, HH Ardinger, SE Wallace, A Amemiya, LJH Bean, TD Bird, CR Dolan, CT Fong, RJH Smith, and K Stephens, eds, University of Washington, Seattle
- University of Washington, Seattle. All rights reserved., Seattle (WA).
- Portugues R, and Engert F (2009) The neural basis of visual behaviors in the larval zebrafish. *Current opinion in neurobiology* 19:644-647.

- Prober DA, Rihel J, Onah AA, Sung RJ, and Schier AF (2006) Hypocretin/orexin overexpression induces an insomnia-like phenotype in zebrafish. *The Journal of neuroscience : the official journal of the Society for Neuroscience* 26:13400-13410.
- Ramsey TL, Liu Q, and Brennan MD (2014) Replication of SULT4A1-1 as a pharmacogenetic marker of olanzapine response and evidence of lower weight gain in the high response group. *Pharmacogenomics* 15:933-939.
- Ramsey TL, Meltzer HY, Brock GN, Mehrotra B, Jayathilake K, Bobo WV, and Brennan MD (2011) Evidence for a SULT4A1 haplotype correlating with baseline psychopathology and atypical antipsychotic response. *Pharmacogenomics* 12:471-480.
- Rapaport DH, Wong LL, Wood ED, Yasumura D, and LaVail MM (2004) Timing and topography of cell genesis in the rat retina. *The Journal of comparative neurology* 474:304-324.
- Rehse PH, Zhou M, and Lin SX (2002) Crystal structure of human dehydroepiandrosterone sulphotransferase in complex with substrate. *The Biochemical journal* 364:165-171.
- Renninger SL, Gesemann M, and Neuhauss SC (2011) Cone arrestin confers cone vision of high temporal resolution in zebrafish larvae. *The European journal of neuroscience* 33:658-667.
- Richardson GS (2005) The human circadian system in normal and disordered sleep. *The Journal of clinical psychiatry* 66 Suppl 9:3-9; quiz 42-43.
- Rossi A, Kontarakis Z, Gerri C, Nolte H, Holper S, Kruger M, and Stainier DY (2015) Genetic compensation induced by deleterious mutations but not gene knockdowns. *Nature* 524:230-233.
- Sakakibara Y, Yanagisawa K, Katafuchi J, Ringer DP, Takami Y, Nakayama T, Suiko M, and Liu MC (1998) Molecular cloning, expression, and characterization of novel human SULT1C sulfotransferases that catalyze the sulfonation of N-hydroxy-2-acetylaminofluorene. *The Journal of biological chemistry* 273:33929-33935.
- Sakurai T, Amemiya A, Ishii M, Matsuzaki I, Chemelli RM, Tanaka H, Williams SC, Richardson JA, Kozlowski GP, Wilson S, Arch JR, Buckingham RE, Haynes AC, Carr SA, Annan RS, McNulty DE, Liu WS, Terrett JA, Elshourbagy NA, Bergsma DJ, and Yanagisawa M (1998) Orexins and orexin receptors: a family of hypothalamic neuropeptides and G protein-coupled receptors that regulate feeding behavior. *Cell* 92:573-585.
- Salman ED, Faye-Petersen O, and Falany CN (2011) Hydroxysteroid sulfotransferase 2B1b expression and localization in normal human brain. *Hormone molecular biology and clinical investigation* 8:445-454.
- Salman ED, Kadlubar SA, and Falany CN (2009) Expression and localization of cytosolic sulfotransferase (SULT) 1A1 and SULT1A3 in normal human brain. *Drug metabolism and disposition: the biological fate of chemicals* 37:706-709.
- Schmidt M, Paes K, De Maziere A, Smyczek T, Yang S, Gray A, French D, Kasman I, Klumperman J, Rice DS, and Ye W (2007) EGFL7 regulates the collective migration of endothelial cells by restricting their spatial distribution. *Development (Cambridge, England)* 134:2913-2923.

- Sidharthan NP, Butcher NJ, Mitchell DJ, and Minchin RF (2014) Expression of the orphan cytosolic sulfotransferase SULT4A1 and its major splice variant in human tissues and cells: dimerization, degradation and polyubiquitination. *PloS one* 9:e101520.
- Stainier DY, Kontarakis Z, and Rossi A (2015) Making sense of anti-sense data. *Developmental cell* 32:7-8.
- Stanley EL, Hume R, and Coughtrie MW (2005) Expression profiling of human fetal cytosolic sulfotransferases involved in steroid and thyroid hormone metabolism and in detoxification. *Molecular and cellular endocrinology* 240:32-42.
- Stewart A, Wong K, Cachat J, Gaikwad S, Kyzar E, Wu N, Hart P, Piet V, Utterback E, Elegante M, Tien D, and Kalueff AV (2011) Zebrafish models to study drug abuse-related phenotypes. *Reviews in the neurosciences* 22:95-105.
- Stewart AM, Nguyen M, Wong K, Poudel MK, and Kalueff AV (2014) Developing zebrafish models of autism spectrum disorder (ASD). *Progress in neuro-psychopharmacology & biological psychiatry* 50:27-36.
- Summerton J, and Weller D (1997) Morpholino antisense oligomers: design, preparation, and properties. *Antisense & nucleic acid drug development* 7:187-195.
- Sun Z, Li H, Shu XH, Shi H, Chen XY, Kong QY, Wu ML, and Liu J (2012) Distinct sulfonation activities in resveratrol-sensitive and resveratrol-insensitive human glioblastoma cells. *The FEBS journal* 279:2381-2392.
- Sutherland HG, Mumford GK, Newton K, Ford LV, Farrall R, Dellaire G, Caceres JF, and Bickmore WA (2001) Large-scale identification of mammalian proteins localized to nuclear sub-compartments. *Human molecular genetics* 10:1995-2011.
- Tappeiner C, Gerber S, Enzmann V, Balmer J, Jazwinska A, and Tschopp M (2012) Visual acuity and contrast sensitivity of adult zebrafish. *Frontiers in zoology* 9:10.
- Teramoto T, Sakakibara Y, Liu MC, Suiko M, Kimura M, and Kakuta Y (2009) Snapshot of a Michaelis complex in a sulfuryl transfer reaction: Crystal structure of a mouse sulfotransferase, mSULT1D1, complexed with donor substrate and acceptor substrate. *Biochemical and biophysical research communications* 383:83-87.
- Thannickal TC, Moore RY, Nienhuis R, Ramanathan L, Gulyani S, Aldrich M, Cornford M, and Siegel JM (2000) Reduced number of hypocretin neurons in human narcolepsy. *Neuron* 27:469-474.
- Theorell H, and McKee JS (1961) Mechanism of action of liver alcohol dehydrogenase. *Nature* 192:47-50.
- Thomas HR, Percival SM, Yoder BK, and Parant JM (2014) High-throughput genome editing and phenotyping facilitated by high resolution melting curve analysis. *PloS one* 9:e114632.
- Tibbs ZE, Rohn-Glowaki KJ, Crittenden F, Guidry AL, and Falany CN (2014) Structural plasticity in the human cytosolic sulfotransferase dimer and its role in substrate selectivity and catalysis. *Drug metabolism and pharmacokinetics*.
- Timbrell JA, Harland SJ, and Facchini V (1980) Polymorphic acetylation of hydralazine. *Clinical pharmacology and therapeutics* 28:350-355.
- Trapnell C, Pachter L, and Salzberg SL (2009) TopHat: discovering splice junctions with RNA-Seq. *Bioinformatics (Oxford, England)* 25:1105-1111.

- Trapnell C, Williams BA, Pertea G, Mortazavi A, Kwan G, van Baren MJ, Salzberg SL, Wold BJ, and Pachter L (2010) Transcript assembly and quantification by RNA-Seq reveals unannotated transcripts and isoform switching during cell differentiation. *Nature biotechnology* 28:511-515.
- Ulke-Lemee A, Trinkle-Mulcahy L, Chaulk S, Bernstein NK, Morrice N, Glover M, Lamond AI, and Moorhead GB (2007) The nuclear PP1 interacting protein ZAP3 (ZAP) is a putative nucleoside kinase that complexes with SAM68, CIA, NF110/45, and HNRNP-G. *Biochimica et biophysica acta* 1774:1339-1350.
- Vallada HP, Gill M, Sham P, Lim LC, Nanko S, Asherson P, Murray RM, McGuffin P, Owen M, and Collier D (1995) Linkage studies on chromosome 22 in familial schizophrenia. *American journal of medical genetics* 60:139-146.
- Vallner JJ, Stewart JT, Kotzan JA, Kirsten EB, and Honigberg IL (1981) Pharmacokinetics and bioavailability of hydromorphone following intravenous and oral administration to human subjects. *Journal of clinical pharmacology* 21:152-156.
- Wada Y, Sugiyama J, Okano T, and Fukada Y (2006) GRK1 and GRK7: unique cellular distribution and widely different activities of opsin phosphorylation in the zebrafish rods and cones. *Journal of neurochemistry* 98:824-837.
- Wang ET, Sandberg R, Luo S, Khrebtkova I, Zhang L, Mayr C, Kingsmore SF, Schroth GP, and Burge CB (2008) Alternative isoform regulation in human tissue transcriptomes. *Nature* 456:470-476.
- Wang J, Yin L, and Lazar MA (2006) The orphan nuclear receptor Rev-erb alpha regulates circadian expression of plasminogen activator inhibitor type 1. *The Journal of biological chemistry* 281:33842-33848.
- Wang Z, Gerstein M, and Snyder M (2009) RNA-Seq: a revolutionary tool for transcriptomics. *Nature reviews Genetics* 10:57-63.
- Weatherly DB, Atwood JA, 3rd, Minning TA, Cavola C, Tarleton RL, and Orlando R (2005) A Heuristic method for assigning a false-discovery rate for protein identifications from Mascot database search results. *Molecular & cellular proteomics : MCP* 4:762-772.
- Weinshilboum R (1988) Pharmacogenetics of methylation: relationship to drug metabolism. *Clinical biochemistry* 21:201-210.
- Weitzner B, Meehan T, Xu Q, and Dunbrack RL, Jr. (2009) An unusually small dimer interface is observed in all available crystal structures of cytosolic sulfotransferases. *Proteins* 75:289-295.
- Wetts R, and Fraser SE (1988) Multipotent precursors can give rise to all major cell types of the frog retina. *Science (New York, NY)* 239:1142-1145.
- Whitmore D, Foulkes NS, Strahle U, and Sassone-Corsi P (1998) Zebrafish Clock rhythmic expression reveals independent peripheral circadian oscillators. *Nature neuroscience* 1:701-707.
- Wilson HL, Wong AC, Shaw SR, Tse WY, Stapleton GA, Phelan MC, Hu S, Marshall J, and McDermid HE (2003) Molecular characterisation of the 22q13 deletion syndrome supports the role of haploinsufficiency of SHANK3/PROSAP2 in the major neurological symptoms. *Journal of medical genetics* 40:575-584.

- Xing Y, Yu T, Wu YN, Roy M, Kim J, and Lee C (2006) An expectation-maximization algorithm for probabilistic reconstructions of full-length isoforms from splice graphs. *Nucleic acids research* 34:3150-3160.
- Yaffe MB, Schutkowski M, Shen M, Zhou XZ, Stukenberg PT, Rahfeld JU, Xu J, Kuang J, Kirschner MW, Fischer G, Cantley LC, and Lu KP (1997) Sequence-specific and phosphorylation-dependent proline isomerization: a potential mitotic regulatory mechanism. *Science (New York, NY)* 278:1957-1960.
- Yamajuku D, Shibata Y, Kitazawa M, Katakura T, Urata H, Kojima T, Nakata O, and Hashimoto S (2010) Identification of functional clock-controlled elements involved in differential timing of Per1 and Per2 transcription. *Nucleic acids research* 38:7964-7973.
- Yokogawa T, Marin W, Faraco J, Pezeron G, Appelbaum L, Zhang J, Rosa F, Mourrain P, and Mignot E (2007) Characterization of sleep in zebrafish and insomnia in hypocretin receptor mutants. *PLoS biology* 5:e277.
- Young RW (1985) Cell differentiation in the retina of the mouse. *The Anatomical record* 212:199-205.
- Zhdanova IV (2006) Sleep in zebrafish. *Zebrafish* 3:215-226.
- Zhdanova IV (2011) Sleep and its regulation in zebrafish. *Reviews in the neurosciences* 22:27-36.
- Zhdanova IV, Wang SY, Leclair OU, and Danilova NP (2001) Melatonin promotes sleep-like state in zebrafish. *Brain research* 903:263-268.
- Zhdanova IV, Yu L, Lopez-Patino M, Shang E, Kishi S, and Guelin E (2008) Aging of the circadian system in zebrafish and the effects of melatonin on sleep and cognitive performance. *Brain research bulletin* 75:433-441.
- Zhu K, Zhao J, Lubman DM, Miller FR, and Barder TJ (2005) Protein pI shifts due to posttranslational modifications in the separation and characterization of proteins. *Analytical chemistry* 77:2745-2755.

APPENDIX A


INSTITUTIONAL ANIMAL CARE AND USE COMMITTEE APPROVAL

UAB THE UNIVERSITY OF ALABAMA AT BIRMINGHAM
Institutional Animal Care and Use Committee (IACUC)

MEMORANDUM

DATE: 20-Apr-2015

TO: Falany, Charles Napoleon

FROM: 
 Robert A. Kesterson, Ph.D., Chair
 Institutional Animal Care and Use Committee (IACUC)

SUBJECT: NOTICE OF APPROVAL

The following application was approved by the University of Alabama at Birmingham Institutional Animal Care and Use Committee (IACUC) on 20-Apr-2015.

Protocol PI: Falany, Charles Napoleon

Title: SULT4A1 in Zebrafish Development

Sponsor: National Institute of Mental Health/NIH/DHHS

Animal Project Number (APN): IACUC-09641

This institution has an Animal Welfare Assurance on file with the Office of Laboratory Animal Welfare (OLAW), is registered as a Research Facility with the USDA, and is accredited by the Association for Assessment and Accreditation of Laboratory Animal Care International (AAALAC).

Institutional Animal Care and Use Committee (IACUC)		Mailing Address:
CH19 Suite 403		CH19 Suite 403
933 19th Street South		1530 3rd Ave S
(205) 934-7892		Birmingham, AL 35294-0019
FAX (205) 934-1188		